

---

This is an electronic reprint of the original article.  
This reprint may differ from the original in pagination and typographic detail.

Rönn, Kristian; Swarts, Andre; Kalaskar, Vickey; Alger, Terry; Tripathi, Rupali; Keskinvääli, Juha; Kaario, Ossi; Santasalo-Aarnio, Annukka; Reitz, Rolf; Larmi, Martti

## Low-speed pre-ignition and super-knock in boosted spark-ignition engines : A review

*Published in:*  
Progress in Energy and Combustion Science

*DOI:*  
[10.1016/j.pecs.2022.101064](https://doi.org/10.1016/j.pecs.2022.101064)

Published: 01/03/2023

*Document Version*  
Publisher's PDF, also known as Version of record

*Published under the following license:*  
CC BY

*Please cite the original version:*  
Rönn, K., Swarts, A., Kalaskar, V., Alger, T., Tripathi, R., Keskinvääli, J., Kaario, O., Santasalo-Aarnio, A., Reitz, R., & Larmi, M. (2023). Low-speed pre-ignition and super-knock in boosted spark-ignition engines : A review. *Progress in Energy and Combustion Science*, 95, Article 101064. <https://doi.org/10.1016/j.pecs.2022.101064>

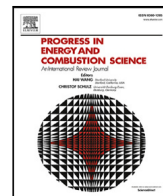
---

This material is protected by copyright and other intellectual property rights, and duplication or sale of all or part of any of the repository collections is not permitted, except that material may be duplicated by you for your research use or educational purposes in electronic or print form. You must obtain permission for any other use. Electronic or print copies may not be offered, whether for sale or otherwise to anyone who is not an authorised user.



Contents lists available at ScienceDirect

# Progress in Energy and Combustion Science

journal homepage: [www.elsevier.com/locate/pecs](http://www.elsevier.com/locate/pecs)

## Low-speed pre-ignition and super-knock in boosted spark-ignition engines: A review

Kristian Rönn<sup>a,\*</sup>, Andre Swarts<sup>b</sup>, Vickey Kalaskar<sup>b</sup>, Terry Alger<sup>b</sup>, Rupali Tripathi<sup>c</sup>, Juha Keskinen<sup>c</sup>, Ossi Kaario<sup>a</sup>, Annukka Santasalo-Aarnio<sup>a</sup>, Rolf Reitz<sup>d</sup>, Martti Larmi<sup>a</sup>

<sup>a</sup> Department of Mechanical Engineering, School of Engineering, Aalto University, FI-00076 Aalto, Finland

<sup>b</sup> Automotive Propulsion Systems, Powertrain Engineering Division, Southwest Research Institute, TX, USA

<sup>c</sup> Technology Centre, Neste Corporation, 06101 Porvoo, Finland

<sup>d</sup> Engine Research Center, University of Wisconsin-Madison, 1500 Engineering Drive, Madison, WI 53705, USA

### ARTICLE INFO

#### Keywords:

SI engine  
Autoignition  
Super-knock  
Low-speed pre-ignition  
Combustion

### ABSTRACT

The introduction of downsized, turbocharged Gasoline Direct Injection (GDI) engines in the automotive market has led to a rapid increase in research on Low-speed Pre-ignition (LSPI) and super-knock as abnormal combustion phenomena within the last decade. The former is characterized as an early ignition of the fuel–air mixture, primarily initiated by an oil–fuel droplet or detached deposit. Meanwhile, super-knock is an occasional development from pre-ignition to high intensity knocking through detonation, which is either initiated by a shock wave interacting with a propagating reaction and cylinder surfaces or inside a hotspot with a suitable heat release and reactivity gradient. The phenomenon can be divided into four stages, including LSPI precursor initiation, establishment and propagation of a pre-ignited flame, autoignition of end-gases and development to a detonation. LSPI and super-knock are rare phenomena, difficult to observe optically in engines, and differences in methodologies and setups between steady-state experiments can lead to discrepancies in results. Experimental research has included more detailed approaches using glow plug-equipped engines, constant volume combustion chambers and rapid compression machines. In addition, the improved availability of mechanisms for fuel and lubricant surrogates has allowed researchers to model the oil–fuel interaction at the cylinder walls, evaporation and autoignition of oil–fuel droplets and regimes for different propagation modes of an autoignition reaction wave. This paper presents a comprehensive review of the underlying phenomena behind LSPI and its development to super-knock. Furthermore, it presents the methodology in experimental research and draws conclusions for mitigating strategies based on studies involving fuel, oil and engine parameters. Finally, it discusses the prerequisites for LSPI from oil–fuel droplets and the future needs of research as original equipment manufacturers (OEM) and lubricant industry have already adopted some proven solutions to their products.

### 1. Introduction

As shown in a report by the International Energy Agency [1], the development of engine displacements in the light-duty vehicle market of advanced economies has shown a clear downward trend in 2005–2017. This development can be largely attributed to the rapid regulatory restriction related to emissions and fuel consumption. However, the evolution of power ratings has not followed in the same direction, as it in fact has shown a moderate increase within the same time frame.

The opposite trends of engine displacement and power output have been achieved by widely adapting turbocharging in modern light-duty vehicles, enabling improved volumetric efficiencies. In order to

counteract a reduction in displacement, forced induction of air is applied, allowing a higher Indicated Mean Effective Pressure (IMEP). An extensive study by Petitjean et al. [2] shows that turbocharging allows for a 30% reduction in displacement, 8–10% increase in fuel economy and additional improvements in torque as compared to naturally aspirated gasoline engines with equivalent power outputs. Furthermore, an aggressively downsized 1.2 l engine improved the fuel economy by almost 15% when compared to a 2.0 l turbocharged engine [3].

Conventional knock limits the potential of achieving higher efficiencies in Spark-ignition (SI) engines, as the thermal conditions in the cylinder introduce autoignition of unburned end-gases before the

\* Correspondence to: Aalto University, School of Engineering, Department of Mechanical Engineering, Research Group of Energy Conversion, P.O. Box 14300, FI-00076 Aalto, Finland.

E-mail address: [kristian.ronn@aalto.fi](mailto:kristian.ronn@aalto.fi) (K. Rönn).

<https://doi.org/10.1016/j.pecs.2022.101064>

Received 8 August 2022; Received in revised form 18 November 2022; Accepted 25 November 2022

Available online 20 December 2022

0360-1285/© 2022 The Authors. Published by Elsevier Ltd. This is an open access article under the CC BY license (<http://creativecommons.org/licenses/by/4.0/>).

**ABBREVIATIONS**

AKI	Anti-knock Index
ATDC	After Top Dead Center
BSFC	Brake-specific Fuel Consumption
BTDC	Before Top Dead Center
CAD	Crank Angle Degrees
CFD	Computational Fluid Dynamics
CFR	Cooperative Fuel Research
CoV	Coefficient of Variation
DCN	Derived Cetane Number
ECU	Engine Control Unit
EGR	Exhaust Gas Recirculation
GDI	Gasoline Direct Injection
IDT	Ignition Delay Time
IMEP	Indicated Mean Effective Pressure
IQT	Ignition Quality Tester
KI	Knock Intensity
KLSA	Knock Limited Spark Advance
LES	Large Eddy Simulation
LSPI	Low-speed Pre-ignition
LTHR	Low-temperature Heat Release
MoDTC	Molybdenum Dithio Carbamate
MON	Motor Octane Number
NTC	Negative Temperature Coefficient
OS	Octane Sensitivity
PCV	Positive Crankcase Ventilation
PFI	Port Fuel Injection
PMI	Particulate Matter Index
PRF	Primary Reference Fuel
RANS	Reynolds-averaged Navier-Stokes
RCEM	Rapid Compression and Expansion Machine
RCM	Rapid Compression Machine
RON	Research Octane Number
SOC	Start of Combustion
SOI	Start of Injection
SOK	Start of Knock
TDC	Top Dead Center
ZnDTP	Zinc Dialkyl Dithio Phosphate

**SYMBOLS**

$\lambda$	Ratio of air mass and stoichiometric air mass
$\phi$	Equivalence Ratio
$p_{EOC}$	End of compression pressure
$p_{in}$	Intake pressure
$T_{EOC}$	End of compression temperature
$T_{in}$	Intake temperature
$a$	Speed of Sound
$D_{CJ}$	Chapman–Jouguet detonation velocity
$r_c$	Critical radius for autoignition
$r_f$	Critical radius for stable flame
$S_L$	Laminar flame speed

spark-ignited flame consumes them. This form of abnormal combustion has been widely investigated during the last century. However, another destructive phenomenon has emerged with the popularization of downsized, boosted engines. As downsizing increases the pressure trajectory in the cylinder, the susceptibility for pre-ignition increases. The resulting temperature and pressure rise from this early flame

development causes further increase of in-cylinder pressure and temperature during the compression stroke, increasing the probability of detonation-induced super-knock (also referred to as mega-knock or deto-knock). Super-knock emerges as an abrupt and intensive rise in cylinder pressure, induced by a strong, supersonic detonation wave after autoignition [4,5]. This chain of events is not independently initiated in modern automotive engines but requires a pre-ignited flame to develop before the spark timing, simultaneously compressing unburned gases to autoignition. Therefore, Low-speed Pre-ignition (LSPI) is a prerequisite for super-knock. LSPI is also referred to as pre-ignition, stochastic pre-ignition and abnormal combustion in literature. The low-speed pre-ignition regime in a turbocharged engine is mainly concentrated at the 15–24 bar Brake Mean Effective Pressure (BMEP) and 1500–2000 rpm region. This region is attainable in commercial GDI engines [3,6].

The impacts of different engine parameters and fuel and lubricant formulations on LSPI and super-knock have been studied [7–9], but yet many questions about causing mechanisms and the affecting parameters remain unanswered. At least two review papers related to pre-ignition have already been published [10,11]. However, much research has been published since then and more detailed approaches on oil reactivity and detonation development have been included. Furthermore, with the introduction of standardized LSPI testing in recent years, new parameters, such as engine and oil aging have gained attraction. Thus, the objective of this review is to identify underlying mechanisms and various parameters that impact the magnitude of these events in SI engines.

This article provides a comprehensive review of research in LSPI and super-knock based on steady-state experiments, numerical simulations and optical diagnostics, highlighting recent progress in the development of turbocharged SI engines. First, the development of LSPI and its later development to super-knock are presented. Then, the effects of fuel and oil properties and engine parameters on LSPI and super-knock are reviewed. Finally, the role of oil-fuel droplets in causing LSPI, the prevalence of pre-ignition beyond gasoline engines and potential future research topics are discussed.

## 2. Development to LSPI and super-knock

The in-cylinder pressure curves for two cycles during the late compression strokes and power strokes are visible in Fig. 1. One can notice that the red pressure curve begins to deviate from the curve of a normal cycle at 10 Crank Angle Degrees (CAD) Before Top Dead Center (BTDC) and finally evolves to an extreme form of knocking, reaching a maximum pressure of almost 200 bar. This is an example of LSPI followed by super-knock.

The development to LSPI and super-knock can be divided into 4 steps as presented in Yu et al. [12] and Fig. 2.

1. Initiation mechanism: The source for pre-ignition, such as an oil-fuel droplet or a deposit, is created.
2. Pre-ignition: The heat release from the initiation mechanism is sufficient in order to ignite the surrounding fuel–air mixture and form a propagating flame.
3. Autoignition: The pre-ignited flame compresses end-gases, in which one or multiple hotspots of spatial thermal gradients autoignite.
4. Super-knock: Depending on the coupling between the autoignition-derived pressure wave and reaction front, the mixture may exhibit detonation, characterized by a strong rise and oscillation in pressure.

As shown in the aforementioned steps, super-knock, as opposed to conventional knock, is not an indicator of excessively advanced spark-timing. Conventional knock is characterized as low-intensity oscillation of the pressure and is simply eliminated by the Engine Control Unit

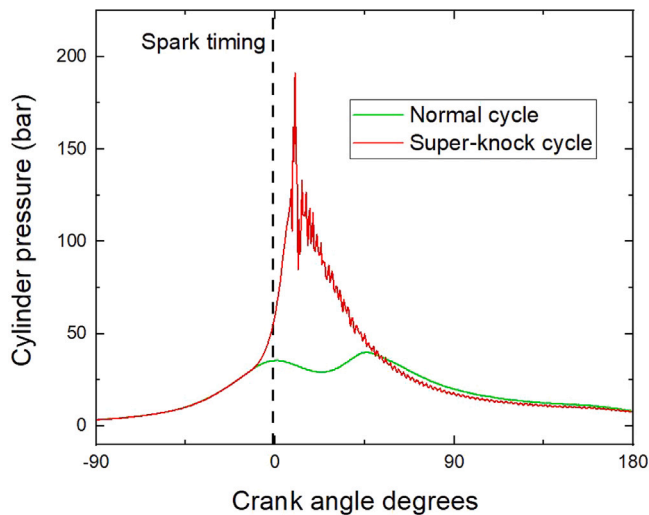


Fig. 1. Pressure curves of a normal cycle and a pre-ignition event with super-knock.

(ECU) through spark retardation. Strategies for reducing conventional knock are well known and standardized tests for deriving fuel knock resistance have been used for almost a century now. Methods for suppressing conventional knock are provided in [10,13].

In addition, it is important to note that LSPI and super-knock are separate phenomena. LSPI appears as a premature ignition and development of a flame, while super-knock is attributed to end-gas autoignition outside of this flame, leading to developing detonation and subsequent pressure oscillation of high intensity. LSPI is a prerequisite for super-knock to occur, but not all LSPI cycles develop into super-knock. Depending on various stochastic factors, such as pre-ignition timing and location, inhomogeneities and thermal gradients in the end-gases, the pre-ignited flame may or may not autoignite and detonate. Therefore, the outcome of LSPI may vary between no knock, slight knock and super-knock. This paper approaches pre-ignition and super-knock in different sections. The pathways to LSPI and super-knock are shown in Fig. 3.

## 2.1. Initiation of LSPI precursors

### 2.1.1. Mixture of oil and fuel droplets

The mechanism of oil–fuel droplet entrainment as the LSPI precursor is supported by repeated results presented in Section 4, which show that changes in fuel injection strategies, fuel volatility and oil composition significantly affect the presence of LSPI. In addition, high-speed in-cylinder imaging by Lauer et al. [14] shows that some LSPI cycles ignite spontaneously without prior light emission, as would be the case if a burning particle initiated LSPI. A weak fluorescent signal was detected from a droplet (a fluorescence agent was mixed in the oil) in [15].

In the case of droplet-initiated pre-ignition, as shown in Fig. 4, the fuel spray impinges on the cylinder liner before complete vaporization, dilutes the oil and changes the chemical and physical properties, including composition, viscosity and surface tension. The impinged fuel creates a layer on the oil film, after which fuel vaporization, heat transfer and mass diffusion dictate the composition of the mixture that forms before the top ring scrapes it off. Following this, the fuel–oil-mixture is collected at the piston crevice, from which it is released into the combustion chamber. Motored cycles at low speeds reveal that fuel and oil are accumulated at the top land, with release from the crevice and piston crown [16,17]. Computational Fluid Dynamics (CFD) derived trajectories from the crown at regions close to the fuel impingement region agreed reasonably well with pre-ignition locations

in optical studies [18]. The experiments by Tormos et al. [19], in which the release of oil was quantified by installing an absorbing paper above a motored engine at 500–3000 rpm with the cylinder head missing, revealed that the quantity of oil released per cycle would increase with faster engine speed up to 2500 rpm.

A 3D piston ring dynamic model was applied by Zahdeh et al. [7] to simulate interaction between the compression rings, piston and bore and gas flow rates between cavities at the piston rings. The results showed that the pressure at the ring crevice is higher than the combustion chamber pressure from 85 CAD After Top Dead Center (ATDC) to 117 CAD BTDC. This means that reverse blow-by occurs from the middle of the power stroke until the early compression stroke. The model did not include oil behavior, but the pressure difference indicates that reverse blow-by could be a pathway for droplet detachment. The same simulation also resulted in extreme ring acceleration exceeding 1000 g as a result of impacts with the ring grooves and the cylinder wall, which should also enhance the detachment of droplets.

Recent research has also considered splashing as an outcome of the interactions between the fuel spray and the oil film. This was indicated through Laser Induced Fluorescence (LIF) experiments with optical separation of oil and fuel traces. The images showed secondary droplets, which contained both fluids, detaching from the relatively thick (80  $\mu\text{m}$ ) oil film. These droplets could be larger than the oil film thickness [21].

As a result of the fuel impingement, two layers of liquid initially exist between the cylinder liner and the gaseous mixture. A thin oil layer with a thickness smaller than the top ring-liner clearance is maintained by the oil control ring at the liner, whereas a cool fuel layer is generated between the oil layer and the gas phase. Heat diffuses from the liner through the film towards the fuel–gas interface. Additionally, convective heat transfer occurs at the fuel film–gas interface. The temperature of the fuel film rises and evaporation of fuel components occurs [22]. The energy balance at the interface becomes:

$$k \frac{dT}{dx} = \dot{m} \times HoV + h(T_{\text{int}} - T_{\infty}) \quad (1)$$

where  $k$  is the heat conductivity (W/(mK)),  $\dot{m}$  is the evaporation mass rate (kg/(m<sup>2</sup>s)),  $HoV$  is the heat of vaporization (J/kg) and  $h$  is the convective heat transfer coefficient at the fuel film–gas interface (W/(m<sup>2</sup>K)). Zhang et al. [22] showed that the evaporation of lighter fuel components is already rapid for a 20  $\mu\text{m}$  film during the late intake stroke, and reduces fast as the volatile species have evaporated and the gas pressure begins to increase during the compression stroke.

Meanwhile, mass transfer of both oil and fuel species dilute both the fuel and oil layer. Oil species, with carbon chain lengths ranging from C<sub>15</sub> to C<sub>40</sub>, tend to diffuse slower than smaller fuel species. However, the increase of oil species concentrations at the gas interface is enhanced by the evaporation of fuel. A methodology to improve the predictions of diffusion coefficients of fuel species in high carbon chain length oils through machine learning and neural networks combined with empirical correlations was proposed by Mariani et al. [23].

The accumulated mixture in the top ring zone is composed of both fuel and oil-related species, the latter of which are heavier in molecular weight. Lee et al. [24] sampled this mixture from a naturally aspirated gasoline engine with indirect injection, and analysis with field ionization-mass spectroscopy and gas chromatography revealed that at 75% load and 1500 rpm almost 40% of the mixture mass comprised volatile species, mainly consisting of C<sub>6</sub> – C<sub>15</sub> aromatics. Alger and Briggs [25] compared LSPI performances and analyzed crevice samples of Primary Reference Fuel (PRF) and toluene standard fuel surrogates, finding that the latter enhanced both LSPI and the formation of heavier aromatics and mid-range paraffins (which were not present in either fuel). The pathways for the formation of these species in the crevice have not been specified. Sampling from an air-cooled engine with a carburetor at no-load operation also showed that higher boiling point aromatics were retained from the fuel with oil species in the top ring zone [26]. Similarly, sampling from the piston skirt for 25 min at

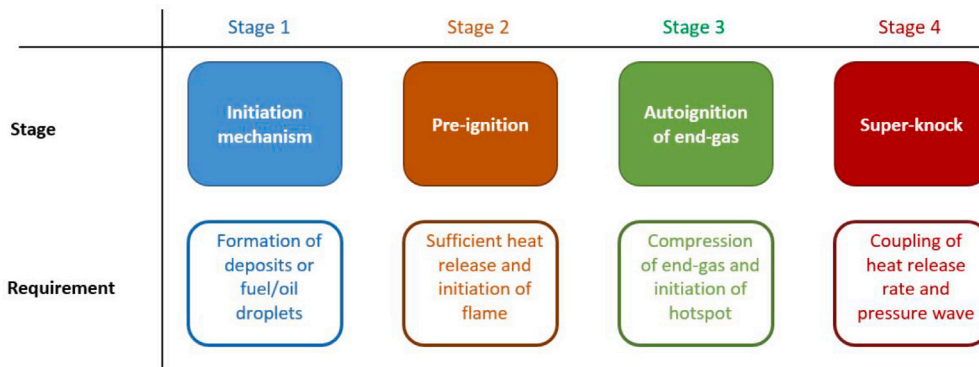


Fig. 2. Stages of super-knock development.

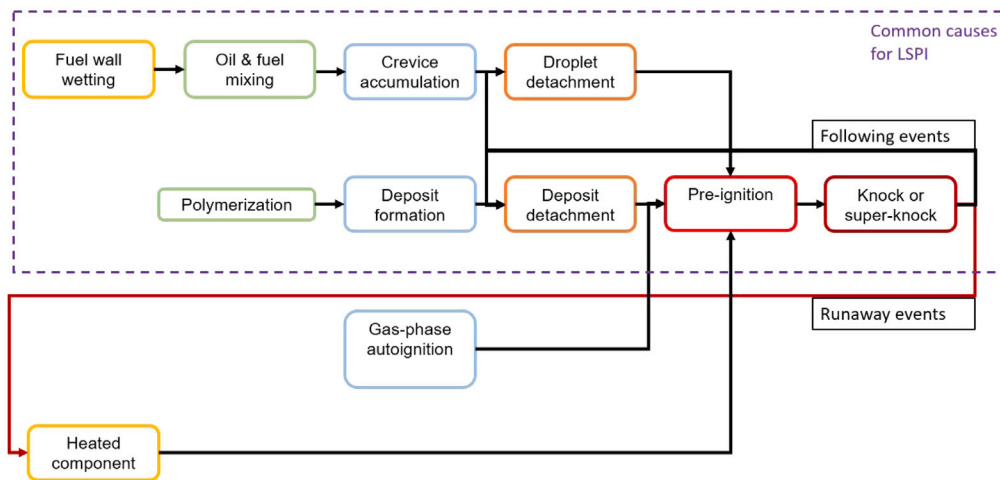


Fig. 3. Possible pathways for LSPI formation.

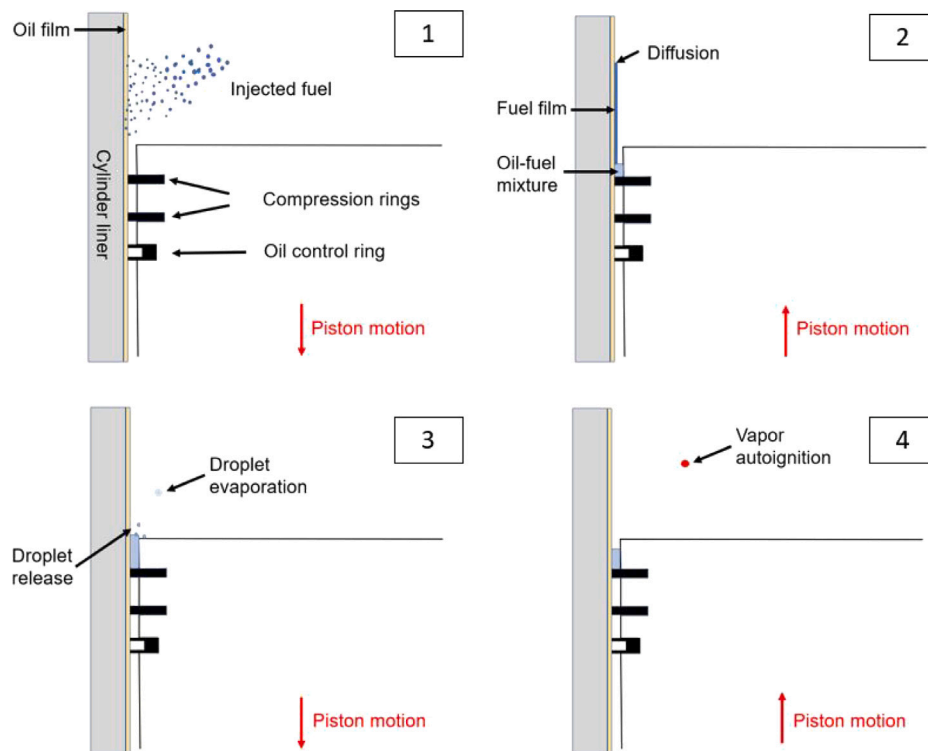


Fig. 4. Illustration of the pathway to LSPI through oil-fuel interaction. Based on [20].

low-speed and low-load starting and warm-up conditions showed that higher boiling point fuel species were favored [27].

The importance of piston crown and crevice geometry was shown in Amann et al. [28], as an increased height of the top land crevice promoted LSPI. In addition, a chamfer with a wide angle at the piston crown would reduce LSPI by allowing the flame to penetrate the crevice and consume the collected hydrocarbons before they would be released into the combustion chamber. Reducing the crevice volume may be insufficient as the LSPI frequency increased for a 0.35 cm<sup>3</sup> crevice as compared to 0.63 cm<sup>3</sup> [7].

Following the release of the droplet of oil and fuel into the combustion chamber, it would undergo evaporation, mixing with the charge and autoignition. The two former steps comprise a physical Ignition Delay Time (IDT), whereas the time required until a steep rise in the heat release rate occurs comprises the chemical IDT. The total IDT is then a combination of both physical and chemical IDTs. As shown by Kuti et al. [29], already a 1% volume fraction of C<sub>16</sub> – C<sub>18</sub> lubricant surrogates blended into iso-octane showed 15% shorter total IDTs in an Ignition Quality Tester (IQT) at 15 bar and 680–873 K. A 10% volume fraction of these species showed a much more significant reduction in total IDTs. The reduction with 10% addition was even stronger for base oils and a commercial lubricant with an additive package at the lower temperatures. CFD simulations by Distaso et al. [30] with n-hexadecane/iso-octane at these conditions showed that the reduction in total IDTs can be attributed to the larger Low-temperature Heat Release (LTHR) for lubricant species than in iso-octane. The higher LTHR enhances vaporization (and lowers physical IDT), especially at ambient temperatures above 800 K, whereas the chemical IDT would be effectively reduced at temperatures below 750 K, as the intermediate stage in iso-octane ignition diminishes. The GasLube mechanism was later used to develop a correlation for the relative impact of n-hexadecane addition on iso-octane chemical IDT [31].

The effect of oil droplets on the ignitibility of an ambient fuel mixture is dependent on the rate of droplet evaporation and the chemical IDT of the ambient mixture. Therefore, Fei et al. [32–35] conducted Rapid Compression Machine (RCM) studies with commercial oil and argon/nitrogen diluted iso-octane–air mixtures. At low temperatures (680 K, <16 bar & 740 K, <20 bar), the oil droplet would enhance ignition significantly. However, as the pressure would increase, the difference in IDTs between the cases with and without an oil droplet would diminish [34].

The pre-ignition appears to be enhanced when mixing fuel into the oil droplet. Qi et al. [36] found the earliest pre-ignition for an injected droplet containing 75% oil and 25% gasoline in a single-cylinder engine with a compression ratio of 14:1. Furthermore, a few percent of naphtha increased the ignition tendency of a group III base stock [37], but reduced it at higher fractions. Tao et al. measured enhanced autoignition for gasoline–oil droplets when increasing the gasoline fraction from 0 to 20% at 1 bar and 723–873 K ambient conditions [38]. Qian et al. [39] recorded the evaporation of oil droplets containing 0%–20% gasoline at 573–773 K ambient temperatures and atmospheric pressure. The increased ratio of gasoline enhanced the fluctuations in droplet size during evaporation as bubbles would form and rupture the droplet.

### 2.1.2. Glowing particles

LSPI precursors are sometimes characterized in optical studies as a glowing particle igniting the charge before the spark [14,15,40,41]. The particles have been identified as solid as their sizes do not change and they can rebound from the piston head or cylinder walls [16,40,42]. The glowing particles have in particular been initiated from the pressure oscillation during an LSPI cycle. Some of these particles would survive the gas exchange, heat up during the next regular cycle and cause a new LSPI event, as outlined in Fig. 5.

High-speed imaging has verified this process as the normal cycle after the first LSPI cycle would contain a high level of particles, which

presumably were caused by deposits detaching, and then finally a visible glowing particle would ignite the charge during the following compression stroke [14,15,42,43]. This explains the intermittent pattern between LSPI cycles and normal cycles which are often reported in literature. Deposit detachment and ignition was optically investigated by Zöbinger et al. [41] (Fig. 6), where a pre-ignition and super-knock event was initiated by a glowing object, causing a high number of burning particles in the following cycles. A glowing particle may also account for initial LSPI events, as was the case in Okada et al. [40]. Also in this case, a large amount of particles were visible after the super-knock, causing following pre-ignition events. Döhler and Pritze [43] detected a diffusively burning lump creating glowing particles during the power stroke. These particles kept glowing during the exhaust and intake strokes until causing pre-ignition. They proposed that these were caused by oil–fuel droplets that were ejected from the crevice and ignited during the cycle before pre-ignition. This would indicate that not all glowing particles originate from detached deposits and that oil–fuel droplets would not require vaporization and vapor autoignition during the compression stroke to cause pre-ignition. The following cycles after strong pre-ignition exhibited again a high number of particles [43]. It is possible that the knocking releases more droplets from the crevice [15,42,44].

It has been reported that deposits are produced as a result of polymerization at the cylinder surfaces. The fuel/air equivalence ratio ( $\phi$ ) and coolant temperature can have significant effects on combustion-chamber deposit formation. Aromatics promote deposit buildup and the number of side chains increased the deposit formation. [45,46]

Particle-initiated pre-ignition has been studied experimentally by high-speed imaging and deliberately feeding carbon particles of varying temperatures and size. Okada et al. [40] used optical tools to investigate the in-cylinder state prior to combustion and observed particles that likely were the source of pre-ignition. They also injected soot collected from the exhaust pipe and artificially generated carbon black (20–100 nm) and larger combustible particles at room temperature into the combustion chamber, finding that pre-ignition occurs for the latter. In another study, Wang et al. [47] injected particles of different temperatures and sizes and observed that particles of higher temperatures and larger sizes can initiate early pre-ignition, leading to super-knock.

While studies have shown that large combustible particles, such as deposits can cause LSPI, Gupta et al. [48] investigated the experimental results of Wang [47] with a 0D ignition model. The results indicated that the particles need to heat up sufficiently during the previous cycles as the required initial temperature for a 150  $\mu$ m particle to cause pre-ignition was above 1000 K.

### 2.1.3. Other mechanisms

During surface ignition, the flame is initiated at the boundary layer of a hot component and the gas mixture. Some of the first reported cases of pre-ignition were related to overheated spark plug electrodes [49]. This form of pre-ignition can also occur at high speeds in naturally aspirated engines if the spark plug heat range is insufficient [50,51]. The pre-ignition cycle heats up the surface hotspot further, which can trigger continuous runaway ignition (see Fig. 3), as shown for instance in [52,53]. Surface ignition has been widely investigated at higher engine speeds (> 4000 rpm) [50,51,53–55].

Surface ignition was detected by Ottenwälder et al. [56] and Hulser et al. [57] at 1500 rpm as in some cases the pre-ignition coincided with the spark plug. These studies were conducted at high intake pressures ( $p_{in}$ ) and temperatures (70–100 °C) with retarded spark timing (10 CAD ATDC or later). Winklhofer et al. [58] detected continuous pre-ignition at the exhaust valve with an optical spark plug.

The hot surface is, however, an unlikely cause for pre-ignition in modern commercial engines. Endoscopic access and optical spark plugs show repeatedly that the location of pre-ignition varies and the events occur either as individual or alternating cycles [7,14,59–61].

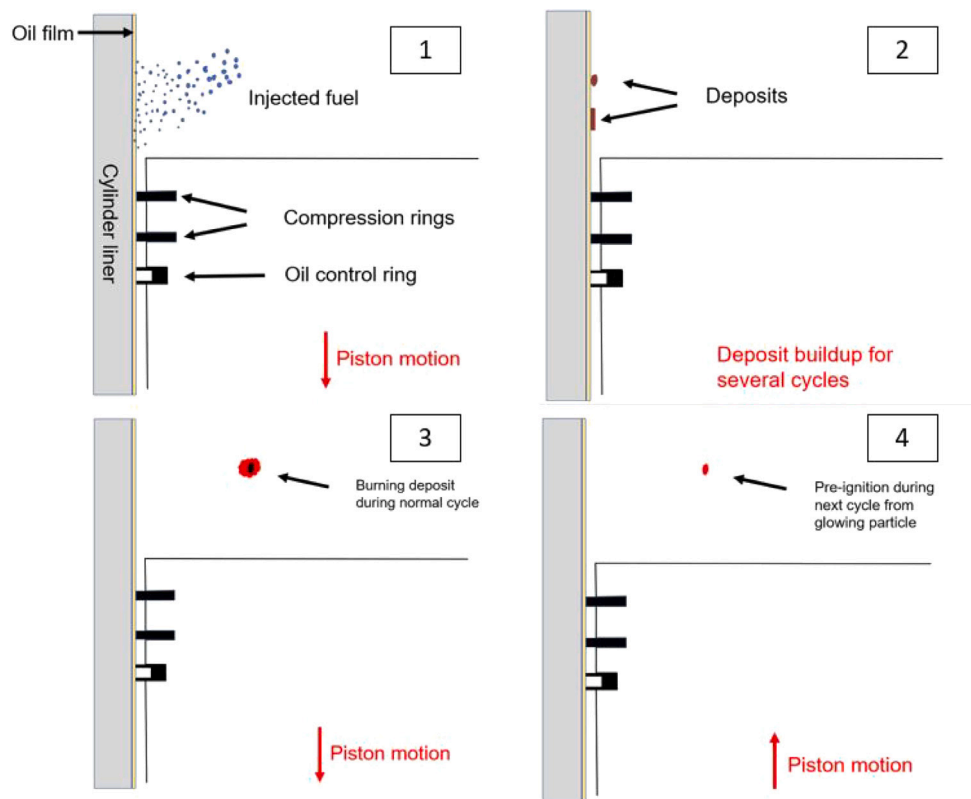


Fig. 5. Illustration of the pathway to LSPI through deposit formation.

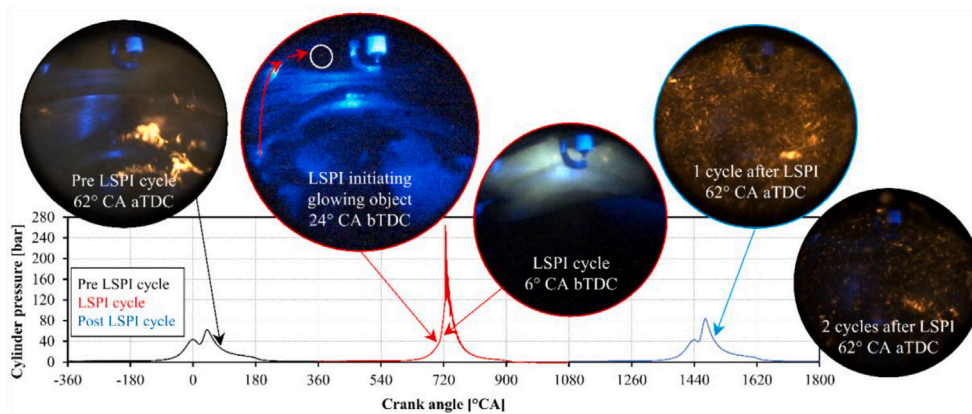


Fig. 6. Formation of a glowing object after a normal cycle, causing pre-ignition. The following cycles show a high amount of burning particles. Source: Reprinted from [41].

Disturbance in the exhaust gas removal leads to an increase in the quantity of hot residual gases during the following cycle. Pre-ignition and super-knock can be the outcome of a misfiring cycle in the same or other cylinders, as the charge ignites in the exhaust manifold and obstructs the flow from open exhaust ports [62].

Based on the spectroscopic work by Kalaskar et al. [63], “soot-like aggregates” appeared to be one of the potential initiators of LSPI and the pre-ignition precursors of a high Particulate Matter Index (PMI) fuel favored wavelengths that were associated with soot-like deposits. Poor mixing and piston wetting contribute to increased unburned hydrocarbon and soot formation, and in some studies higher emissions of these coincide with elevated pre-ignition activity [47,64,65]. However, in other studies, the soot production correlates poorly to pre-ignition [7, 66,67]. Furthermore, a sweep of engine load and Start of Injection (SOI) showed that elevated filter smoke numbers and hydrocarbon emissions

required very early SOI, whereas higher oil dilution was noticed also at retarded SOI for high loads [68]. Although the papers by Swarts et al. [69,70] revealed a strong correlation between LSPI activity and the PMI, it is acknowledged in the latter paper that PMI could simply be a substitute for aromatic content. Based on those experiments where soot production correlates poorly with LSPI and where only larger combustible particles cause LSPI [40], fine soot particles seem like unlikely causes for LSPI as compared to larger particles. In those cases where high soot emissions follow pre-ignition, the improper combustion of the oil droplet may instead be the cause [32,71]. Kar et al. [72] measured spikes in particulate mass emissions after an LSPI cycle, indicating that the pressure oscillation releases combustible pre-ignition precursors, causing a momentary increase in emissions.

## 2.2. Pre-ignition and flame propagation

The initiation of a flame from autoignition must fulfill three criteria as explained in Kalghatgi and Bradley [73]. Firstly, the IDTs of the combustible mixture must be sufficiently short to initiate autoignition. Secondly, the autoignition hotspot must reach a critical radius  $r_c$  for counteracting the heat transfer through conduction to surrounding gases with a sufficient heat release. Thirdly, the radius of the autoignited hot spot must be large enough to initiate a stable flame by reaching the critical radius  $r_f$ . The critical radius  $r_c$  is given as:

$$r_c = \left( \frac{\delta_c k T_a}{A Q E_n \exp(-E_n)} \right)^{1/2} \quad (2)$$

where  $\delta_c$  is the critical Frank-Kamenetskii parameter before ignition [74].  $T_a$  is the ambient temperature,  $k$  is the thermal conductivity,  $A$  is the pre-exponential factor in the Arrhenius equation and  $Q$  is the fuel mass per volume multiplied with the reaction enthalpy.  $E_n$  is expressed as:

$$E_n = \frac{E}{RT_a} \quad (3)$$

where  $E$  is the activation energy.

The laminar flame speed of a fuel is indicative for its propensity to ignite from a hot spot. This propensity is expressed through  $r_f$  [73].

$$\frac{r_f}{\delta} = \exp\left(\frac{\beta}{2} \left(1 - \frac{1}{Le}\right)\right) \quad (4)$$

where  $\delta$  is the laminar flame thickness,  $Le$  is the Lewis number and  $\beta$  is the Zeldovich number.

$$\beta = E(T_b - T_u)/RT_b^2 \quad (5)$$

where  $T_b$  and  $T_u$  are the burned and unburned gas temperatures. The laminar flame thickness is expressed as the kinematic viscosity divided with the laminar flame speed  $S_L$ .

$$\delta = \nu/S_L \quad (6)$$

A larger laminar flame thickness should decrease the propensity of a fuel to initiate a flame.

The rate at which combustion occurs after pre-ignition is dictated by the laminar flame speed and wrinkling from turbulence. An increased flame speed can consume the unburned gases faster, leaving less time for autoignition to occur. Furthermore, the turbulence may dissipate radicals and thermal inhomogeneities at hotspots, retarding autoignition. On the other hand, a higher flame speed increases the heat release rate, which increases the heating of end-gases and promotes autoignition [75].

## 2.3. Autoignition

For almost a century, the resistance of a fuel to undergo autoignition has been represented by its Research Octane Number (RON), Motor Octane Number (MON), Anti-knock Index (AKI) and Octane Sensitivity (OS), where AKI is the average and OS is the difference of RON and MON. MON is operated at a higher temperature and speed than RON [76]. These indicators are derived empirically using PRFs in a Cooperative Fuel Research (CFR) engine, which is based on specifications from the 1920s [77]. Modern turbocharged, GDI engines operate on significantly lower temperature trajectories as compared to MON tests, and thereby MON correlates rather poorly with real-world performance. The compression-profile is closer to that of a RON measurement and even beyond it [78,79].

Autoignition occurs as a result of a chain of reactions, resulting in a rapid rise in OH and CH radical concentrations, pressure and temperature. Therefore, generally the IDT in homogeneous reactors is defined as the time taken to achieve local maximum for one of these metrics. The IDT varies strongly based on the molecular structure of the fuel.

Depending on the fuel's structure, IDT can decrease with increasing temperature or in some cases an increase of IDT is observed with an increase in temperature. This anomaly, where even at lower temperatures ignition propensity is increased, is known as NTC. The NTC behavior occurs due to a specific kind of branching reactions where two OH radicals are produced from one. This is referred as low-temperature chemistry and is common in fuels having long carbon chains. The understanding of the elementary reactions that govern autoignition and low-temperature combustion has been developing over decades and a detailed information can be found in the study of Cai et al. [80]. Lubricants consist of long carbon chain components, and therefore can be emulated by chemically reactive long chain alkane surrogates. IQT studies have reported that the total IDT reduces significantly when the injected fuel is diluted with even a small amount of lubricant oil [29,30].

End-gas autoignition after pre-ignition has been detected both close to the cylinder wall and ahead of the pre-ignited flame front [81]. The magnitude of pressure oscillation after autoignition is given as its Knock Intensity (KI). This quantity can be expressed as maximum value, integrated or derived values. A description and comparison of various approaches in terms of signal-to-noise ratio for conventional knocking are provided in [82]. Methods used in super-knock studies include the integral of the high-pass filtered pressure signal with respect to CAD [83] and the difference between minimum and maximum values from the knock signal, which was defined by subtracting a three-point averaged value from the pressure curve [84].

The development to super-knock is partly dictated by several stochastic factors. Previous studies have shown that the probabilities for very high knock intensity and maximum pressure tend to increase if Start of Combustion (SOC) occurs significantly before the spark timing and Start of Knock (SOK) occurs close to TDC, but heavy variation can be found in the peak pressure between LSPI cycles with the same SOC or SOK [83,85,86]. In addition, the average peak pressure of LSPI cycles reached a plateau when SOC occurred earlier than 10 CAD BTDC [87]. Furthermore, the knock intensity was weakly correlated to the thermal conditions and burned mass fraction during knock onset [83].

## 2.4. Development to detonation

The final step to super-knock is the detonation of unburned end-gases. An illustration of this process is shown in Fig. 7.

A combination of global and local phenomena dictates the outcome of an engine cycle. Global phenomena, which can be controlled and measured during steady-state experiments, include the trapped mass, mean values of the cylinder pressure and mixture stoichiometry, Exhaust Gas Recirculation (EGR) rate and tumble ratio. Local phenomena on the other hand include several stochastic factors, such as turbulent flow and variations in temperature, pressure and mixture homogeneity. Their spatial and temporal scales can be very small, within the range of micrometers to millimeters and few microseconds to a few CAD. The combination of these global and local phenomena lead to cyclic combustion variability [88].

Unlike experimental setups, certain modeling approaches capture the impact of local phenomena. Robert et al. [89] used a reactive and compressible Large Eddy Simulation (LES) solver for simulating knock formation for 15 cycles of different spark timings. The spark was therefore used as a substitute for the pre-ignition initiation. They noticed that when advancing the spark timing from 8 CAD ATDC, the knock intensity would initially increase proportionally to the mass burned by autoignition. At the earliest spark timings at TDC and 4 CAD BTDC, a transition to detonation would begin, leading to a much higher knock intensity. They highlight that the use of Reynolds-averaged Navier-Stokes (RANS) simulations poses a challenge due to the sporadic nature of super-knock cycles [89].

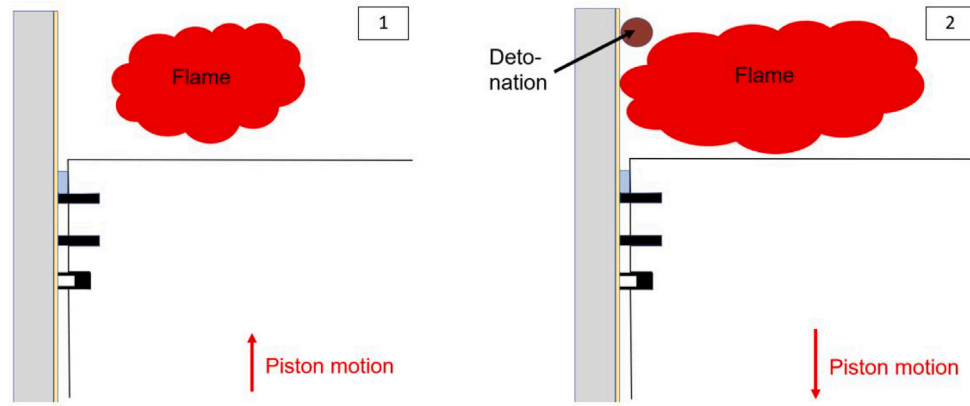


Fig. 7. Illustration of detonation formation.

#### 2.4.1. Propagation modes of autoignition reaction fronts

The classification of propagation modes after autoignition was presented by Zeldovich [90] as follows:

- $u > D_{CJ} > a$ : Propagation of a weak detonation wave.
- $D_{CJ} \geq u > a$ : Detonation with a compressing shock wave.
- $a > u > u_f$ : Subsonic propagation.
- $u_f > u$ : Flame development generated by diffusion and heat conduction.

where  $D_{CJ}$  is the Chapman–Jouguet detonation velocity:

$$D_{CJ} = \sqrt{2(\gamma^2 - 1)Q_d} \quad (7)$$

where  $\gamma$  is the ratio of specific heats and  $Q_d$  is the heat release from a unit of mixture mass [89]. The propagation modes can be plotted into a detonation peninsula expressed with two dimensionless parameters,  $\xi$  and  $\varepsilon$  [4].  $\xi$  expresses the inverse ratio of reaction wave velocity  $u$  to the acoustic velocity  $a$ .

$$\xi = a/u \quad (8)$$

The reaction wave velocity is inversely proportional to the gradient of IDT with respect to the distance  $r$  from the center of a hotspot.

$$u = \left( \frac{\partial \tau_i}{\partial r} \right)^{-1} \quad (9)$$

This can be rewritten with the IDT sensitivity and temperature gradient:

$$u = \left( \frac{\partial \tau_i}{\partial T} \times \frac{\partial T}{\partial r} \right)^{-1} \quad (10)$$

One can notice that a reduced sensitivity of the IDT to temperature and increased thermal homogeneity increase the reaction wave velocity and reduces the value of  $\xi$ . Thus, the propagation can approach characteristics of thermal explosion. However, at slow velocities the process is enhanced by shock waves and heat transfer. Spontaneous propagation occupies the regime between the point of homogeneous combustion and Chapman–Jouguet (CJ) point on the detonation adiabat. The CJ point is the minimum velocity of a steady spontaneous wave [91]. This part of the detonation adiabat corresponds to weak detonations.

The parameter  $\xi$  is used to classify the propagation modes.

- Thermal explosion:  $\xi = 0$
- Supersonic autoignitive wave:  $\xi_l > \xi > 0$
- Developing detonation:  $\xi_u > \xi \geq \xi_l$
- Subsonic autoignitive deflagration:  $a/SL > \xi \geq \xi_u$
- Subsonic laminar burning:  $\xi \geq a/S_L$

The lower and upper limits for developing detonation,  $\xi_l$  and  $\xi_u$  can be plotted against the dimensionless parameter  $\varepsilon$  [92].

$$\varepsilon = \frac{r_0}{a \times \tau_e} \quad (11)$$

where  $r_0$  denotes the initial hotspot radius and  $\tau_e$  is the excitation time. The initial hotspot radius  $r_0$  and thermal gradient ( $\partial T/\partial r$ ) in Eq. (10) can be approximated in computational studies. Values of 5 mm and 1 cm have been used for the radius [73,89], while values between  $-1$  and  $-2$  K/mm have been used for the gradient [73,93]. The hotspot temperature at autoignition was estimated by Rudloff et al. [94] by adjusting the hotspot temperature at intake valve closure (IVC) for reaching unity with the Livengood–Wu integral during autoignition. However, also in this case, the temperature gradient requires that the hotspot radius is assumed.

Peters et al. [95] has proposed a turbulence theory based on dissipation elements, each of which are limited to the gradient trajectories between a local minimum and maximum temperature. The joint probability density of temperature gradients and their lengths could then be used to calculate the detonation probability at each cell of an engine CFD model.

The excitation time refers to the period, during which the chemical energy in the hotspot is mostly released. This time, often calculated as the period when the heat release rises from 5% to its maximum is very short, generally in the order of microseconds [89,96–98]. This value has been simulated to decrease with increasing pressure and temperature for dimethyl ether (DME) and various gasoline surrogates [98,99].

In a completely homogeneous mixture, ignition would occur simultaneously throughout the mixture, causing constant-volume combustion and a uniform rise in pressure. Complete homogeneity is virtually impossible, due to the inevitable spatial and temporal variations of temperature and mixture homogeneity that emerge from charge stratification, residual gases and heat transfer at the walls [4].

Quasi-homogeneous conditions with very low gradients can, however, cause extremely rapid reaction wave propagation beyond the Chapman–Jouguet conditions, thus exhibiting no coupling between the shock wave and reaction wave as a thermal explosion [100]. The rapid combustion does not allow the burnt gases to expand, resulting in a fast and smooth pressure rise, and is attractive for combustion applications, due to the significant improvement in efficiency that it offers. Hence, its use in both internal combustion engines and gas turbines is studied in the forms of homogeneous charge compression ignition (HCCI) and shockless explosion combustion (SEC) [93,101]. Both of these concepts are challenging to execute homogeneously, largely due to the inevitable thermal or mixture stratification in HCCI and the varying residence time of the injected fuel in SEC [102,103]. The need for optimal SEC has driven research in fuel tailoring, in which the purpose is to find suitable fuels that exhibit very small IDT sensitivities to temperatures

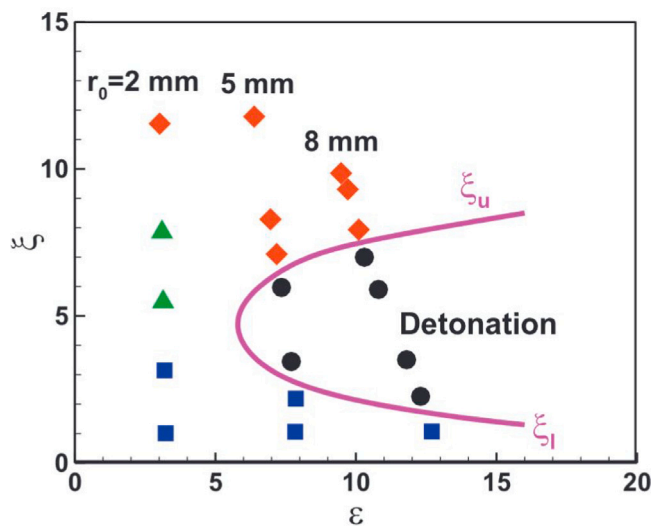


Fig. 8. Regions of propagation modes for dimethyl ether and air at 982 K and 40.5 bar. Black circles: Detonation; blue squares: supersonic autoignition reaction wave; green triangles: transonic regime; red diamonds: subsonic deflagration. Source: Reprinted from [97].

for a wide range. Given a vanishing sensitivity for temperature or proper mixture stratification, quasi-homogeneous combustion could be reached despite inhomogeneities in the gas temperature [93,99].

As the parameter  $\epsilon$  approaches zero, the combustion process inside the hotspot becomes isobaric. In contrary, an approach towards infinity indicates isochoric combustion leading to isentropic expansion [96]. A coupling of the reaction and sonic wave occurs when the distance traveled by the sound during the excitation time is lower than the distance of the constant temperature gradient in the hotspot. Therefore, long excitation times have been desired for detonation prevention [99]. It has been shown for various fuels that  $\xi_u$ , which is the limit between subsonic deflagration and developing detonation, increases for higher values of  $\epsilon$ , translating to larger initial hotspot size and shorter excitation times. This is visible in Fig. 8 for a DME/air mixture at 982 K and 40.5 bar.

The shape of this detonation peninsula seems to be fuel-dependent, but the detonation regime generally becomes wider for an increase in  $\epsilon$ , as shown for syngas [4],  $\text{CH}_4$  [104], TRF [105] and Hydrogen [106] in various 1-d simulations. Consequently, fuel blends that exhibit a slow rise in heat release during the excitation period are attractive for detonation prevention. For instance, an investigation by Vinkeloe et al. [93] revealed that a substitution of  $\text{H}_2$  with  $\text{CH}_4$  in DME-containing stoichiometric ternary blends slows down the excitation time at 33 bars. The boundaries of developing detonation for DME were determined by Dai et al. [97], showing a C-shaped curve that becomes narrower as the hotspot temperature increases from 802 K (before NTC) to 982 K (NTC) and 1035 K (after NTC) at 40.5 bar. Their results indicate that the initial temperature and its related chemistry and energy density are factors in the limits of propagation modes.

As a result of mass and thermal diffusion within the hotspot, the reaction wave velocity has been reported to differ from the one that was calculated from initial conditions. Thus, a modification of  $\xi$  was used by Dai et al. [107] and Dai et al. [108].  $\xi_u$  is based on the sound speed at  $r_0/2$  and the average reaction wave speed within the hotspot.

Both Robert et al. [89] and Zhang et al. [109] concluded in their simulations that a detonation can be triggered by pressure waves that were created by other hotspots. This was observed by Blumenthal et al. [110] in a shock tube. LES simulations by Pan et al. [111] showed that several adjacent autoigniting hotspots can merge and yield a developing detonation. The merging of flame kernels leading to a transition to detonation between the flame and the end-wall was observed by Blumenthal et al. [110] in a shock tube.

#### 2.4.2. Detonation induction from reflected shock waves

Both experimental studies using rapid compression machines and constant volume combustion bombs have observed shock wave reflection induced detonation near the wall. A series of schlieren images at an initial pressure of 5 bar taken by [112] showed that the rapidly accelerating hydrogen flame creates a shock wave, which reflects first at the right-side wall and the left-side perforated plate before autoignition and detonation close to the Chapman–Jouguet point occurring at the third reflection. Zhang et al. [109] showed detonation with 2d-simulations of stoichiometric hydrogen combustion when strong pressure waves reflected at the end-wall.

Similar development is illustrated in Fig. 9 (cases a and b). Wang et al. [113,114] and Liu et al. [115] ignited an iso-octane flame with a spark in an RCM, causing autoignition in the compressed end-gases and the generation of a shock wave, which reflects on the cylinder wall and triggers detonation. Meanwhile, when 80% excess air was added (case c), the detonation was avoided and a supersonic autoignitive wave occurred instead.

It is reported that the shock wave intensifies prior to detonation [113]. The intensification depends on the interaction between primary and secondary flames and shock waves, as shown in a numerical study of  $\text{H}_2/\text{O}_2$  mixtures by Xu et al. [116]. As the initially smooth deflagration interacts with the oscillating shock wave, the flame surface becomes distorted and larger, accelerating it, increasing flow velocity and mass and heat transfer to the unburned region. A significantly cooler secondary flame is generated, resulting in deceleration, which may be momentarily enhanced by the flow from the reflected shock wave traveling in the opposite direction. The oncoming shock wave also heats up the region between the primary and secondary flames, which increases reactivity and intensifies the shock wave. The outcome of these regular interactions between flame regions and shock waves is an intensifying primary shock wave and the formation of secondary shock waves that are generated from the enhanced chemical reactions after the primary shock wave. The coupling of one of these shock waves cause a developing detonation [116].

Chamber geometry can affect the formation of developing detonation, as it dictates the convergence of shock waves. The shock waves travel both in a radial and axial direction of the chamber, converging with each other, subsequently initiating detonation [116].

#### 2.5. Oscillation modes and damage

In addition, the severity and locations of damage caused by detonation waves can be attributed to different modes of convergence. Experimental and numerical results by Xu et al. [117] indicate that the most intense energy convergence occurs as a result of simultaneous convergence of axial and radial waves at the middle of the chamber. Meanwhile, the intensity of energy convergence of a radial wave at the edges could be damped by ensuring enough clearance to avoid vertices.

Whereas conventional knock is often characterized by low-intensive pressure pulses and gradual wear on hardware, a single super-knock cycle may cause abrupt engine failure. Studies have reported pressure wave amplitudes beyond 160 bar [118]. The amplitude reduces throughout the power stroke. Only a minor deviance in exhaust pressure was detected between normal cycles and pre-ignition cycles with high peak pressures [119]. Various types of damage have been reported by authors, including a broken spark plug electrode, melted exhaust valve (caused by fragment from the electrode being stuck between the valve and seat), eroded piston crown and cylinder head and fractured piston ring land [13,83,120]. An example of broken piston ring lands is shown in Fig. 10. Damage on piston rings includes various degrees of coating deterioration, such as chipping, cracking and a widespread loss of the coating material [121].

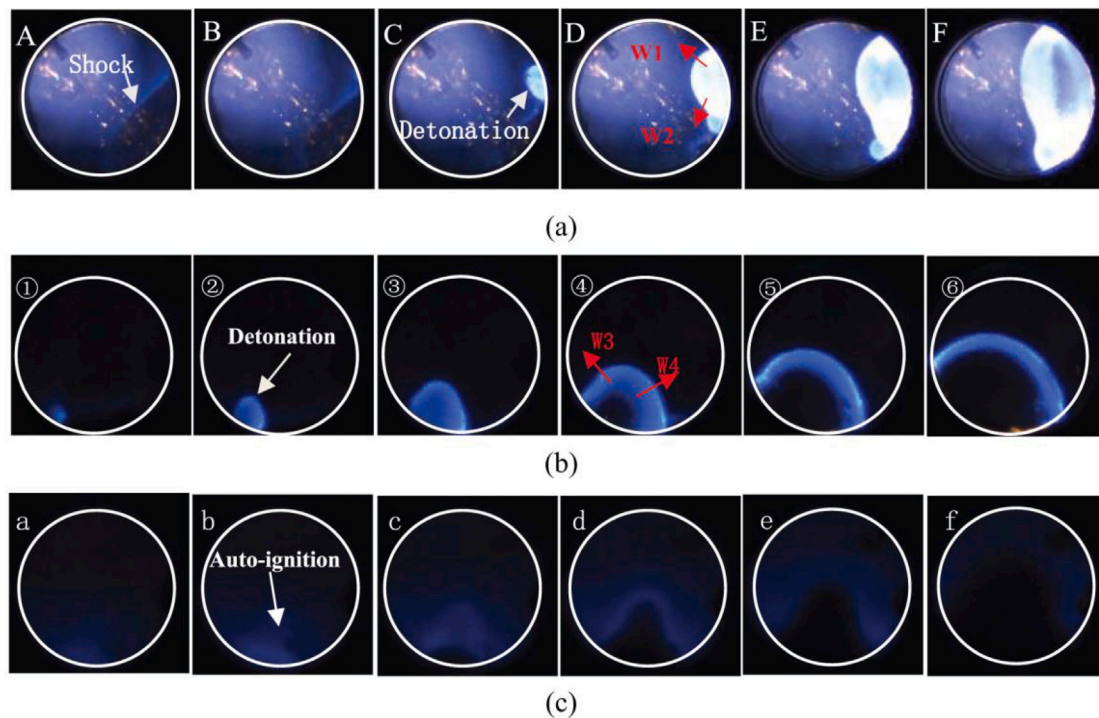


Fig. 9. Combustion modes of iso-octane after autoignition. (a)  $\lambda = 1.0$  (b)  $\lambda = 1.6$  (c)  $\lambda = 1.8$ . Source: Reprinted from [115].



Fig. 10. Damage caused by super-knock to piston ring lands.

### 3. Methodology in research

#### 3.1. Steady-state experiments

The most common method for studying LSPI is to use steady-state engine operation with short health check intervals between the test segments of high loads and low speeds. Both single-cylinder research engines and multi-cylinder commercial engines are widely used in research.

An overview of 71 experimental gasoline pre-ignition investigations in this literature review revealed that the most common investigated

range is within 1500–2000 rpm. Four publications by Southwest Research Institute included measurements at 1250 rpm [8,9,25,122], whereas high-speed (> 4000 rpm) experiments on surface-induced pre-ignition have been published by Sasaki et al. [50,54], Cavina et al. [53, 55] and Mogi et al. [51]. It is also possible to adopt an externally driven charger for reaching boost pressures and loads above those of commercial turbocharged engines [123]. It is common to disconnect the positive crankcase ventilation (PCV) to eliminate the potential impact of oil mist recirculation from the crankcase into the intake air [59,61,124,125].

A piezoelectric sensor is installed through the cylinder head for high-resolution pressure measurements. A high resolution (up to 0.1

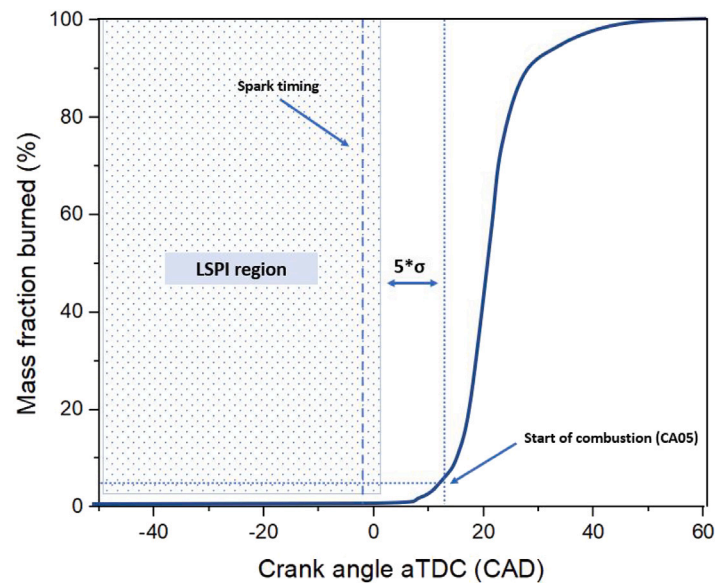


Fig. 11. Illustration of LSPI detection based on a CA05 SOC and  $5\sigma$  margin [127].

CAD) of data sampling is recommended at pre-ignition relevant timings (i.e., from the earliest expected SOC to the middle of the power stroke). A high-pass filter with cutoff frequency at 4 kHz was applied in Zhou et al. [118] for canceling out in-cylinder noise. The frequency of knocking after pre-ignition can exceed 20 kHz as it shifts upwards from conventional knock [126].

### 3.1.1. Statistical analysis

An LSPI event is identified if the pressure curve-derived SOC of a cycle occurs significantly before the mean SOC of all cycles during testing. A suitable margin, such as 5 standard deviations of the SOC, is applied to exclude spark-initiated cycles with abnormally early SOC. Therefore, as illustrated in Fig. 11, it is possible that pre-ignition is detected after the spark timing, as the SOC of an ordinary cycle occurs several CAD after the spark. However, super-knock is unlikely to occur after such late pre-ignition, due to the thermal conditions of end-gases being similar to those of ordinary cycles [85].

The definition of a positive pre-ignition cycle is based on the assumption that the SOC data is normally distributed (skew = 0 and kurtosis = 3). Experimental data can deviate from this assumption, and thus, false positive or negative events are possible without adjustments. The required standard score (e.g.,  $-5$  as suggested above) for a normal distribution can be transformed into an adjusted standard score for a non-normal distribution (skew  $\neq 0$  and kurtosis  $\neq 3$ ) with a method presented in Boese et al. [128] and Fleishman [129]. The method has its limitations if the distribution is heavily skewed or platykurtic (kurtosis  $< 3$ ).

As will be shown in Section 4.3.5, the engine aging and switching between engines affects the LSPI rates in a complicated manner. Thus, it is motivated to stabilize the engine as in [130] before LSPI tests of fuels and lubricants and to normalize the LSPI count to account for differences between engine hours and setups using reference tests [131, 132].

LSPI and super-knock may occur in consecutive or alternating series, as shown by Dahnz et al. [60], who noticed that up to 75% of pre-ignitions occurred in groups of two to seven cycles. The alternating series of LSPI and super-knock have been found by several other authors [119,133,134]. This indicates a dependency between events, thus distorting the statistical reliability of the results. An example of an LSPI/super-knock sequence is shown in Fig. 12. Statistical reliability can be improved by separating independent events from following events in the data post-processing with a determined number of dependent cycles [61,135,136].

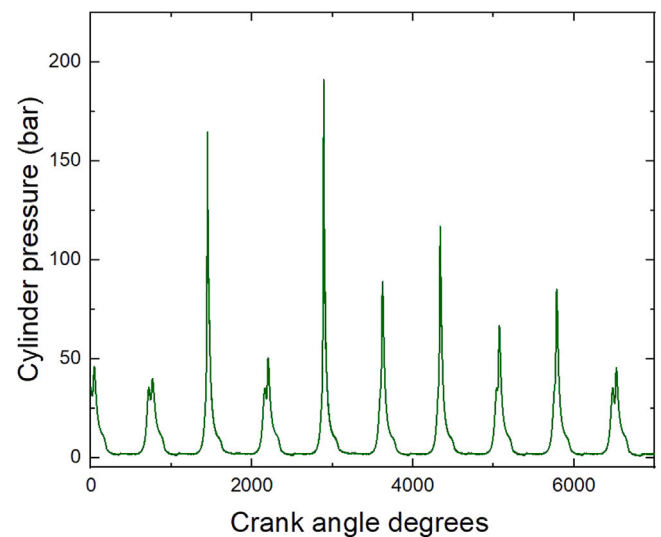


Fig. 12. Example of an LSPI/super-knock sequence.

### 3.1.2. Detection methods

Kaul et al. [137] used time-delay embedding of cylinder pressure and principal component analysis, detecting pre-ignition from a deviation in the cylinder pressure trajectory up to 1.6 CAD earlier than could be identified through direct statistical analysis of the pressure data. However, this approach would also require cylinder pressure as available data during operation.

Fast flame ionization detection was applied by Haenel et al. [138], showing that a peak in total hydrocarbon emissions would occur before an LSPI cycle. This motivated researchers to develop an early-warning and prevention system with ion current sensors in the exhaust system [139]. The method was deemed inadequate as no correlation between hydrocarbon emissions and the ion signal was found. In addition, several authors report a spike in emissions after the LSPI event. Kar et al. [72] found a spike in particulate mass after an LSPI cycle, but without a corresponding rise in particulate number, indicating that quite large particulates have been formed. Magar et al. [42] detected increased oil emissions after pre-ignition with a mass spectrometer, while Moriyoshi et al. [140] measured increased oil consumption after

pre-ignition with a sulfur analyzer. A wide-band  $O_2$  sensor at the exhaust port revealed a spike in exhaust gas richness after an LSPI cycle, more so than a simulated cycle with heavily advanced spark timing [9]. These results support the conclusion that an LSPI event combusts and releases deposits or liquid droplets inside the cylinder.

A bandpass filtered AC ion signal inside the cylinder was utilized for detecting a pre-ignited flame during its propagation. The early detection of a pre-ignited flame would then allow to mitigate the knock intensity through immediate enrichment [139]. Kumano et al. [141] could detect pre-ignition cycles with the integral of the ion signal intensity. Tong et al. [142] found that the ion current signal inside the combustion chamber provides a robust replacement for the pressure trace SOC detection and that bandpass filtering or the integral of the signal provides good correlation with the knock signal from the engine's knock sensor. A pre-ignition cycle with heavy knocking could be identified through the ion current signal, as the amplitude was an order of magnitude higher compared to normal cycles [143]. Reliable detection of LSPI with this method becomes difficult if it occurs close to the spark timing as the flame has less time to reach the detector. This was apparent in one test sequence by Wang et al. [144], where only 14.3% of LSPI cycles were detected due to them occurring relatively late. Deep learning models were used to detect pre-ignition from pre-processed exhaust backpressure and lambda sensor input, returning an 85% accuracy in detecting pre-ignition cycles in a test set of 44,290 cycles, 350 of which were pre-ignition cycles [145].

### 3.1.3. Glowplug measurements

Various studies have examined the propensity of fuels to undergo surface ignition by deliberately causing a hotspot with a glowplug. The resistance of a fuel against this type of pre-ignition would then be characterized as a minimum value in glowplug temperature or electrical energy for achieving a certain frequency of LSPI. The higher this value, commonly denoted as a glowplug pre-ignition temperature index or pre-ignition rating, becomes, the less prone the gaseous mixture is to pre-ignition from a hot object. A description of a glowplug test setup and precautions is given by Yu et al. [12]. They highlight that a feedback control of the tip temperature with power reduction after pre-ignition is crucial in order to avoid runaway ignition and maintain statistical reliability.

## 3.2. On-road experiments

Generally, pre-ignition is studied at 1500–2000 rpm for steady-state conditions, but positive cycles have also been reported for transient conditions at 3000–4000 rpm [146]. Moriyoshi et al. [140] found that transient operation would be more prone to pre-ignition than steady-state operation.

On-road measurements provide important data on the incidence of LSPI in the real-world operation. However, the transient conditions demand changing spark timings, complicating the statistical analysis. Positive cycles may then be detected by setting threshold values for the SOC or peak pressure and individually analyzing the cycles that exceed them [146]. Alternatively, super-knock cycles may be detected through the lambda sensor, if the ECU responds to LSPI with enrichment [147].

Since the on-road testing is affected by surrounding traffic and the selected route, there will be differences in the time spent at LSPI-relevant conditions. This effect may be mitigated by detecting an LSPI-prone region in the operating conditions and normalizing the results with respect to the time spent within that region [147]. While on-road testing provides information on the tendency of pre-ignition to occur in transient operation, its utility in fuel, lubricant and engine parameter testing is challenging due to the large number of variables that it introduces.

## 4. Parametric studies

### 4.1. Impact of fuel parameters on LSPI

Researched factors of the fuel impact on LSPI can be divided into two categories, these being the chemical composition and physical properties. Research on chemical composition has been largely concentrated on ethanol and aromatics. Meanwhile, laminar flame speed, volatility and HoV are relevant physical properties, as they should describe the formation of initiation mechanisms or the ignition susceptibility of the mixture.

#### 4.1.1. Octane rating

Steady-state experiments have generated no significant correlations between RON, MON and LSPI frequencies [66,148,149]. One would expect that fuel autoignition chemistry affects LSPI as the gasoline comprises a fraction of the droplet composition and ambient gas mixture before pre-ignition. The slower ignition of suspended PRF-oil droplets with ambient air at 573 K was evident with higher RON of the PRF blend [150]. However, constant volume combustion chamber studies at this temperature showed a diminishing impact of the RON of a oil–fuel droplet on the total IDT at chamber air pressures above 20 bar [151].

A high autoignition resistance is provided by branched aromatics, iso-paraffins and ethanol. Aromatics generally exhibit very high RONs, largely depending on the number and location of alkyl groups. Moreover, ethanol, for which some studies have revealed an LSPI promoting impact at high concentrations, exhibits a high autoignition resistance, as estimates vary at RON108–128 and MON90–93 [152,153]. As will be shown in Section 4.1.3, especially aromatics can severely enhance pre-ignition through fuel wall wetting and top ring zone retention, which dominate over potential benefits from octane numbers.

An increased octane number however allows for advanced spark timing, thus reducing the time available for pre-ignition. The advanced knock limit improves the load, which can be compensated with a reduction in boost pressure. This indirect benefit of increased RON explains the slight reduction in LSPI when comparing RON91, RON95 and RON98 fuels with rather similar distillation curves [7]. Furthermore, the autoignition resistance appears to be influential if the common causes for LSPI are diminished. This was shown by applying a narrow fuel injection spray targeting for reduced wall wetting, while increasing  $p_{in}$  until pre-ignition would occur [56]. It became apparent through simulations and optical studies at high  $p_{in}$  and intake temperature ( $T_{in}$ ) that fuels of relatively low autoignition resistance, including RON95E0, RON95E10 and iso-octane, would exhibit bulk autoignition, whereas some autoignition resistant alcohols and ketones would not. Even in this case, the resulting correlation between RON and the critical  $p_{in}$  for 0.1% LSPI frequency was rather modest ( $R^2 = 0.63$ ). In the case of surface ignition at 4400 rpm, the MON correlated well to the required spark-plug center electrode temperature for pre-ignition, whereas at 1600 rpm, RON showed a better correlation [50,54].

#### 4.1.2. Laminar flame speed

As previously mentioned in Section 2.2, the laminar flame speed is related to the susceptibility of a fuel to exhibit a stable flame. Budak et al. [154] reported no correlation between  $1/S_L$  at 1 bar and 120 °C and required glowplug temperature for 2% LSPI frequency. Meanwhile, Kalghatgi & Bradley [73] presented a significant correlation ( $R^2 = 0.83$ ) between  $1/S_L$  at 3.04 bar and 450 K and the required electric power in a heated coil for pre-ignition, using data of 15 paraffins, olefins, naphthenes, aromatics and alcohols from [155,156]. Variation in the estimated laminar flame speed had no clear effect on steady-state LSPI frequencies in Jatana et al. [136]. However, their results indicated that higher flame speeds could advance the SOC, reduce the delay time between SOC and peak pressure and increase the knock intensity.

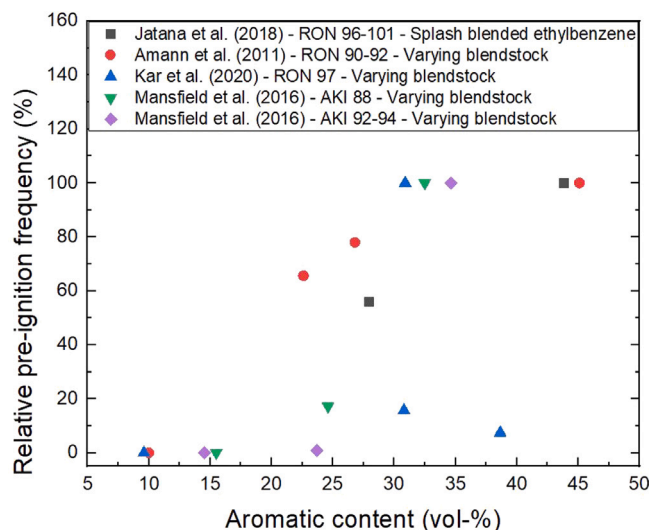


Fig. 13. Effect of aromatic content on pre-ignition frequency. Frequency calculated from total pre-ignition cycles (including following cycles) and data obtained from [9, 72,136,158].

#### 4.1.3. Altering the chemical composition

The general view in literature is that high aromatic content and less volatile gasoline composition (i.e., the end third of the distillation curve) are the key properties in gasoline that increase LSPI [9,65, 67,72,136,149,157–159]. Fig. 13 shows the increasing trend in pre-ignition from aromatic content, as the lowest relative frequencies were found for volume fractions below 20%. Meanwhile, the highest relative frequencies were found for volume fractions above 30%. An exception for the trend is visible in the data by Kar et al. [72], where the highest frequency was obtained for 30.9 vol-%, whereas a fraction of 38.7 vol-% yielded much less pre-ignition. However, this can be explained by an opposite order in C10+ aromatics (19.9 vol-% and 5.1 vol-%). Thus, future analysis on the impact of aromatics should be broken down to the numbers and lengths of their alkyl groups.

Heavier aromatics, with boiling points ranging up to 193 °C of 4-tert-butyltoluene [160], are prone to deposit formation [45]. The inherent correlation between aromatics and the upper half of the distillation curve was pointed out by both Swarts et al. [70] and Tanaka et al. [161], as is the particular relevance of C9+ aromatics [72]. Using a modern engine, Sethi et al. [162] showed that aromatic-rich fuels did not stand out as more susceptible to pre-ignition than saturates and olefins, albeit the lack of distillation properties limits the analysis of their relative impact.

Costanzo et al. [66] showed by supplementing a premium certification fuel with 30% of alternative components that the pre-ignition frequency increases rapidly as the boiling point of a component exceeds 130 °C. The substitution shifts the distillation curve of the gasoline and in the case of an aromatic substance with a single ethyl or propyl group or multiple methyl groups (such as ethylbenzene, cumene and trimethylbenzene) the upper half of distillation points will increase and more liquid fuel will remain on the oil film and top ring zone. The importance of the upper half of the distillation range was also visible in a comparison between pure toluene (110 °C) and diisobutylene (104 °C) and a premium certification gasoline. A refinery-based gasoline extends its upper half of distillation from these temperatures to approximately 200 °C, making it more prone to LSPI. These less volatile components not only enhance the fuel impingement but also reduce the evaporation of the impinged fuel from the liner leading to more fuel being collected in the top ring zone [67].

The distillation points T50–T80 in refinery-based gasoline have been repeatedly shown as important factors for LSPI mitigation [59,64,69,

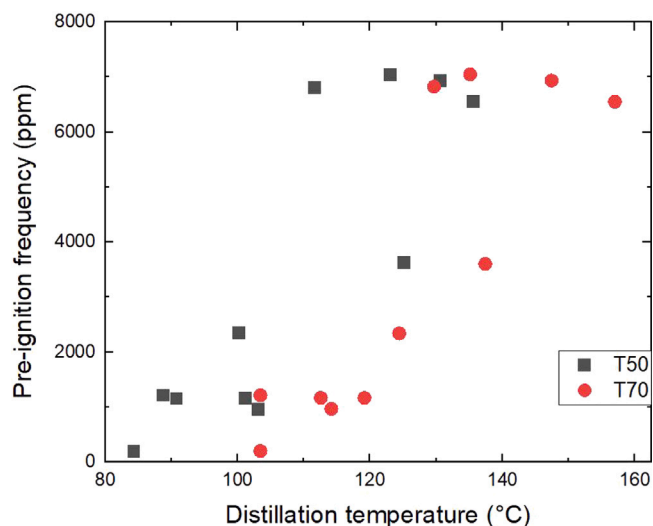


Fig. 14. Effect of distillation temperatures T50 and T70 on pre-ignition frequency. Source: Data obtained from [148].

148,149]. Fig. 14 presents results from Chapman et al. [148] for the impact of T50 and T70.

The significance of T90, T95 and final boiling point is more challenging to infer as results vary from no correlation [69,148] to moderate and good correlations [86,163,164]. Kocsis et al. [149] found a slight increasing impact from T90 on LSPI. Meanwhile, an increase of the V150 (vaporized fraction at 150 °C) reduces pre-ignition [164].

Jatana et al. [136] studied the effect of cyclopentanone, 2-methyl-1-butanol and ethylbenzene on LSPI by blending them in 25 wt% quantities in the same gasoline blendstock. The results show that the addition of the assessed compounds generated roughly double the LSPI events compared to the reference gasoline through reduced vaporization. The added compounds generated roughly the same amount of LSPI events, despite their different physical and chemical properties. They conclude that the physical properties (volatility and HoV) of the gasoline blends could explain the LSPI event counts, while the LSPI characteristics are differentiated by the chemical/kinetic properties of the gasoline blends.

Analysis beyond the LSPI frequencies is useful to determine the relative impacts of the volatility and autoignition chemistry of pure fuels on the formation of LSPI. Deliberate injection of an oil droplet into different port-injected gasoline compositions revealed that the SOC occurs earlier with increased aromatic and olefin content and decreased paraffin content for constant RON. This observation was only detected for oil injection before 50 CAD BTDC, but does nevertheless indicate that the promoting impact of aromatic species is not only restricted to their high boiling points [165]. Glowplug measurements have not been able to explain the enhancing role of aromatics, as several of them, including xylene, toluene and 1,2,4-trimethylbenzene, turned out to be more resistant towards ignition than cycloalkanes, olefins or oxygenates [166,167].

Crevice accumulation is not only dictated by the fuel impingement on the liner. Investigations of fuel dilution by Colomer et al. [67] and Splitter et al. [68] were conducted using LIF in vicinity to the dry oil sump. The analysis revealed that the dilution of relatively volatile iso-octane (boiling point at 99 °C) can at some engine conditions, especially at those of late injection, be significant. The region of engine conditions where iso-octane causes fuel dilution also exhibited a high ratio of ambient pressure to vapor pressure of the fuel.

In addition to fuel wall wetting, the retention of the fuel in the top ring zone is critical for LSPI. The LSPI experiments by Colomer et al. [67] included three gasoline compositions, two of which had almost the same fractions of saturates, olefins and aromatics but different

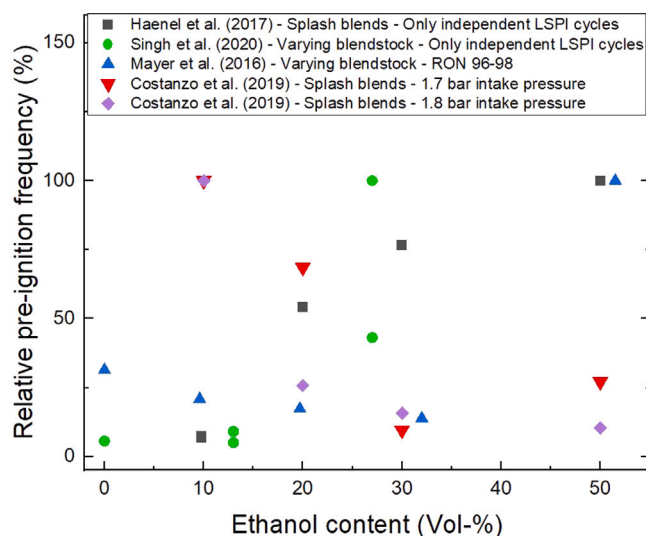


Fig. 15. Effect of ethanol content on pre-ignition frequency.  
Source: Data obtained from [66,138,157,164].

distillation curves. The heavier of these two saturate-rich fuels had a distillation curve close to the third fuel, which contained less saturates and more aromatics. Combined analysis of fuel dilution in oil through LIF and the need for excess fueling to maintain stoichiometric exhaust lambda revealed that although a volatile fuel with low distillation temperatures could at late injection increase fuel dilution, its impact on fueling was low as the impinged fuel evaporates instead of being retained at the liner or top ring zone. Meanwhile, the aromatic-rich fuel required excess fueling due to top ring zone retention, and in this case the pre-ignition count would increase accordingly at late SOI. The saturate-rich fuel with high distillation temperatures caused fuel retention and pre-ignition values between those of the volatile and aromatic-rich fuels.

The impacts of ethanol addition on pre-ignition in engines for various studies are presented in Fig. 15. Singh et al. [157] studied the effect of ethanol on the LSPI by experimenting with five different gasolines with 0 vol-%, 13 vol-% and 27 vol-% ethanol content. The study concluded that the addition of ethanol increases LSPI. However, the ethanol additions were made on different hydrocarbon gasoline blendstocks. Haenel et al. [138] also noticed the increased amount of LSPI events with increasing ethanol content using a regular E10 gasoline as a blendstock/reference to which desired amount of ethanol was splash blended. The LSPI density was shown to increase from the E10 base level 271/292 ppm to 2167 ppm, 3063 ppm and 4000 ppm with E20, E30 and E50 gasoline, respectively [138]. A slight promoting effect of ethanol was also reported by Kocsis et al. [149].

It is considered that the impact of ethanol on LSPI is heavily dictated by mixture preparation. The injected volume of ethanol as compared to gasoline is high, and thus the duration of injection is long, enhancing the impingement on walls and the piston crown. In addition, it creates a significant charge cooling effect on surrounding gases. This can be beneficial for LSPI mitigation by delaying ignition through lower mixture temperatures, but may also lead to postponed evaporation during injection and increased impingement and interaction with oil on cylinder walls. The switch in weight between these effects may be the reasons for heavy variation in LSPI in Mayer et al. [164], which showed a mitigating impact within the range 0%–30%, but a sharp rise within 30%–50%. The mitigating effect of ethanol when aiming for high pre-ignition frequencies with direct injection is shown in Günther et al. [168] and Pischinger et al. [169]. The authors applied high temperature and pressure intake conditions and heavily retarded combustion phasing to trigger gas-phase pre-ignition at a relatively

high frequency. Splash blended E20 would have similar IDTs as E85 and E100, but the latter blends would be more resistant against pre-ignition. This can be attributed to the charge cooling as the increase in pre-ignition resistance was not as distinct with Port Fuel Injection (PFI) at high  $T_{in}$ . The E20, having a higher RON and charge cooling effect, was more resistant than splash blended ETBE20 for both direct injection and PFI. The approach for direct injection was continued by Ottenwälder et al. [56], in which wall wetting and glow ignition were further counteracted, resulting in a very good resistance from ethanol against LSPI. Moreover, Costanzo et al. [66] reported a mitigating effect when increasing splash blended ethanol content from 10 to 50 %. They used a newly formulated, more LSPI-resistant lubricant and the liner temperature was suspected to be higher than in referred studies, in which case the fuel–oil interaction should have less of an effect on pre-ignition rates. Amann et al. [9] reported that the addition of 10 mass-% ethanol with varying blendstock reduces the number of independent LSPI events, but the number of cycles per LSPI cluster would increase at the baseline conditions.

The charge cooling effect of a fuel depends on its injected mass and heat of vaporization and may affect both the formation of pre-ignition mechanisms and the propensity of a fuel to autoignite. Using the narrow spray strategy for avoidance of wall wetting, Ottenwälder et al. [56] found that the specific heat of vaporization ( $\text{kJ}/\text{kg}_{\text{air}}$ ) would correlate with the critical  $p_{in}$  for pre-ignition with  $R^2 = 0.56$ , deriving a mitigating effect.

The study by Ottenwälder et al. [56] (at  $T_{in} = 100$  °C) showed that ketones and alcohols required a much higher critical  $p_{in}$  ( $> 3.0$  bar) for achieving 0.1% LSPI frequency than RON95E0, RON95E10 and iso-octane ( $< 2.0$  bar). Particularly good resistances were shown by 2-butanone and ethanol, which did not reach 0.1% even when the  $p_{in}$  was increased to the maximum available value of 3.65 bar. Furthermore, it became apparent through optical imaging that the pre-ignition of conventional fuels occurred more on the exhaust side, presumably due to a higher heat transfer from the walls to the mixture. Simulations of the thermal conditions and the scattered locations of pre-ignition indicate that bulk gas autoignition would be the source in this case. Meanwhile, the pre-ignition sites of 2-methylfuran, iso-butanol and 1-propanol would be concentrated at the spark plug, thus indicating glow ignition [56]. An increase in ethanol content in certification gasoline caused a reduction in glowplug temperature at up to 50 vol-% for direct injection and 20 w-% for PFI [66,166]. In the contrary, splash blended E20, M20 and ETBE20 with RON95 base fuel were more resistant to glowplug ignition than RON95E0, whereas fuels with even higher ethanol content, i.e., E85 and E100, were less resistant to glowplug ignition than E20 [169]. The impact of ethanol addition on glowplug temperature index could thus be a balance between increased charge cooling with direct injection (leading to increased heat transfer from the boundary layer to the cooler mixture) and an increased ignition tendency at high-temperatures. The good performances of 2-butanone and iso-propanol are apparent when comparing glowplug temperatures with ethanol [154,166,169].

Paraffins were shown to quench LSPI when compared to aromatics, olefins and ethanol [149]. Steady-state results for olefinic compounds have not yet indicated such a strong promoting effect of olefins on LSPI as in the case with aromatics. Kocsis et al. [149] found a slightly mitigating impact of them, as opposed to the enhancement from aromatics. Mansfield et al. [135] compared the fits of different regression models with varying mathematical forms and fuel components as independent variables using experimental results from ten “US regular octane” commercial fuels. The best performing fit was attributed to an exponential function with the sum of the volumetric shares of olefins and aromatics as variables. However, the relative importance of olefins was not determined due to a limited dataset.

#### 4.1.4. Additives

Nomura et al. [170] studied the effect of methylcyclopentadienyl manganese tricarbonyl (MMT) on the LSPI propensity. The addition of 15 ppm of MMT increased the number of LSPI events with at least 160 bar peak pressures for all the tested gasoline grades, and the biggest change was from 2 events/h to over 40 events/h. The gasolines with LSPI increasing factors, i.e. high aromatic content and low volatility, reacted more strongly to the addition of MMT. The MMT was hypothesized to generate small incandescent manganese oxide particles in the combustion chamber upon the oxidation/burning of the manganese complex compound. These particles then act as the ignition source for the fuel to generate LSPI.

The effect of gasoline detergent additive on the LSPI was assessed by Zahdeh et al. [7]. The used detergent additive package contained a kerosene type solvent according to the supplier. Although the content of the high boiling detergent package solvent was below 0.4% of the whole gasoline blend it was shown to increase the LSPI events over two-fold compared to unadditized reference fuel. The result highlights how big of an impact the small but very harmful fractions in the gasoline might have regarding the LSPI count. Although typically the detergent packages are used in the level hundreds of ppm (in volume), the high boiling components in the package alters the end distillation properties that favors the LSPI phenomenon. Chapman et al. [87] varied the concentrations of three detergent chemistries, finding that the number of LSPI cycles would exceed those of an unadditized gasoline when any of the detergents were blended at a treat rate of 5 times the Top Tier gasoline specifications.

Meanwhile, it was shown by Joedicke et al. [171] that a unadditized fuel would increase the injection duration at 19 bar BMEP and 1500 rpm due to injector tip deposit formation, also leading to an increase in cycles with peak pressures exceeding 100 bar. Colliou et al. [65] reported a slightly decreasing trend in LSPI when using 1000 ppm of a deposit control additive in an extended test. The aforementioned studies indicate that the detergent has potential to both promote and mitigate LSPI. Firstly, it counteracts injector fouling and deposit buildup, decreasing the formation of LSPI precursors. Secondly, similarly to the used gasoline, the heavy hydrocarbon composition of the detergent package enhances LSPI, especially if used above normal treat rates. The latter of these effects is assumed to dominate in Zahdeh et al. [7] as no cleaning effect was noticed. However, the detailed assessment of the effect of detergent additives (or any other organic additives) is challenging as there are multiple additive suppliers with their own additive packages and formulations, which typically are not disclosed to the public. In this regard the detailed evaluation of the detergent would require samples, detailed information of the additives and close collaboration with the additive suppliers.

#### 4.2. Impact of oil parameters on LSPI

Studies show that oil additive properties strongly affect LSPI formation. The base oil is treated with various additives including detergents, antiwear additives, soot dispersants, viscosity improvers, oxidation inhibitors, corrosion inhibitors, friction modifiers, pour point depressants, foam inhibitors and metal deactivators [172]. The detergent is often highlighted as a strong influencer on LSPI. Another important factor is the ratio of antiwear additives due to their mitigating effect on LSPI.

Literature does not indicate a significant impact from additives beyond detergents and antiwear additives. This was shown in Kassai et al. [163], Ritchie et al. [173] and Takeuchi et al. [174] for poly-methacrylate or olefin copolymer viscosity index improvers, dispersant molecular weights, phenolic, aminic or sulfurized ester antioxidants or glycerol monooleate as a friction modifier. However, an increased dispersant treat rate was proven beneficial in Fletcher et al. [131].

#### 4.2.1. Viscosity, volatility and base oil properties

Experiments concerning base oil properties have concentrated on the effect of the API group. It is reported that higher groups (III and IV) of base oils exhibit higher derived cetane numbers and lower total IDTs than lower groups (I and II) when mixed with gasoline or iso-octane in IQT measurements [29,175]. This impact is also apparent in ignition measurements of oil in constant-pressure air flow at 50 bar and below 800 K, whereas at higher temperatures the difference is reduced [176]. The higher reactivity of group III as compared to groups I and II is attributed to the increased content of saturates and decreasing content of aromatics [29,175,177]. Surprisingly, Takeuchi et al. [174] found a decreasing trend in LSPI frequency with increasing base oil group, as groups III and IV (polyalphaolefin) exhibited lower LSPI frequencies than groups I and II when using the same additive package. Therefore, LSPI behavior has not yet been explained through base oil reactivity, albeit additional investigations would be desirable.

As fuel-oil interaction, droplet detachment and vaporization are generally considered as steps for LSPI, it is reasonable to study the impacts of viscosity and volatility. Volatility shows no significant effect on LSPI propensity. Takeuchi et al. [174] compared Noack volatilities ranging 5–25% and found a very weak correlation. In addition, Kocsis et al. [122] found no consistent trend from increased volatility as it varied by detergent composition.

The effort to achieve lower fuel consumption and emissions has included the introduction of thinner engine oils to the market. IDT measurements at high-temperature atmospheric conditions in a co-flow burner show slightly increased tendency of autoignition for lower viscosity [178]. This impact was also noticed with deliberate injection of oil droplets into the cylinder [37].

Andrews et al. [132] showed a statistically significant increase in LSPI with higher KV100 viscosity of the oil. Furthermore, Takeuchi et al. [174] found higher rates for a polyalphaolefin with 8 cSt than one with 4 cSt KV100. Ritchie et al. [173] did not find statistical significance when comparing SAE grades 0W-16, 0W-30, 10W-30, despite the slight decreasing trend in LSPI in this order. Moreover, no clear impact of SAE grades of synthetic oils was detected by Teng et al. [133] or Kubach et al. [61]. The impact of viscosity index was not deemed significant in Andrews et al. [132], whereas in Magar et al. [42] the addition of a viscosity improver to a 0W-40 lubricant for increased viscosity would reduce LSPI.

The results indicate that the reduction in oil viscosity does not cause a clear impact on the formation of LSPI. Variations in oil temperature or viscosity caused no clear effect on oil release rates from the piston crevice and crown during motored operation [19,179]. LIF measurements of a GDI spray showed slightly enhanced fuel deposition for a more viscous oil film at 70 bar injection pressure, but a reversed trend at 150 bar [180].

#### 4.2.2. Detergent additives

The detergents are composed of a polar head group containing an anionic functional group associated with a metal cation (mainly Ca<sup>2+</sup> and Mg<sup>2+</sup>) and a hydrocarbon tail. The purposes of metallic detergents in lubricants include suspending insoluble combustion products, mitigating corrosion through neutralization of acidic products from combustion and oil oxidation (in the case of overbased detergents) and maintain a proper antiwear and friction performance [181].

The harmful impact of calcium in detergents was already addressed in the early 1970s as part of a study on deposit-initiated pre-ignition [182]. The promoting effect has since then been confirmed by several other studies [20,64,119,122,131,163,173,174,183–186]. The steep increase in LSPI for a calcium content between 1000 and 2500 ppm is visible in Fig. 16.

The only exception to our knowledge was shown in [187] where the LSPI activity was kept virtually the same, despite the calcium content varying more than an order of magnitude. In this case, the load was maintained at a moderate level (13 bar IMEPg) contrary to

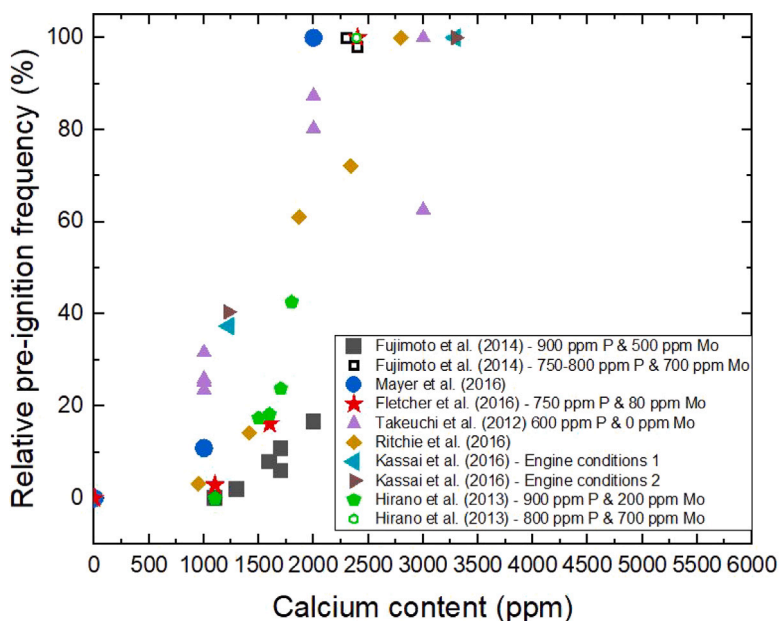


Fig. 16. Effect of calcium content in oil detergents on pre-ignition frequency. Hollow symbols indicate a change in phosphorus and molybdenum content. The highest frequency for each dataset has a relative frequency of 100%. Data obtained from [20,131,163,173,174,183,184]. Only independent LSPI cycles counted in [20,163].

the near maximum load that is normally used in lubricant-related LSPI studies. This may suggest that the impact of calcium is biased towards higher engine conditions, especially as the same study showed that the increased calcium content would promote LSPI at 16 bar IMEPg.

The functional group of the calcium additive may vary between sulfanate, phenate, salicylate and calixarene [188]. No significant differences on LSPI have been noticed between the three former options [131,163,173,174]. No significant impact has been attributed to the change in total base number [174] or the alkylate backbone type [173]. A typical calcium content of oils that have not been formulated for LSPI mitigation is over 2000 ppm and a replacement of half of the content with an LSPI-neutral detergent additive would decrease LSPI significantly.

Interestingly, it is widely reported that a partial or complete substitution of calcium for magnesium suppresses the formation of LSPI [72, 122,131,147,163,173,184,189,190]. In fact, magnesium appears to be neutral (Fig. 17) to pre-ignition frequencies, despite overbased magnesium sulfonate being beneficial for increasing total base number [131]. A magnesium detergent was also beneficial for reaching sufficient anti-rust performance [189].

The magnesium may be added to the detergent either as a sulfonate or salicylate, the latter of which performed better in a silicone rubber compatibility test [191]. It was shown by Kaneko et al. [192] that carbonate containing micelles from overbased magnesium sulfonate would deteriorate the poly-phosphate tribolayer and inhibit MoS<sub>2</sub> formation, thus also counteracting the friction reduction provided by Molybdenum Dithio Carbamate (MoDTC) and Zinc Dialkyl Dithio Phosphate (ZnDTP). The increase in friction coefficients in the boundary and thin film regimes for an all magnesium formulation was reported in Gupta et al. [190], which was also reflected in deteriorated fuel economy as compared to an all calcium formulation. The friction performance was improved by adopting a borated dispersant [192].

Corresponding studies with other metals have shown promising effects, such as in the case of potassium [193]. A partial substitution of calcium with lithium also showed benefits, whereas experiments by Ritchie et al. [173], Kassai et al. [163] and Fletcher et al. [131] indicate that sodium in the detergent promotes LSPI, likely even more than calcium. Deliberate injection of sodium sulfonate containing oil lead to slightly earlier SOC than a base oil [165].

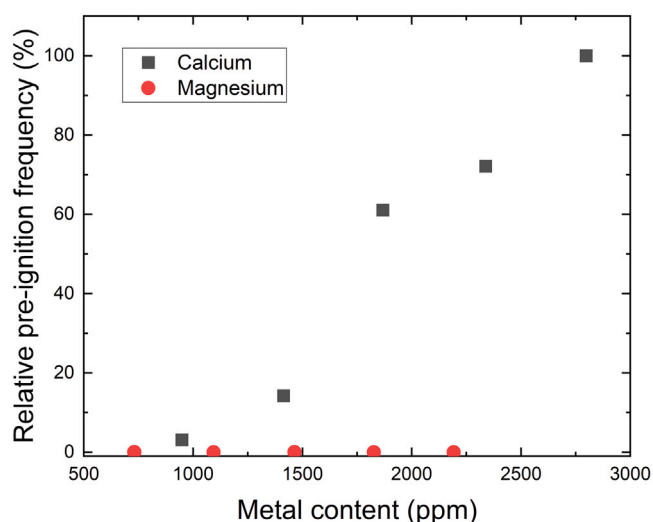


Fig. 17. Effect of calcium (sulfonate) and magnesium content on pre-ignition frequency in single-metal detergents.

Source: Data obtained from [173].

#### 4.2.3. Friction modifiers and antiwear additives

Molybdenum as an anti-oxidant or as the friction modifier Molybdenum Dithio Carbamate (MoDTC) and the antiwear additive Zinc Dialkyl Dithio Phosphate (ZnDTP) have been identified as quenchers of LSPI [163,173,174,183,184]. An ashless antioxidant also showed promising results in [159]. The impact of molybdenum is shown in Fig. 18.

The phosphorus content is reported to dominate over the zinc content in mitigating LSPI [131], whereas increasing the alkyl length in ZnDTP showed slight but no statistically significant increase in LSPI [173]. ZnDTP may produced using differently structured alcohols and a ZnDTP produced with a secondary alcohol would be more effective against LSPI than one made with a primary alcohol [131].

ZnDTP and MoDTC have multifunctional purposes, as they not only provide friction and wear protection but also function as antioxidants. ZnDTP stabilizes highly reactive radicals and peroxides,

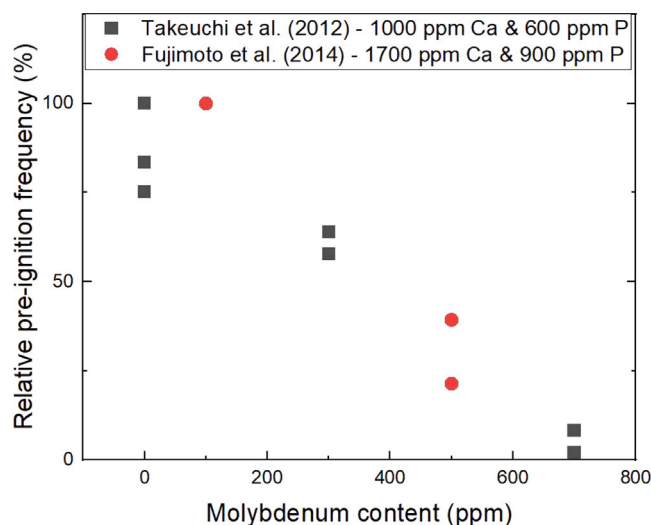


Fig. 18. Impact of Molybdenum content on pre-ignition.  
Source: Data obtained from [174,183].

which possibly counteracts pre-ignition [20,184,194]. The addition of MoDTC and ZnDTC to ZnDTP exhibit synergy in friction and antioxidant performance [195,196]. Phosphorus can cause poisoning of catalytic converters. These limitations and interdependencies show the importance of finding a proper balance between additives.

Titanium was highlighted for its antiwear and friction performance [197]. In addition, 800–1000 ppm of titanium has been shown to effectively mitigate LSPI for an all calcium oil formulation [190,198].

#### 4.2.4. Oil aging, contamination and dilution

Oil-related experiments are mainly conducted with fresh lubricants. However, several experiments within recent years have extended the test matrix to include aged oil as well. In addition to a change in physical properties from fuel dilution, the long duration at engine conditions reduces the total base number. Typically, the aging process includes hundreds of hours of engine operation, but alternative methods, where the oil is oxidized at elevated temperatures in the presence of a catalyst, have also been used [175,176].

Oil aging can show a promoting trend on LSPI. Hirano et al. [20] aged the same Mo-containing oil for 30,000 km in two different cars, finding that one three-folded the LSPI frequency as compared to a fresh oil, whereas the other did not degrade LSPI performance. In fact, it was shown that the number of events would elevate after 50–100 h of operation [20,146,162] (Fig. 19). The authors repeated LSPI testing with a fresh oil after the aging study and noticed less pre-ignitions than during the peaks at 50–100 h of aging. The pre-ignition frequencies decreased in some cases as the aging continued beyond 100 h.

Little research has concentrated on the combined effects of oil formulations and aging. The benefits of magnesium appear to hold throughout aging [147,198], whereas the mitigating impacts from molybdenum and titanium deteriorated (Fig. 20).

In Haenel et al. [185], a 10,000 miles aged LSPI-resistant formulation showed twice as many independent pre-ignition events as compared to a fresh one. In this case, both magnesium and molybdenum were included in the additive package. Swarts et al. [199] did not find any evidence of oil aging during single 12-hour steady-state engine tests for LSPI.

No significant change in Derived Cetane Numbers (DCN) was attributed to the oxidation of a Ca-containing 0W-30 lubricant [175]. Constant-pressure ignition measurements, in which 100 h aged and 144 h oxidized group I and III oils with API SN Plus additive package showed slightly slower ignition as compared to fresh oils [176]. However, engine wear can introduce Fe and Cu into the oil and thereby aged

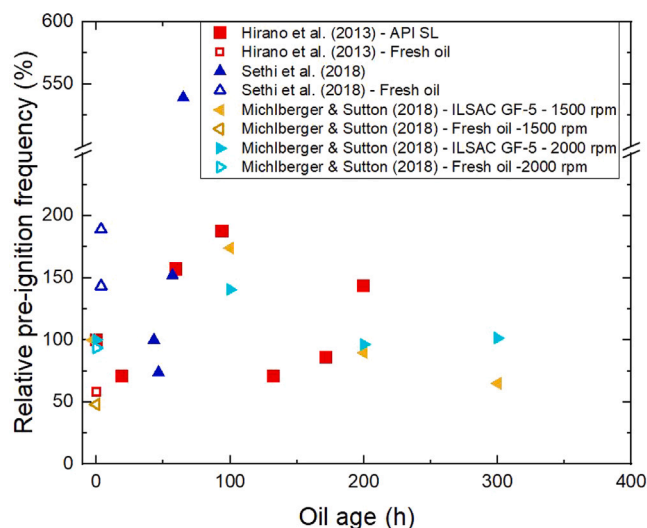


Fig. 19. Impact of oil aging on pre-ignition. Results normalized to the frequency of the first test of each oil. Hollow symbols represent results for fresh oils tested after the aged oils. Data obtained from [20,146,162]. Only independent cycles counted in [162].

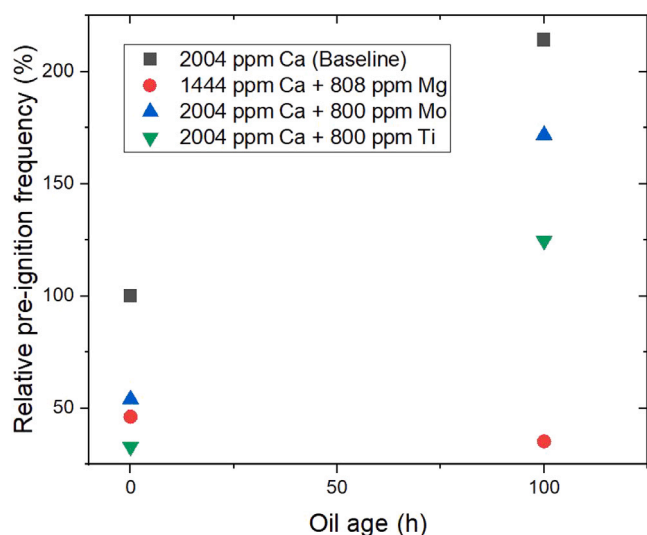


Fig. 20. Impact of oil aging on pre-ignition for four different formulations. Frequency normalized to a fresh baseline oil formulation and corrected for engine effects using reference tests and linear interpolation for engine hours.  
Source: Data obtained from [198].

oil contained more of these metals than a fresh oil [162]. A manual increment of these metals as naphthenates into the oil promoted LSPI both for a low and mid-level calcium content [20].

Engine runs at LSPI conditions can cause significantly increased fuel dilution, which affects the physical properties of the oil. In fact, only 50,000 cycles of LSPI conditions with a commercial engine caused enough dilution (9%) to reduce the KV100 of fresh oil by 42%, almost covering the viscosity difference between fresh 5W-30 and 15W-50 oils [61]. Still, the global dilution levels (without aging and fuel added directly to the oil pan) do not show a significant change in pre-ignition counts [185]. This further indicates that a reduction in oil viscosity has no clear trend on the outcome, as already stated in Section 4.2.1. The role of the fuel and oil interaction is thus limited to increased crevice accumulation and potential chemical effects prior to ignition.

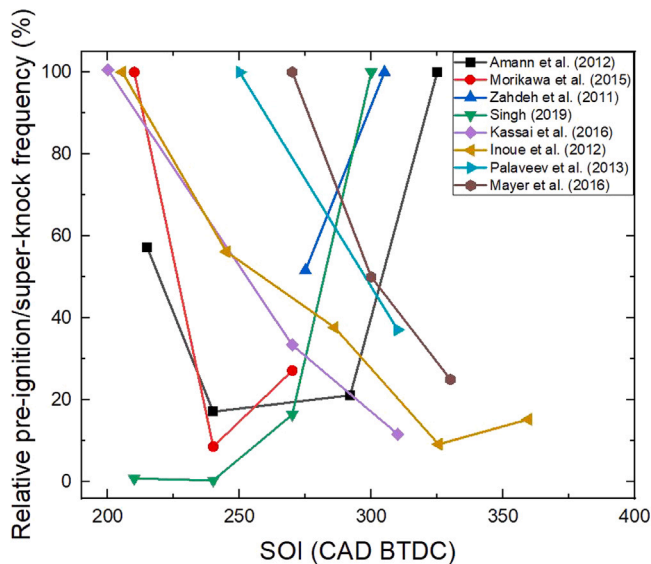


Fig. 21. Impact of SOI on pre-ignition or super-knock frequency (only super-knock cycles counted in [125]). Data obtained from [7,28,59,119,125,163,200,202]. Independent pre-ignition cycles counted in [28,119,163].

### 4.3. Impact of engine parameters on LSPI

#### 4.3.1. Injection strategy

The benefits of GDI over other injection technologies comprise reduced mixture temperatures due to in-cylinder evaporation and increased flexibility in injection timing and mixture homogeneity. As the fuel-wall interactions are an important step for the formation of deposits and release of fuel-oil droplets, one should consider the effects of different injections strategies, including fuel pressure, injection targeting and timing, on LSPI.

Amann et al. [28] showed that the lowest number of pre-ignition events would result for SOI between 292 and 240 CAD BTDC, with higher occurrence at SOI before or after this interval. An SOI of 240 CAD BTDC was also found to be optimal for an intake side-mounted injector in [119], whereas a retardation of SOI to 210 CAD BTDC would deteriorate the LSPI performance more than an advancement. Zahdeh, et al. [7] showed the mitigating influence of SOI at 275 CAD BTDC compared to 305 CAD BTDC for a side-mounted injector, which was targeting the liner. Singh [200] reduced pre-ignition clearly by retarding SOI of a central direct injector past 270 CAD BTDC, which did, however, lower IMEP and increase the Coefficient of Variation (CoV) of IMEP.

Meanwhile, several studies have revealed that pre-ignition increases with the retardation of SOI from 300 CAD BTDC. Kassai et al. [163] and Inoue et al. [125] reported a consistent increase in LSPI and super-knock, respectively, when retarding the SOI for a side-mounted injector from 310 to 200 CAD BTDC. Han et al. [201] shows slightly less pre-ignition for the timing of the first injection (SOI1) in a split injection strategy at 310 CAD BTDC compared to 290 CAD BTDC and 330 CAD BTDC with a 6-hole injector. Intake side-mounted swirl and multihole injectors produced less pre-ignition at 310 CAD BTDC than at 270 and 250 CAD BTDC [59,61]. Mayer et al. [202] found significant increase of the pre-ignition frequency by retarding the SOI. Especially with lateral injector position at early SOI of 330 CAD BTDC strong piston crown wetting occurred, which, however, evaporated rapidly due to the high piston temperatures. Retarding the SOI led to an increased wall wetting by fuel impingement. Overall, it appears that retarded injection risks an increase in pre-ignition, at least when using a side-mounted injector (Fig. 21).

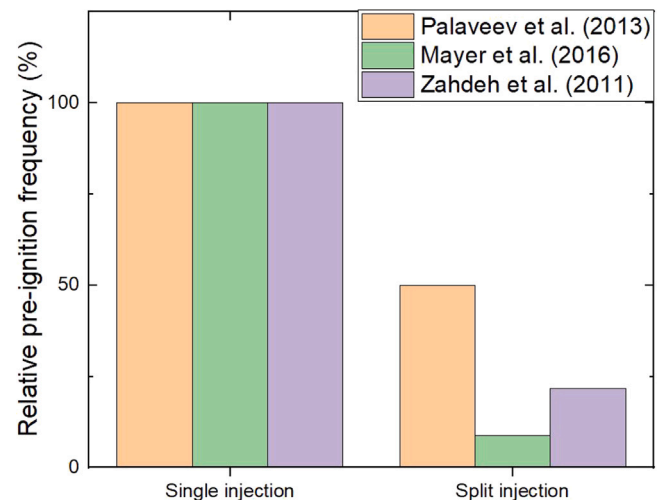


Fig. 22. Effect of split injection on pre-ignition. Source: Data obtained from [7,59,164].

Split injection shows repeatedly benefits. Mayer et al. [164] reduced the pre-ignition propensity of E50 by approximately 90% by changing to split injection with a side-mounted 7-hole injector. Palaveev et al. [59] halved pre-ignition events by switching from single injection at 290 CAD BTDC to a split injection with about 20% of the injected mass close to the spark timing. Zahdeh et al. [7] decreased LSPI by 78% with a transition from single injection at 305 CAD BTDC to optimized split injection. The impacts of split injection strategies on LSPI in these studies are shown in Fig. 22.

Xu et al. [159] found that the pre-ignition frequency can be suppressed to a third of that of single injection by using equally split injection pulses, with the SOI1 maintained at 275 CAD BTDC and end of the second injection at 190 CAD BTDC. A triple injection strategy by Arnold et al. [203] reduced wall wetting by a factor of 5 in CFD simulations as compared to a single injection strategy and almost completely eliminated the occurrence of LSPI in experiments.

Singh et al. [204] applied a split injection strategy for pre-ignition suppression in a turbocharged engine using gasoline in the first pulse, and gasoline, ethanol, methanol or water in the second pulse (which was injected late in the compression stroke). All of these strategies turned out to mitigate pre-ignition as compared to single injection, but late injection of gasoline and the alcohols also decreased IMEP and increased CoV IMEP when the fraction of the second injection was increased. Water injection was beneficial in reducing the pre-ignition count when injected during the intake or compression strokes (charge cooling effect) or late exhaust stroke (quenching pre-ignition precursors) without the compromises on IMEP and CoV IMEP. Furthermore, Singh et al. [205] applied two or three injection pulses for mitigating pre-ignition, while calibrating the SOI and duration of injection to mitigate the compromises on IMEP and combustion instability. They showed that when a small mass of fuel was delivered in the last injection pulse close to TDC, the IMEP and CoV IMEP could be compromised little, while still mitigating pre-ignition as compared to single injection.

A sweep of SOI2 from 183 CAD BTDC to 143 CAD BTDC indicated lower pre-ignition frequency for an earlier second injection in Han et al. [201]. Moreover, an increased fuel ratio of the second injection from 17 to 27 and 40% at 163 CAD BTDC SOI2 lead to more pre-ignition [201]. A CFD model explained this through a higher wall film thickness during the compression stroke. Meanwhile, a sweep of the ratio for the second injection from 37 to 63% revealed the lowest pre-ignition frequency when at least half of the fuel is injected in the second pulse for SOI1 300 CAD BTDC and SOI2 210 CAD BTDC, but the CoV IMEP would increase with a higher fraction of the second injection [205].

Although the current vehicle fleet comprises primarily GDI engine technology and LSPI is often attributed to its related engine parameters, PFI technology can exhibit it [28]. Singh [200] reported that PFI caused only slightly less pre-ignition than a central direct injector, but significantly more as compared to a lateral direct injector. Enhanced impingement is expected when the end of injection is delayed to after intake valve opening (IVO), as was the case in Han et al. [201]. However, in Amann et al. [28], a change from open valve injection to closed valve injection yielded no significant differences in the results.

Injection pressures of GDI systems have been reaching values about one order of magnitude higher than PFI engines to ensure efficient evaporation and homogenization within the limited time available until ignition. An increased injection pressure is critical for better atomization, but the higher momentum also increases the penetration of the spray. Thus, the impact of fuel pressure on pre-ignition is not straightforward, as these factors cause opposing effects on the magnitude of fuel wall impingement. In a study by Liu et al. [180], increased fuel pressure from 70 bar to 150 bar with constant injected mass caused less deposited fuel in the oil in LIF measurements of a GDI spray. LIF measurements in a pressure vessel showed that the reduction in deposited fuel amount with increasing injection pressure is emphasized at boosted pressures [206]. These results can be attributed to a higher incident velocity, which promotes splashing, and enhanced mixing of fuel and air. However, a reduction of the rail pressure from 150 bar to 70 bar reduced LSPI by almost a factor of 10 while using a side-mounted injector with a spray modified to target the opposite wall for liner wetting (SOI 305 CAD BTDC) [7]. Morikawa et al. [119] changed the fuel pressure from 80 bar to 100 and 120 bar and noticed that LSPI frequency was the lowest at 80 bar. Singh et al. [205] studied the IMEP, CoV of IMEP and pre-ignition frequency for three different fuel injection pressures (130, 150 and 170 bar) both for single injection and split injection with a small fraction of fuel injected at SOI2 30 CAD BTDC. The highest fuel injection pressure provided a slightly higher IMEP, but also an increasing trend in pre-ignition.

Injector location and orientation affect spray direction and amount of fuel impingement on cylinder walls. The LSPI occurrence is obviously sensitive to the spray pattern. This was shown in studies by Splitter et al. [187,207], where the centrally-mounted injector was rotated 45–180° to direct the spray towards the wall instead of the spark plug, resulting in following LSPI cycles. This modification would also reduce oil pressure with increased oil dilution [187]. The behavior can be explained through increased fuel impingement, but an increasingly inhomogeneous mixing with air was also indicated. A swirl injector promoted LSPI as compared to a six-hole injector, with an increased droplet number and more concentrated distribution at 180 CAD BTDC [59]. Meanwhile, increasing the bent angle and narrowing the spray of a side-mounted multi-hole injector directed the fuel towards the piston crown instead of the liner, resulting in effective LSPI mitigation [7].

The effect of equivalence ratio on LSPI in gasoline SI engines is not straightforward. For premixed homogeneous mixtures, the IDT tends to increase for leaner mixtures. However, in case of a fuel–oil droplet causing LSPI, the evaporation introduces a locally rich region with higher reactivity than the surrounding mean mixture [208]. Amann et al. [9], Xu et al. [159] and Zahdeh et al. [7] found that the LSPI frequency reduced during fuel enrichment (exhaust  $\lambda=0.8\text{--}0.95$ ), whereas a stoichiometric or slightly lean mixture (exhaust  $\lambda=1.05\text{--}1.1$ ) increases LSPI. Moreover, the detrimental impact of slightly lean operation is apparent in Inoue et al. [125], where a transition from stoichiometric operation to  $\lambda=1.13$  caused a 3-fold increase in super-knock cycles. The benefits of fuel enrichment in GDI and PFI engines were shown by Han et al. [201]. The GDI results are plotted in Fig. 23.

Although it has been shown that fuel enrichment can be favorable in terms of LSPI, continuous enrichment is not desirable due to deteriorated fuel economy. Okada et al. [40] reported that immediate

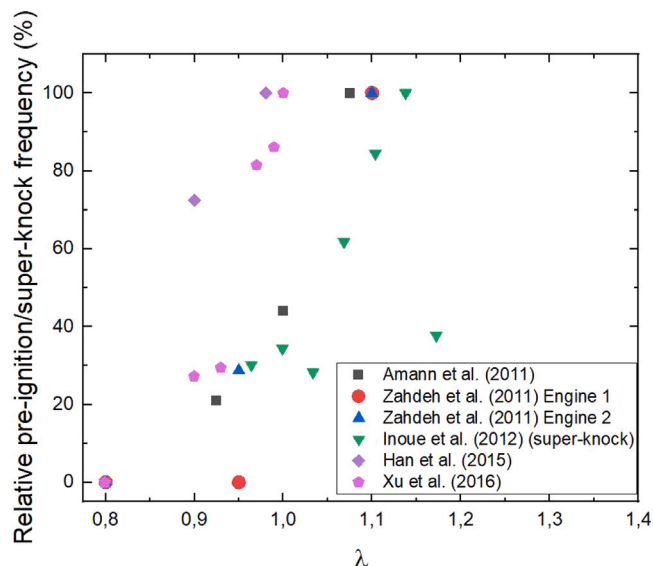


Fig. 23. Impact of  $\lambda$  on pre-ignition (only super-knock cycles counted in [125]). Data obtained from [7,9,125,201]. Independent pre-ignition cycles counted in [9].

enrichment during the normal cycle after an initial LSPI event would almost completely eliminate following LSPI cycles. However, if the enrichment started two cycles after the initial LSPI event, the following LSPI cycle would not be as effectively mitigated. This indicates that the benefits of enrichment are not only attributed to the charge conditions during the compression stroke, but also to the combustion process and exhaust composition of the previous normal cycle.

Pischinger et al. [169] reported a lower thermal threshold for surface ignition when using a RON95E0 gasoline in slightly lean conditions ( $\lambda = 1.1$ ), whereas rich conditions at  $\lambda = 0.7$  (and constant  $p_{in}$ ) would result in an over 50 K glowplug temperature increase (Fig. 24). This can be explained by a reduced cooling effect from decreased GDI fueling and a higher isentropic exponent, leading to increased temperatures at the end of compression. Meanwhile, Yu et al. [12] found that the required glowplug temperature reaches its lowest value at stoichiometric or slightly rich conditions. In this case the engine was equipped with PFI, which should mitigate the charge cooling effect, thus making enrichment less effective.

The mitigating impact of enrichment is presumably due to a combination of the cooling effect and the reduced oxidation of particles that were released during the previous LSPI cycle. It should however be noted that the enrichment increases injection duration and mass, which in turn favor wall wetting. Based on previously mentioned results, the oxygen-deprived conditions and cooler charge from slight enrichment outweigh the negative effect from accumulation of fuel on the oil film. However, enrichment increases fuel consumption and deteriorates catalyst performance, thus limiting its feasibility to only temporary use.

#### 4.3.2. Gas exchange

The scavenging is crucial in eliminating particles after a super-knock cycle and mitigate the risk of following LSPI cycles. This would explain why the number of following LSPI cycles remained low when using an electrically driven supercharged engine (having higher  $p_{in}$  than exhaust pressure) with a large valve overlap, as shown in the work of Kuboyama et al. [15]. In turbocharged engines, the insufficient scavenging has been attributed to LSPI, in particular during super-knock series. These findings are supported by optical investigations showing a high density of particles in the combustion chamber after a pre-ignition event as mentioned in Section 2.1.2. In addition to enhanced removal of initiation mechanisms, the scavenging of residual gases decreases the temperature of unburned gases, thus decreasing the

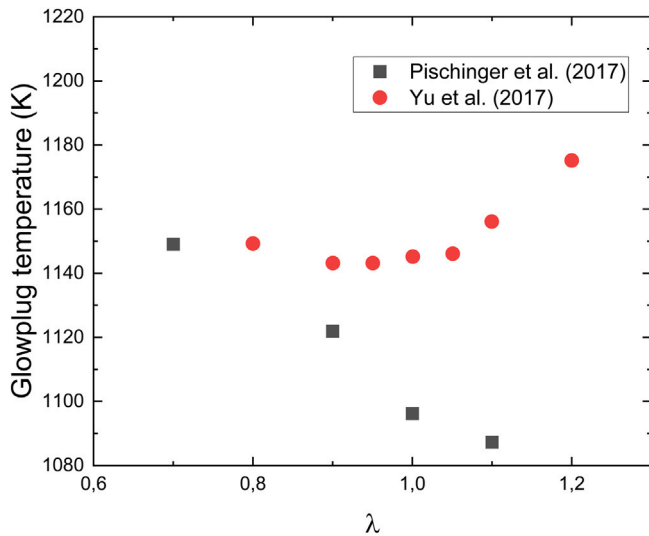


Fig. 24. Impact of  $\lambda$  on glowplug temperature index.  
Source: Data obtained from [12,169].

propensity of surface ignition. This was also reported in the work of Pischinger et al. [169], in which a 10 CAD valve overlap would increase the glowplug temperature by approximately 20 K for a chosen surface-ignition frequency. However, Inoue et al. [125] advanced the intake cam phasing by 30 CAD from a baseline IVO of 390 CAD BTDC and IVC of 174 CAD BTDC, leading to a higher frequency in super-knock with increased valve overlap. Moreover, the increased mass of air bypassing combustion through increased valve overlap makes the exhaust gases lean, which reduces catalyst compatibility [209].

Exhaust back pressure limits turbocharger efficiency and enhances conventional knock, as part of the hot exhaust gases remain in the cylinder [210]. Exhaust back pressure was also shown to enhance LSPI severely in [207]. The exhaust gas residuals increase the polytropic constant, causing higher End of Compression Pressure ( $p_{EOC}$ ) and End of Compression Temperature ( $T_{EOC}$ ) at stoichiometric operation [207]. The quantity of residual gases is dependent on the intake valve timing. At certain timings, the exhaust gas pressure wave from the previous cylinder will reduce the scavenging of residual gases.

Gao et al. [62] detected pre-ignition in misfiring cylinders and the cylinders next and last in the firing order as counted from the misfired cylinder. Moreover, pressure oscillation from the combustion of unburned gases in the exhaust pipe was connected to super-knock in the cylinder that followed in the firing order. This was attributed to the fact that the unburned mixture would burn in the exhaust pipe and can produce pressure waves. The stronger the pressure fluctuation, the higher was also the intensity of knock in the power cylinder.

Singh [200] carried out experiments on the impact of exhaust back pressure on pre-ignition. These experiments were conducted separately for constant  $T_{in}$  (increased  $p_{in}$  with higher back pressure) and constant  $p_{in}$  (lower  $T_{in}$  with higher back pressure). It was shown that pre-ignition was promoted by higher  $T_{in}$  for cases when  $p_{in}$  was higher than exhaust back pressure and the scavenging of precursors is effective. When both exhaust back pressure and  $p_{in}$  are increased, the scavenging is less effective due to the increased back pressure. The temperature near TDC was also calculated to increase in this case. An exponential increase in pre-ignition tendency was then observed (Fig. 25).

The closing of tumble flaps enables increased charge motion. This should reduce fuel impingement on the walls and enhance evaporation, which would explain the reduced pre-ignition events with an intake side-mounted injector [59,61]. Radwan et al. [211] investigated the effect of induction manifold angles on pre-ignition with a Ricardo E6 variable compression engine, equipped with a glowplug. A manifold

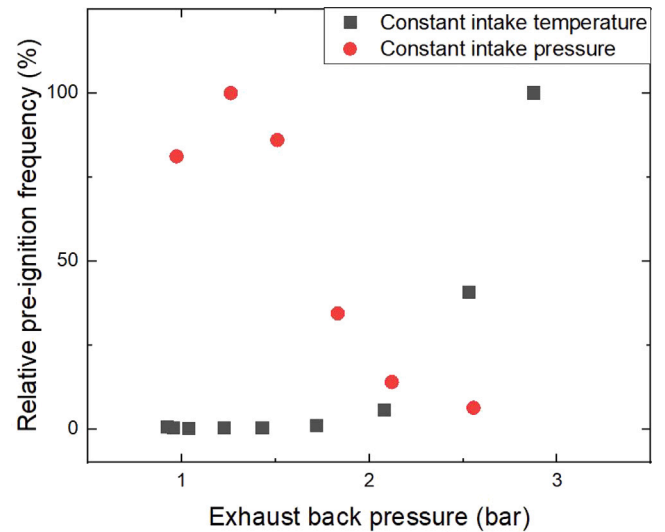


Fig. 25. Pre-ignition count with varying exhaust back pressure, when  $T_{in}$  (squares) and  $p_{in}$  (circles) are kept constant.  
Source: Data obtained from [200].

angle of 40°–50° yielded better surface ignition resistance than 30°, 60° or 90°.

#### 4.3.3. External exhaust gas recirculation

External EGR can be used to advance the knock limit by diluting the unburned mixture with relatively inert exhaust gases from previous cycles. In addition, it offers effective  $\text{NO}_x$  mitigation and exhaust temperature reduction without the fuel consumption increase from mixture enrichment or the degradation of aftertreatment systems during stratified lean burn. EGR may be conducted internally or with a valve-controlled external loop, the latter of which may use a cooler to maintain low temperatures within the intake manifold. Low-pressure EGR is generated by directing a fraction of the post-turbine gases through a cooler to the compressor, and the following improvement in fuel consumption is attributed to the advancing of combustion phasing, low heat transfer and avoidance of rich fueling. This strategy has improved fuel consumption at 2000 rpm and high loads [210,212]. The improvement was reached by advancing CA50 and eliminating the need for overfueling, the latter of which improved fuel consumption significantly as compared to combustion phasing alone [210].

The addition of EGR will contribute to a higher cylinder pressure in order to maintain a high intake air flow. Meanwhile, the rise of in-cylinder temperatures is affected by the change in the ratio of specific heats. EGR offers a lower ratio of specific heats than air. However, as constant equivalence ratio is applied, the addition of EGR also reduces the fractions of fuel-related hydrocarbons, which offer significantly lower heat capacity ratio  $\gamma$  than the gases in EGR. Therefore, the change in end-gas temperature trajectories is limited (and might even increase before start of combustion) when adding EGR, while maintaining a constant value of  $\lambda = 1$  [213].

Considering the aforementioned results, it is unlikely that thermodynamic cooling of unburned gases is behind the suppressive impact of EGR on pre-ignition but rather the quenching of reactions caused by chemical dilution. The mitigating impact of EGR on glowplug ignition was clearly shown [12].

The mitigating effect of cooled EGR on pre-ignition was shown by Zaccardi and Serrano [208] for constant load operation with RON97E5 and advancing combustion phasing through improved Knock-limited Spark Advance (KLSA). Amann et al. [8] reduced LSPI by using low-pressure cooled EGR in moderate levels, while maintaining constant combustion phasing or advancing the spark timing to KLSA. The results

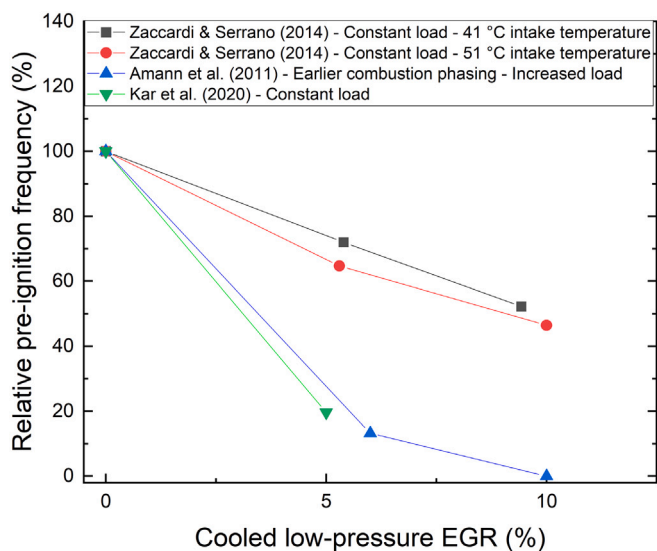


Fig. 26. Impact of low-pressure cooled EGR on pre-ignition frequency. Source: Data obtained from [8,72,208].

in Fig. 26 indicate a consistent reduction in LSPI as the EGR rate approaches 10%.

It should be noted that the increment of EGR may result in promoted deposit buildup. High-load operation at 5% low-pressure cooled EGR would again be beneficial as compared to 0% in terms of LSPI mitigation in Kar et al. [72]. However, the following operation without EGR showed more LSPI than corresponding operation before using EGR. Borescope images revealed significant deposit buildup after the 160,000 cycle EGR operation. Repeating this procedure with an improved oil formulation resulted in no LSPI before, during and after EGR operation, despite the deposit buildup.

The immediate benefits of EGR are comprehensive. Its inhibiting effect on super-knock formation is not only limited to less frequent pre-ignition but also includes the suppressive effect on the knocking itself. The latter effect will be addressed in Section 4.5.2.

#### 4.3.4. Measures to restrict oil transport and carryover

As droplet release from the top land is a pathway to LSPI, measures to mitigate lubricant oil consumption are attractive solutions. Transient engine operation showed that oil that had been accumulated in the crevice was burned during acceleration, resulting in increased oil consumption. Several pre-ignition cycles were detected during steady-state conditions immediately after the acceleration [140]. Increasing the tension of the top ring [42] and the oil control ring [7] resulted in reduced LSPI. Furthermore, increasing the wear resistance of the top ring and conformability of the oil control ring allows for reduced oil consumption and blow-by. Suggestions for improved ring designs were given in Sekarapandian et al. [214], including U-flex oil control rings instead of three-piece oil control rings and double layer physical vapor deposition coating with nitrided steel instead of plasma-coating on the top rings. An improved ring pack with smaller ring gaps and a modified third land reduced both oil consumption and pre-ignition during steady-state tests [140]. However, high-speed camera footage from motored operation suggests that the piston ring gap is a less frequent source for droplet intrusion as compared to the piston crevice or crown [17].

PCV recirculates blow-by gases from the crankcase to the intake manifold. The PCV includes an oil separator, but oil mist may enter the intake manifold. A slightly higher frequency of LSPI was noticed for PCV as compared to open air ventilation in Morikawa et al. [119]. Luo et al. [134] and Inoue et al. [125] reported that the LSPI/super-knock could be lowered with improved oil separator efficiency. No significant impact of the PCV was found in [124].

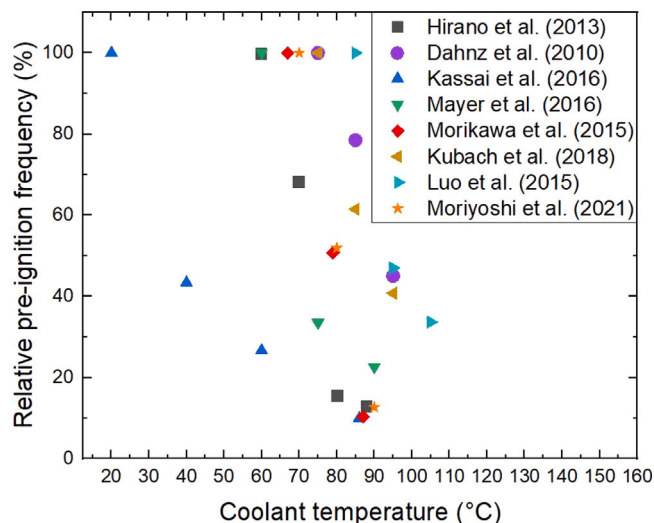


Fig. 27. Impact of coolant temperature on pre-ignition. Data obtained from [20,60,61,119,134,140,163,202]. Only independent LSPI cycles counted in [20,140,163].

#### 4.3.5. Engine aging and cleanliness

A reduction in LSPI activity over multiple tests was ascribed to a gradual deterioration of the engine [199]. This phenomenon was first observed by Andrews et al. [132] and confirmed by Kocsis et al. [149] wherein extended testing on the same engine required an appropriate adjustment to the measured activity to account for the change in severity of the engine. Swarts et al. [199] additionally demonstrated that new engines would undergo a rapid decrease in severity during initial LSPI testing, even after break-in, and would continue to deteriorate, albeit it a slower rate, after this stabilization. The paper also showed that different engines behave differently during the stabilization and stabilized phases and also different from each other, reinforcing the need for continual reference testing to enable quantitative comparisons. A reduction was also noticed by Sethi et al. [162] after approx 200 h and by Michlberger et al. [146] during 76,250 miles of engine operation. Kocsis et al. [149] applied a correction to the measured LSPI events per test to account for not only changes within an engine due to aging, but also differences between different engines of the same type.

Disassembly and cleaning of an existing LSPI test engine revealed no impact on activity, indicating a negligible impact from deposits [130]. Consequently, the reduced activity was attributed to impaired oil transport at the liner resulting from increased wear with a fuel-diluted oil.

#### 4.3.6. Coolant and oil temperature

Increasing the coolant temperature restricts the formation of LSPI precursors. It is directly linked to the surface temperatures of the cylinder, and since a high local temperature improves splashing and the evaporation of the volatile species, both the deposit mass [46] and fuel-oil film thickness during compression will be reduced. The reduction in LSPI from higher coolant temperature has been reported by several studies [7,20,60,61,72,119,134,140,163,202,203,215] and a temperature of 95 °C can be deduced as sufficient (Fig. 27). Hirano et al. [20] and Zahdeh et al. [7] also noticed a simultaneous reduction in crankcase oil dilution and the filter smoke number, respectively. To our knowledge, the only exceptions for reduced pre-ignition with increased coolant temperature was shown by Han et al. [201] and Mounce [216], the former of which noticed a small increase in pre-ignition when changing coolant temperature from 88 to 98 °C with split injection.

Results also suggest that a cooled piston yield higher LSPI counts than high-temperature conditions [7,202]. The improved evaporation

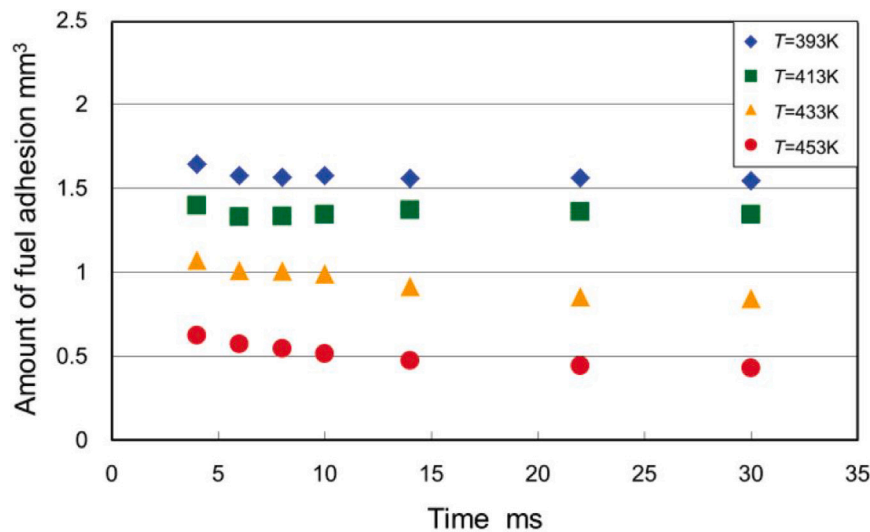


Fig. 28. The amount of fuel adhesion onto a 10  $\mu\text{m}$  oil film for varying wall temperature. LIF measurements of 100 bar injection at 90 mm distance and 70° angle. Source: Reprinted from [217] with permission from SAE.

of fuel was indicated by lower filter smoke number and hydrocarbon emissions [7]. Mounce [216] found that oil temperature was a significant positive determinant for LSPI activity in the range 75 to 95 °C whereas coolant temperature was not significant. On the contrary, a reduction in oil temperature increased LSPI in [202].

The often reported benefits of higher coolant temperatures can be attributed to mitigated fuel adhesion on the oil film and faster evaporation of the volatile species. Fuel adhesion experiments (Fig. 28) with a 100 bar single-hole injection onto a 10  $\mu\text{m}$  oil film by Kouchi et al. [217] show a clear reduction in the amount of fuel on the liner as the wall temperature becomes higher, which was attributed to the Leidenfrost effect.

The impact of wall temperature on fuel–oil film thickness reduction was shown by Zhang et al. [22] using a numerical model with multicomponent fuel and oil formulations that takes into account mass and heat transfer at the fuel–oil film and boundary movement through evaporation (Fig. 29). The fuel film was formed at 100 CAD ATDC and the simulation terminated at 100 CAD BTDC when the upwards traveling piston is assumed to reach the film and collect the mixture into the crevice. One can notice that the initial thickness of the film has a strong impact on the final thickness, more so than the liner temperature and vertical location on the liner (20 to 100 CAD BTDC). However, for a 20  $\mu\text{m}$  thickness, the sensitivity to liner temperature is strong between 400 and 500 K. Therefore, it is likely that some LSPI cycles in the aforementioned studies have been prevented by the Leidenfrost effect and enhanced evaporation of fuel due to a higher coolant temperature.

#### 4.3.7. Intake conditions

The increased boosting of downsized engines is the main cause for why LSPI and super-knock have become a critical issue for the automotive industry. Zahdeh et al. [7] increased the manifold air pressure by 0.2 bar (or 10%) resulting in twice as many LSPI cycles. Super-knock occurred for  $p_{\text{in}}$  exceeding 1.9 bar in Inoue et al. [125] and the frequency would reach 800 ppm for 2.3 bar. However, in this case, a positive event was defined both through early ignition and knocking, making it difficult to assess whether the development is due to increased risk of LSPI or detonation.

Glowplug measurements with a certification fuel by Yu et al. [12] resulted in a lower resistance for glowplug ignition following a rise in  $p_{\text{in}}$ , both for fixed intake air mass and temperature. It has also been shown by various studies that the chemical IDTs of gasolines and their surrogate blends reduce with increasing pressures as measured

in RCMs [218–220]. The rise in  $p_{\text{EOC}}$  from 13 bar to 25 bar at 850 K shortened the total IDT of a suspended oil droplet in a stoichiometric iso-octane/ $\text{O}_2$ /Ar blend from 6.5 to 4.2 ms [165], while at lower temperatures (740 K) the total IDT would remain almost the same as the pressure approached 20 bar [34]. Faster ignition was also detected for elevated pressures in fuel–oil droplet constant-volume measurements at 573 K [151]. These results indicate that the gaseous fuel–air mixture increases its reactivity at boosted condition, while the effect of an oil or fuel–oil droplet can vary by the conditions. Whether the droplet is volatile and reactive enough to cause pre-ignition at these boosted conditions will be discussed in section 5.1.

The intake air temperature affects the formation of pre-ignition precursors and their propensity to initiate a flame. Firstly, a minimum  $T_{\text{in}}$  should be chosen in order to ensure proper evaporation of the liquid fuel for mitigation of wall wetting. Improved evaporation of injected fuel is presumably the reason for less pre-ignition when increasing the manifold air temperature from 20 °C with split injection [201]. Secondly, a maximum limit should be decided, as an excessive  $T_{\text{in}}$  will elevate the mixture temperature throughout the compression stroke, leading to more susceptible conditions for the fuel–air mixture to ignite from a pre-ignition precursor. Glowplug ignition propensity of a certification gasoline for an elevating  $T_{\text{in}}$  has been investigated by Yu et al. [12] both for a constant  $p_{\text{in}}$  (reducing charge density) and air mass. In both cases, the propensity for glowplug ignition increased for a sweep of the  $T_{\text{in}}$  from 40 °C to 100 °C.

Kar et al. [72] reported increased LSPI for a higher  $T_{\text{in}}$ . Changing the temperature between 26 and 42 °C was considered insignificant for the frequency of LSPI with super-knock in Inoue et al. [125]. Meanwhile, Zahdeh et al. [7] reported a promoting influence for 50 °C manifold air temperature as compared to 30 °C with constant MAP. However, the same study found that the detrimental impact of a higher temperature after the charge air cooler can be eliminated with a sufficiently high oil control ring tension.

#### 4.3.8. Spark parameters

A heavy retardation of the spark timing from the knock limit tends to increase the CoV IMEP and exhaust temperatures towards the turbine inlet limit. No significant change in LSPI was noticed by Morikawa et al. when retarding the timing by 5 CAD [119]. The retardation slightly decreased super-knock in Inoue et al. [125].

The spark plug itself is an unlikely cause for pre-ignition and super-knock in modern gasoline engines. This is evident in investigations by Inoue et al. [125], where the heat range or electrode designs did not affect super-knock frequencies.

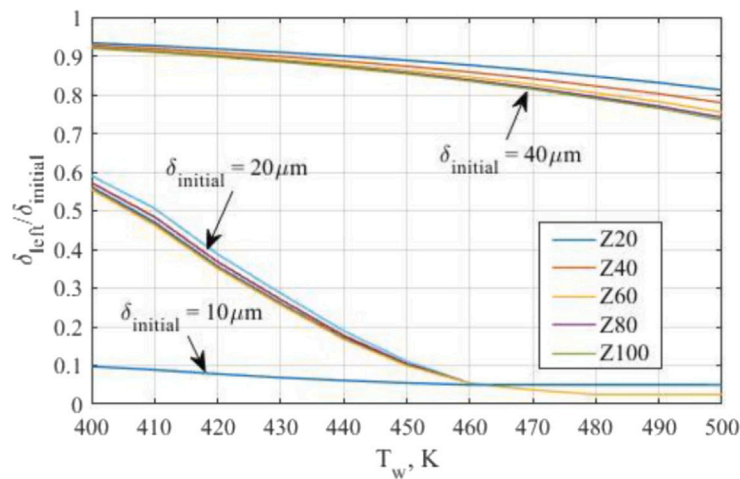


Fig. 29. The ratio of fuel–oil film thickness at various points of the compression stroke and initial thickness with respect to cylinder wall temperatures. Source: Reprinted from [22] with permission from SAE.

#### 4.4. Impact of fuel parameters on super-knock

As already explained in Section 2, autoignition is a step in the development to super-knock. Therefore, super-knock peak-pressures and KI can be expected to relate well to the change in octane numbers. Mansfield et al. [158] compared AKI 88 and AKI 94 gasolines without significant differences in median LSPI SOC, yet finding clear dissimilarity in the following frequency of autoignition and median peak pressures. Only 2% of the LSPI cycles exhibited autoignition with AKI 94, whereas the corresponding share for AKI 88 was 56%. Moreover, the share of heat released from autoignition was less than 10% for the high-grade fuel and 10–55% for the low-grade fuel. Thus, it is not surprising that the peak pressure were about 30 bar higher for the latter fuel. In Hulser et al. [57], only 2-methyltetrahydrofuran and gasoline (RON88 and RON96) would exhibit heavy knocking after pre-ignition, whereas 2-methylfuran and ethanol (RON101 and RON107) would not.

Haenel et al. [138] and Mayer et al. [164] both reported the mitigating impact of ethanol on the severity of super-knock, but neither attempted to separate the possible confounding impact of octane numbers. Two papers by Swarts et al. [69,70] studied the impact of fuel composition on not only the LSPI frequency but also on the severity of the ensuing super-knock. The study of nine market fuels provided lower knock intensities with increased octane numbers and ethanol content. This was found not to be the case for 17 specially prepared test fuel blends, nine of which contained no ethanol and rest with 15% ethanol content.

#### 4.5. Impact of engine parameters on super-knock

##### 4.5.1. Injection strategy

Singh and Dibble [126] studied the direct injection of excess fuel for mitigating conventional knock and super-knock. Under boosted conditions, a low excess fuel quantity at 5 CAD BTDC led to knock suppression, but beyond a threshold value, higher fueling resulted in pre-ignition events.

A heavy reduction in equivalence ratio should also reduce the probability for LSPI to develop into super-knock. This is apparent in Fig. 9 by Liu et al. [115], where detonation would occur for spark-ignited iso-octane RCM experiments with  $\lambda = 1.0$  and  $\lambda = 1.6$ , but not for  $\lambda = 1.8$ .

##### 4.5.2. Exhaust gas recirculation

The inhibiting effect of EGR on conventional knock has been shown by various studies, manifesting itself through earlier KLSA [210,213] and combustion phasing [8,208]. The slower propagation of a CO<sub>2</sub>

diluted flame mitigated the formation of compression waves [221]. Dai et al. [108] found that the excitation time increases with CO<sub>2</sub> dilution for n-heptane/air mixtures at 40.5 bar and 1000 K, reducing the risk of coupling between the pressure and reaction wave. The location of the peak pressure was retarded for LSPI cycles with increased EGR [8]. This implies that a later pre-ignition or the longer delay between SOC and SOK in a diluted charge allows the expansion stroke to begin before knocking, thus also mitigating the risk of detonations. It is thus no surprise that an increment of EGR has shown suppressed knock intensity for LSPI-initiated knock. This is visible in Amann et al. [8], where an increment of EGR from 0% to 6% and 10% significantly reduced the average knock intensity of LSPI cycles.

## 5. Discussion and future needs

### 5.1. Prerequisites for LSPI from oil

A few simulations have been conducted for identifying threshold conditions for droplets and fuel–air mixtures before pre-ignition. Palaveev et al. [59] conducted numerical modeling for droplets with n-heptane chemistry and n-hexadecane physical properties at high-load conditions and the earliest ignition they could predict was at –3.5 CAD ATDC for a 60  $\mu\text{m}$  droplet with an initial temperature of 470 K and a high initial gas-phase temperature of 450 K. This indicates that enhanced reactivity would be needed for oil droplets to cause LSPI at several CAD BTDC. No autoignition of local n-heptane vapor was found before TDC in [124]. In recent studies, it has become popular to use n-hexadecane as a lubricant surrogate in experimental and numerical studies, as the computed chemical ignition delay times of n-alkanes C<sub>7</sub> – C<sub>16</sub> can show remarkable similarities in the low-temperature region [222,223]. It should however be noted that n-hexadecane represents the lower range of carbon chain lengths in commercial lubricants as the chain length can reach C<sub>40</sub> [224,225]. This difference may still introduce some discrepancy, as up to 25% longer IQT IDTs were shown at the low-temperature region for n-hexadecane as compared to base and commercial oils [29].

It should be noted that the average end of compression temperatures are unlikely to exceed 700 K in turbocharged, GDI engines, as shown in a comparison between different  $T_{in}$ , loads and fuels by Birkigt et al. [226]. They concluded that the temperature at TDC for a 90% load with a RON95 fuel is 661 K. The temperatures at TDC were estimated through rotational coherent anti-Stokes Raman spectroscopy measurements and isentropic calculations for stoichiometric mixtures at 9.3:1 CR, 289 K  $T_{in}$ , 2.01 bar  $p_{in}$ , SOI 300 CAD BTDC and 1800 rpm, thus representing LSPI prone conditions well.

The charge motion affects the homogeneity of mixture stoichiometry and temperature. CFD modeling of the stoichiometric injection from a centrally-mounted injector at 2000 rpm presented distribution of the temperature at TDC ranging between 660 and 750 K, the latter of which would coincide close to the exhaust valve at a locally lean region [124]. Considering that a reactive base oil droplet could enter this region and form a small rich and reactive mixture, the 750 K can be considered to represent the worst case scenario for LSPI to occur. Döhler and Schaffner [120] found through endoscopic access that the most common location for pre-ignition would be close to the exhaust valve. The exhaust valve temperature was determined through infrared measurements to be around 425 °C at 40 CAD BTDC during steady-state, wide-open throttle operation with retarded spark timing.

Based on aforementioned simulations, it appears unlikely that pre-ignition several CAD before TDC could be reached solely with base oil droplets. The chemical reactivity of oil is high but the volatility is low. For instance, Fei et al. [34,35] measured the autoignition of gaseous iso-octane both with and without an oil droplet in an RCM, finding that the droplet would enhance ignition below 16 bar at 680 K and below 20 bar at 740 K, with diminishing impact at the higher pressures. While these temperatures are close to end-of-compression conditions in a gasoline engine, the pressures are below the end-of-compression pressures during heavily boosted operation. However, considering that the droplet temperature influences evaporation, it is necessary to study the constraints for it throughout the compression stroke. Ohtomo et al. [227] and Ohtomo et al. [228] used a Rapid Compression and Expansion Machine (RCEM) to compare total IDTs for oil (API group 3, no additives) droplets at different initial droplet temperatures and diameters in both air and gasoline-air mixtures. A 410 µm droplet required an initial temperature in excess of 250 °C to exhibit vapor ignition during the 25 ms (translating to 1200 rpm) compression stroke (+5 ms at the TDC) (with  $T_{EOC} = 530$  °C and  $p_{EOC} = 19$  bar), and an initial temperature of 335 °C would exhibit vapor ignition and flame propagation in the gasoline-air mixture in 23 cases out of 30 tests. Furthermore, EGR mitigated oil vapor ignition effectively, while RON and equivalence ratio showed only minor impact on the probability of ignition. A reduction in the oil droplet size in RCM tests with ambient air, iso-octane/O<sub>2</sub>/N<sub>2</sub>/Ar and methane/O<sub>2</sub>/N<sub>2</sub>/Ar mixture would enhance earlier ignition of the oil as the droplet temperature rise and evaporation is faster [33,228,229]. This is supported by calculations by Ito et al. [17] where a droplet diameter of 50 µm would almost reach the in-cylinder temperature before TDC. A 0.2 mm oil droplet was calculated to be approximately 1500 times slower to reach the maximum vapor mass fraction on the surface in an inert environment above TDC conditions (773–1023 K and up to 50 bar) as compared to a 0.05 mm diameter [230].

The temperature of the oil film at the liner does not generally exceed 200 °C, and thereby it appears that the oil droplet must be very small in size or heated during the previous cycle. It was determined through numerical simulations that a relatively large droplet (250–500 µm) would survive the previous power and exhaust strokes, resulting in droplet temperatures above 300 °C at the early compression stroke, which is enough to cause ignition [227,228]. Support for this theory is provided by Welling et al. [231], where some deliberately injected oil droplets during the early exhaust stroke would remain in the cylinder and autoignite during the following cycles. Similarly, Döhler and Pritze [43] proposed that diffusively burning droplets survive the gas exchange and initiate pre-ignition during the next cycle based on their optical findings.

Already a small addition of NO (100 ppm) in 25% N<sub>2</sub>-diluted engine operation at 2000 rpm and 19 bar IMEP showed a need for ignition retardation due to knocking [212]. It is known that NO<sub>x</sub> also participates in reactions with the engine oil, as shown by Coultas [232] in engine and nitro-oxidation bench tests. The reaction path initiated through H-abstraction from oil species by NO<sub>2</sub>, forming hydrocarbon radicals that further react to form peroxide species and nitrate esters. These species

decompose to form free radicals. The formation and decomposition of nitrate esters are sensitive to the oil temperature, as the peak of nitrate esters formed at 130 °C, whereas at 150 °C the decomposition back to RO radicals and NO<sub>2</sub> would consume them. The impacts of these or other radicals on oil or oil-fuel reactivity in LSPI-relevant engine conditions would be of interest to predict pre-ignition before TDC.

Lauer et al. [14] first approached to simulate pre-ignition in a stochastic reactor model by injecting an n-heptane droplet at 100 CAD ATDC into a toluene reference fuel. The reactivity of pure n-heptane was deemed too slow to cause pre-ignition, and thereby a small fraction of octylketohydroperoxide was added to the droplet. This triggered autoignition at a timing of −17.5 CAD ATDC, thus corresponding well with pre-ignition cycles in engine experiments. Considering that other modeling efforts with n-heptane also have predicted too slow reactivity for pre-ignition [59], it appears that initial reactions of alkane chain branching occurring before droplet ejection from the crevice is a crucial step for LSPI.

The reason for why a substitution of calcium with magnesium in the oil detergent reduced LSPI still remains unknown. The additives do not show the same consistent difference in IQT measurements as in engine operation, as fuel-oil mixtures containing different levels of calcium and magnesium additives showed no variation in DCN [175]. Combustion bomb measurements in air at 773 K and 45 bar by Kassai et al. [163] showed no reduction in IDT when calcium salicylate, calcium sulphonate or ZnDTP were added to base oil. Similar conclusions can be drawn from IQT measurements at 15 bar and 680–873 K in air by Kuti et al. [29] where total IDTs of 20W-50 with an additive package (including antiwear additives in addition to detergents) did not differ significantly from those of pure base stocks. No significant differences in IDTs could be inferred for 1,157–20,000 ppm calcium containing oils blended in 25% p-xylene during IQT measurements at 30 bar, 10% O<sub>2</sub> and 620–770 K [187]. In fact, IDTs in 50-75 bar, 750–850 K constant-pressure air flow were either similar or longer for high-calcium oil formulations as compared to LSPI-mitigating additive packages [176]. Remembering that the in-cylinder pressure and temperature in a turbocharged engine should not exceed 40 bar and 750 K before ignition, one can notice that the constant-volume and constant-pressure measurements in air at relevant conditions do not exhibit the increased reactivity from Ca-rich lubricant detergents that would be expected based on LSPI measurements. Differential scanning calorimetry at 10 bar measurements exhibited reduced autoignition temperature for an increased amount of calcium detergent, but little difference between magnesium and calcium detergents [184].

On the contrary, increased calcium content in a group 3 oil showed a clear reduction in IDT when injected into high-temperature atmospheric co-flow (1123–1173 K) [233]. No significant impact was found from the addition of Mg [178]. Kassai et al. [234] showed advanced ignition when adding calcium additive into an iso-octane droplet, which was injected to a gaseous PRF mixture in an RCEM. However, they found no significant impact on the IDT when adding calcium into an iso-octane/base oil droplet injected into a methane mixture. This indicates that the effect of calcium is fuel dependent. Moreover, calcium salicylate was shown to promote autoignition and conventional knocking when mixed purely into PRF50, whereas sodium and magnesium would not encourage autoignition [235,236]. It has been indicated that the deposits formed by the addition of calcium salicylate in the fuel would enhance the autoignition [237].

The impact from calcium was theorized by Moriyoshi et al. [238] to be caused by reactions involving CaO and CaCO<sub>3</sub>. Initially, CaCO<sub>3</sub> decomposes to CaO and CO<sub>2</sub>, due to the heat release during combustion. During the next compression stroke, the reverse exothermic reaction occurs and heats up the droplet to a temperature where pre-ignition may take place. This theory would also explain why substitution of calcium with magnesium reduces LSPI, as the reaction enthalpy for the MgO/MgCO<sub>3</sub> reaction is significantly lower than for the corresponding

reaction with calcium [239]. The decomposition and its reverse reaction do not explain the promoting effect of calcium in single-stroke applications, such as the RCEM experiments by Kassai et al. [234]. Therefore, they proposed that the impact may be due to catalytic enhancement of H abstraction [194].

A third theory for the impact of detergents was expressed by Splitter et al. [187], in which the detergent metals would enhance the reactivity of nitro compounds in the oil. This was supported by results showing that the LSPI activity would increase with calcium content at a moderate load with a  $\text{CH}_3\text{NO}_2$  doped RON70 fuel. This effect was not observed without the addition of  $\text{CH}_3\text{NO}_2$ , suggesting that the nitrogen levels in the crevice accumulation have a role in the formation of LSPI.

A mitigating effect of ZnDTP has been concluded through the various engine experiments that were addressed in Section 4.2.3. This effect of ZnDTP was also shown by slower ignition in an RCEM when added in increased amounts to an iso-octane droplet that was injected into a PRF90/air mixture [234]. Furthermore, increased ZnDTP resulted in longer IDTs in high-temperature (1123–1223 K) atmospheric co-flow [178,233]. A high fraction of phosphate (5–10 vol-%) increased the IDT of hexadecane in 573 K air at 4 and 12 bar, whereas 5% of magnesium would not change the IDT [240]. Meanwhile, no impact on autoignition was inferred from the addition of molybdenum and zinc into the fuel itself (PRF50) [241].

### 5.2. Pre-ignition in other engines

Lubricant-initiated pre-ignition is not only restricted to gasoline engines for automotive use but has also been encountered in medium-speed gas engines [242]. In this case, the countermeasures include reduced amount of oil in the combustion chamber, lower compression temperatures and suppressing the flame kernel propagation. In recognition of this Yasueda and coworkers coined the phrase lubricating oil autoignition or LOA [243–245].

A natural gas or dual fuel engine should counteract pre-ignition effectively since cylinder wall wetting and crevice accumulation from impinging fuel droplets are deemed unlikely as the gaseous methane is port-injected and the small fraction of pilot diesel fuel is injected directly close to TDC. Still, pre-ignition has been encountered in small gas and dual fuel engines operating on natural gas and biogas and its probability increases with higher load [246–248]. Surface ignition was ruled out by Königsson [248] as the required glowplug temperature for repeated pre-ignition was approximately 1000 °C and sporadic events would occur at much lower temperatures. As with gasoline engines, the lubricant oil has an influence on pre-ignition. The reduction in chemical IDT is apparent with increased n-hexadecane content into methane [249]. However, the benefits of reduced calcium in the lubricant could not be shown [248].

The delay of pilot fuel SOI for dual fuel combustion caused an increase in LSPI [208]. This was explained to be both due to a longer time available for pre-ignition to occur and an increase in exhaust and residual gas temperatures. An increase in the methane number results in lower intensity of the following knock after pre-ignition [247,248].

Zaccardi and Serrano [208] reported a 9-fold increase in methane-diesel dual fuel LSPI frequency when decreasing  $\phi$  from 1 to 0.75 with a constant pilot SOI and simultaneous rise in intake air pressure (Fig. 30). Thus, the rise in pressure maintains a fixed load and counterbalances the longer IDTs that follow a lower equivalence ratio. Meanwhile, the required  $T_{in}$  for pre-ignition was increased by approximately 50 K when increasing  $\lambda$  from 1.35 to 1.6, while keeping the load constant [247].

As with SI engines, a dual fuel engine with a high compression ratio shows improvement with EGR [208,248]. The trend is apparent despite variations in piston configuration and equivalence ratio [208].

Zaccardi and Serrano [208] noticed that the LSPI rate would increase when decreasing the compression ratio from 17:1 to 16:1 in a multi-cylinder dual fuel engine. The lower compression ratio would produce higher exhaust gas temperatures and residual rates, which

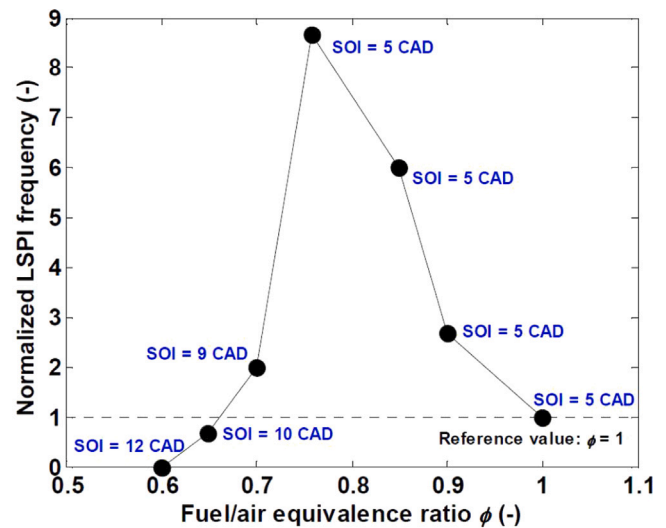


Fig. 30. Impact of equivalence ratio in a single-cylinder 0.5 l methane-diesel dual fuel engine. Increased  $p_{in}$  used for lower  $\phi$  in order to maintain constant load. Source: Reprinted from [208] with permission from SAE.

counteracted the reduced pressure during compression. An increased  $T_{in}$  also enhanced pre-ignition [248], which has been supported through faster ignition of suspended oil droplets in RCM measurements [229].

Green hydrogen is an attractive fuel due to its carbon-free emissions. However, pre-ignition restricted the increment of  $\text{H}_2$  in a 1.3 l single-cylinder diesel dual fuel engine already at intermediate loads (7 bar IMEP) [250].

Liquified petroleum gas (LPG) blends with varying levels of  $\text{C}_3$  and  $\text{C}_4$  with late combustion phasing and high intake air temperature revealed an improved gas phase pre-ignition resistance with higher propane content [251].

Two-stroke engines have exhibited pre-ignition at very high speeds. The reason appears to be slow combustion during the preceding cycle, which leads to immediate combustion during the following compression stroke [252].

### 5.3. Progress and future needs

The conclusions from Sections 4.1–4.3 are shown in Fig. 31, in which the green color indicates a higher likelihood for a mitigating impact against LSPI and the red color indicates a higher likelihood for a promoting impact. Meanwhile, the yellow color indicates that the impact is close to neutral, whereas the impacts of black factors have not been properly concluded yet and can vary heavily between experimental setups.

An adoption of the effective LSPI mitigation strategies allows the automotive industry to continue the downsizing of gasoline engines. Morikawa et al. [119] applied very high  $p_{in}$  in combination with a Ca-free oil and low-pressure EGR or Miller timing, achieving IMEPg values of 28.5 and 30.2 bar at 1500 rpm, respectively. Strategies for highly downsized engine operation were also studied by Martin et al. [209]. Most pre-ignition studies in this review have been performed at loads below these examples and it would be beneficial to expand testing to loads approaching 30 bar IMEP.

Improvements in fuel economy can be reached through further reductions in oil viscosities and lower hydrodynamic friction, although the effect may vary significantly by the vehicle [253]. These improvements have been approached through newly developed viscosity modifiers [254] and sludge handling systems [255]. The boundary lubrication was improved with a borated calcium detergent that reduces boundary friction through promoted  $\text{MoS}_2$  formation [256]. An

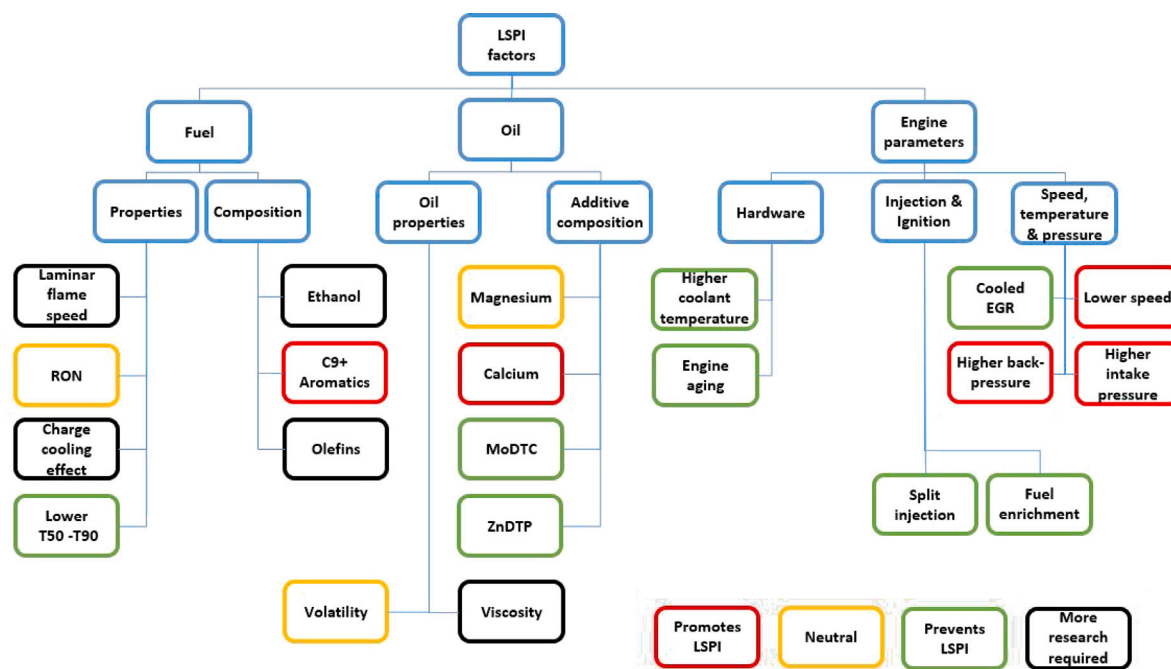


Fig. 31. Factors in the formation of LSPI.

interesting scope would be to compare how these borated detergents compare to carbonate detergents in LSPI tests.

Besides a higher coolant temperature, the increment of cooled low-pressure EGR was found to be a potential remedy for LSPI and super-knock. However, IDT studies of oil–fuel droplets in EGR diluted gasoline mixtures would allow to quantify its impact on LSPI formation. Similarly, variations in the composition of both the droplet and ambient gasoline mixture in IDT studies would be beneficial to understand the impact of fuel formulations on LSPI beyond the susceptibility to cause fuel-wall wetting and top ring zone retention. Furthermore, additional ignition studies on commercial base oils would be beneficial to understand their reactivity as compared to any potential surrogate species.

Despite the significant enhancing impact of calcium-rich oil detergents on LSPI, the pathway through which they activate ignition has not yet been proven in the studied literature. Therefore, elaborate studies on how detergent metals interact with different hydrocarbon chemistries at engine relevant conditions would widen the understanding on why magnesium-based detergents have proven to be a remedy for LSPI. We recommend further fundamental studies on the impact of calcium on the reactivity between heavy fuel components, lubricant components and  $\text{NO}_x$  at conditions relevant to the top ring zone and the compression stroke.

Steady-state engine tests have become the standard to evaluate the impact of oils, fuel, hardware and operational conditions on LSPI. The multi-segment tests published by Southwest Research Institute and FEV established the basis for the development of the Sequence IX engine to evaluate the effect of engine oil on LSPI. The paper by Mounce [216] provided a practical guide to not only the test engine modification and test-stand requirements, but also details of the prove-out and precision matrices required to ultimately arrive at a precision statement of the test. The practice of testing reference oils to allow read-across between different engine is also firmly established. The Sequence IX test was ultimately codified in ASTM D8291 [257] and accepted as the gauge for conformance to LSPI performance requirements in the ILSAC Standards For Passenger Car Engine Oils (GF-6 A and GF-6B), as well as the earlier, interim SN PLUS, and latest American Petroleum Institute (API) service category SP, for gasoline engine oils. The same test method is required for adherence to categories A7/B7 and C6 or

the ACEA European Oil Sequences for Light-duty Engines. An LSPI performance required was also incorporated as a requirement in the second generation (Gen2) of GM dexos1™ oil specification.

Much of the understanding of LSPI is based on these steady state engine tests, supported by real-life, on-road experiences. There has been very little published in the way of transient testing, aimed at replicating the in-vehicle behavior. The performance requirement for the third generation (Gen3) of GM dexos1™ oils incorporate a transient engine test which is expected to be more severe than any of the previous steady-state tests. Very little is known about the details of this test.

## 6. Conclusions

This article provided a review of the phenomena behind LSPI and super-knock in gasoline engines. Furthermore, suitable methods for mitigating LSPI have been presented. LSPI has been a threshold in the further downsizing of gasoline engines through increased boosting, and effective mitigation of this issue will allow further improvements in fuel economy and emissions reductions, while reducing the risk of hardware damage from super-knock. Some of the main findings of this review include:

**Initiation of LSPI precursors:** LSPI is a stochastic phenomenon and occurs every 10,000–100,000 cycles under high-load and low-speed conditions. Oil–fuel droplets that have been ejected from the top ring crevice and deposits can be the precursors for LSPI events. An LSPI event can release more pre-ignition precursors, thereby initiating following LSPI cycles.

**Development to super-knock:** The pre-ignited flame compresses unburned end-gases to the point of autoignition. The following knocking may exhibit very high intensities if a detonation follows the autoignition. This detonation can be the result of an autoignitive reaction wave coupling with the pressure wave in a hotspot or as the result of a shock wave interacting with cylinder surfaces and a propagating flame.

**Impact of fuel parameters:** A high volatility fuel (i.e. by reducing the distillation temperatures T50–T90) substantially reduces LSPI due to mitigated wetting of the cylinder wall and reduced oil–fuel dilution at the top ring crevice. Therefore, fuels with high fractions of C9+ aromatics were susceptible to LSPI. The research octane number has not shown a notable impact on the LSPI frequency, but some studies

indicate a higher average knock intensity after an LSPI event for low-octane fuels. The impact of ethanol varied significantly between studies.

**Impact of oil parameters:** Oils with higher concentrations of calcium have been established as common LSPI promoters, whereas already a partial substitution of calcium for magnesium reduces LSPI. ZnDTP and MoDTC suppress LSPI, while sodium promotes it. LSPI experiments with aged oils have been published within recent years, showing that the aging can affect LSPI frequencies.

**Impact of engine parameters:** Fuel injection strategies that reduce wall impingement, including split injection and spray targeting that avoids the cylinder liner, can effectively reduce LSPI. Late injection timings during the intake stroke have in several studies revealed a promoting impact on LSPI, while increased fuel injection pressure has not shown a mitigating effect despite improved atomization. Fuel enrichment has been shown to mitigate LSPI and can thereby be suitable to mitigate the risk of following events. The integration of cooled EGR and higher coolant temperatures have also counteracted LSPI, and the former of these appears to mitigate the risk of super-knock after an LSPI event. Engine aging tends to reduce the frequency of LSPI.

### CRedit authorship contribution statement

**Kristian Rönn:** Conceptualization, Methodology, Visualization, Roles/Writing – original draft, Writing – review & editing. **Andre Swarts:** Conceptualization, Investigation, Writing – original draft, Writing – review & editing. **Vickey Kalaskar:** Writing – review & editing. **Terry Alger:** Supervision. **Rupali Tripathi:** Roles/Writing – original draft, Writing – review & editing. **Juha Keskinvääli:** Conceptualization, Writing – original draft. **Ossi Kaario:** Conceptualization, Writing – review & editing. **Annukka Santasalo-Aarnio:** Investigation, Validation, Writing – review & editing. **Rolf Reitz:** Writing – review & editing. **Martti Larmi:** Supervision, Writing – review & editing.

### Declaration of competing interest

The authors declare that they have no known competing financial interests or personal relationships that could have appeared to influence the work reported in this paper.

### Data availability

Data will be made available on request.

### Acknowledgments

The authors want to thank the support by the Dean's grant of Aalto University School of Engineering, Henry Ford Foundation of Finland and Technology Industries of Finland, Combustion Engines Branch Group.

### References

- [1] International Energy Agency. Fuel economy in major car markets: Technology and policy drivers 2005–2017. 2019.
- [2] Petitjean D, Bernardini L, Middlemass C, Shahed S. Advanced gasoline engine turbocharging technology for fuel economy improvements. Tech. Rep., (2004-01-0988). SAE Technical Paper; 2004.
- [3] Fraser N, Blaxill H, Lumsden G, Bassett M. Challenges for increased efficiency through gasoline engine downsizing. SAE Int J Engines 2009;2(2009-01-1053):991–1008.
- [4] Bradley D, Morley C, Gu X, Emerson D. Amplified pressure waves during autoignition: relevance to CAI engines. SAE Trans 2002;(2002-01-2868):2679–90.
- [5] Gu X, Emerson D, Bradley D. Modes of reaction front propagation from hot spots. Combust Flame 2003;133(1–2):63–74.
- [6] Björnsson H, Adkin P, Johannesson T, Johansson K, et al. The new volvo drive-e 3-cylinder engines. In: 25th Aachen colloquium automobile and engine technology. 2016.
- [7] Zahdeh A, Rothenberger P, Nguyen W, Anbarasu M, Schmuck-Soldan S, Schaefer J, et al. Fundamental approach to investigate pre-ignition in boosted SI engines. SAE Int J Engines 2011;4(1):246–73.
- [8] Amann M, Alger T, Mehta D. The effect of EGR on low-speed pre-ignition in boosted SI engines. SAE Int J Engines 2011;4(1):235–45.
- [9] Amann M, Mehta D, Alger T. Engine operating condition and gasoline fuel composition effects on low-speed pre-ignition in high-performance spark ignited gasoline engines. SAE Int J Engines 2011;4(1):274–85.
- [10] Wang Z, Liu H, Reitz RD. Knocking combustion in spark-ignition engines. Prog Energy Combust Sci 2017;61:78–112.
- [11] Chapman EM, Costanzo VS. A literature review of abnormal ignition by fuel and lubricant derivatives. SAE Int J Engines 2016;9(1):107–42.
- [12] Yu X, Costanzo V, Chapman E, Davis R. A robust preignition rating methodology: Evaluating the propensity to establish propagating flames under real engine conditions. Tech. Rep., (2017-01-2241). SAE Technical Paper; 2017.
- [13] Attard WP, Toulson E, Watson H, Hamori F. Abnormal combustion including mega knock in a 60% downsized highly turbocharged PFI engine. Tech. Rep., (2010-01-1456). SAE Technical Paper; 2010.
- [14] Lauer T, Heiss M, Bobicic N, Holly W, Pritze S. A comprehensive simulation approach to irregular combustion. Tech. Rep., (2014-01-1214). SAE Technical Paper; 2014.
- [15] Kuboyama T, Moriyoshi Y, Morikawa K. Visualization and analysis of LSPI mechanism caused by oil droplet, particle and deposit in highly boosted SI combustion in low speed range. SAE Int J Engines 2015;8(2):529–37.
- [16] Kassai M, Hashimoto H, Shiraishi T, Teraji A, Noda T. Mechanism analysis on LSPI occurrence in boosted SI engines. Tech. Rep., (2015-01-1867). SAE Technical Paper; 2015.
- [17] Ito T, Abe Y, Tanaka J. Lubricating oil droplets in cylinder on abnormal combustion in supercharged SI engine. Tech. Rep., (2018-32-0008). SAE Technical Paper; 2018.
- [18] Heiss M, Lauer T. Analysis of particle separation with respect to pre-ignition in an si-engine. In: 11th world congress on computational mechanics (WCCM XI), Barcelona, Spain. 2014.
- [19] Tormos B, García JM, Bastidas S, Domínguez B, Oliva F, Cárdenas D. Investigation on low-speed pre-ignition from the quantification and identification of engine oil droplets release under ambient pressure conditions. Measurement 2020;107961.
- [20] Hirano S, Yamashita M, Fujimoto K, Kato K. Investigation of engine oil effect on abnormal combustion in turbocharged direct injection-spark ignition engines (Part 2). Tech. Rep., (2013-01-2569). SAE Technical Paper; 2013.
- [21] Maliha M, Stumpf B, Beyer F, Kühnert M, Kubach H, Roisman I, et al. Optical investigation on the interaction between a fuel-spray and an oil wetted wall with the focus on secondary droplets. Int J Engine Res 2022;14680874221095235.
- [22] Zhang Q, Kalva VT, Tian T. Modeling the evolution of fuel and lubricant interactions on the liner in internal combustion engines. Tech. Rep., (2018-01-0279). SAE Technical Paper; 2018.
- [23] Mariani V, Pulga L, Bianchi GM, Cazzoli G, Falfari S. Neural network-based prediction of liquid-phase diffusion coefficient to model fuel-oil dilution on engine cylinder walls. SAE Int J Engines 2020;13(03-13-05-0041).
- [24] Lee P, Priest M, Stark M, Wilkinson J, Smith LJ, Taylor R, et al. Extraction and tribological investigation of top piston ring zone oil from a gasoline engine. Proc Inst Mech Eng J 2006;220(3):171–80.
- [25] Alger TF, Briggs TE. Chemical analysis of potential initiating fluid for low-speed pre-ignition. In: International conference on knocking in gasoline engines. Springer; 2017, p. 112–20.
- [26] Splitter D, Burrows B, Lewis S. Direct measurement and chemical speciation of top ring zone liquid during engine operation. Tech Rep., (2015-01-0741). SAE Technical Paper; 2015.
- [27] Frottier V, Heywood JB, Hochgreb S. Measurement of gasoline absorption into engine lubricating oil. SAE Trans 1996;1114–21.
- [28] Amann M, Alger T, Westmoreland B, Rothmaier A. The effects of piston crevices and injection strategy on low-speed pre-ignition in boosted SI engines. SAE Int J Engines 2012;5(3):1216–28.
- [29] Kuti OA, Yang SY, Hourani N, Naser N, Roberts WL, Chung SH, et al. A fundamental investigation into the relationship between lubricant composition and fuel ignition quality. Fuel 2015;160:605–13.
- [30] Distaso E, Amirante R, Calò G, De Palma P, Tamburrano P, Reitz R. Predicting lubricant oil induced pre-ignition phenomena in modern gasoline engines: The reduced GasLube reaction mechanism. Fuel 2020;281:118709.
- [31] Distaso E, Amirante R, Calò G, De Palma P, Reitz R. Lubricant-oil-induced pre-ignition phenomena in modern gasoline engines: Using experimental data and numerical chemistry to develop a practical correlation. Tech. Rep., (2021-24-0052). SAE Technical Paper; 2021.
- [32] Fei S, Wang Z, Qi Y, Wang Y, Zhang H. Ignition of a single lubricating oil droplet in combustible ambient gaseous mixture under high-temperature and high-pressure conditions. Combust Sci Technol 2019;191(11):2033–52.
- [33] Fei S, Wang Z, Qi Y, Wang Y. Investigation on ignition of a single lubricating oil droplet in premixed combustible mixture at engine-relevant conditions. Tech. Rep., (2019-01-0298). SAE Technical Paper; 2019.

- [34] Fei S, Qi Y, Wang Y, Zhang H, Wang Z. Study of oil droplet ignition and its induction for pre-ignition under different environmental conditions.
- [35] Fei S, Qi Y, Liu W, Wang Y, Wang Z, Zhang H. Combustion modes induced by oil-droplet gas-phase pre-ignition in the chamber under different environmental conditions. *Combust Sci Technol* 2021;1–19.
- [36] Qi Y, Xu Y, Wang Z, Wang J. The effect of oil intrusion on super knock in gasoline engine. *Tech. Rep.*, (2014-01-1224). SAE Technical Paper; 2014.
- [37] Welling O, Collings N, Williams J, Moss J. Impact of lubricant composition on low-speed pre-ignition. *Tech. Rep.*, (2014-01-1213). SAE Technical Paper; 2014.
- [38] Tao C, Miao K, Tang F, Qian Y, Zhang Y, Meng S, et al. Evaporation and combustion characteristics for a droplet of lubricating oil and gasoline. *Int Commun Heat Mass Transfer* 2021;127:105513.
- [39] Qian Y, Zhao P, Tao C, Meng S, Wei J, Cheng X. Experimental study on evaporation characteristics of lubricating oil/gasoline blended droplet. *Exp Therm Fluid Sci* 2019;103:99–107.
- [40] Okada Y, Miyashita S, Izumi Y, Hayakawa Y. Study of low-speed pre-ignition in boosted spark ignition engine. *SAE Int J Engines* 2014;7(2):584–94.
- [41] Zöbinger N, Schweizer T, Lauer T, Kubach H, Koch T. Experimental and numerical analysis on two-phase induced low-speed pre-ignition. *Energies* 2021;14(16):5063.
- [42] Magar M, Spicher U, Palaveev S, Gohl M, Müller G, Lensch-Franzen C, et al. Experimental studies on the occurrence of low-speed pre-ignition in turbocharged GDI engines. *SAE Int J Engines* 2015;8(2):495–504.
- [43] Döhler A, Pritze S. A contribution to better understanding the pre-ignition phenomenon in highly charged internal combustion engines with direct fuel injection. In: 4th international conference on knocking in gasoline engines (Berlin). 2013, p. 41–61.
- [44] Dingle SF, Cairns A, Zhao H, Williams J, Williams O, Ali R. Lubricant induced pre-ignition in an optical SI engine. *Tech. Rep.*, (2014-01-1222). SAE technical Paper; 2014.
- [45] Cheng S. The impacts of engine operating conditions and fuel compositions on the formation of combustion chamber deposits. *Tech. Rep.*, (2000-01-2025). SAE Technical Paper; 2000.
- [46] Cheng S, Kim C. Effect of engine operating parameters on engine combustion chamber deposits. *Tech. Rep.*, (902108). SAE Technical Paper; 1990.
- [47] Wang Z, Qi Y, Liu H, Long Y, Wang J-X. Experimental study on pre-ignition and super-knock in gasoline engine combustion with carbon particle at elevated temperatures and pressures. *Tech. Rep.*, (2015-01-0752). SAE Technical Paper; 2015.
- [48] Gupta A, Seeley R, Shao H, Remias J, Roos J, Wang Z, et al. Impact of particle characteristics and engine conditions on deposit-induced pre-ignition and superknock in turbocharged gasoline engines. *SAE Int J Fuels Lubr* 2017;10(3):830–41.
- [49] Sparrow SW. Preignition and spark-plugs. *SAE Trans* 1920;412–27.
- [50] Sasaki N, Nakata K, Kawatake K, Sagawa S, Watanabe M, Sone T. The effect of fuel compounds on pre-ignition under high temperature and high pressure condition. *Tech. Rep.*, (2011-01-1984). SAE Technical Paper; 2011.
- [51] Mogi K, Hashizume K, Arisawa K, Kobayashi H. Analysis and avoidance of pre-ignition in SI gasoline engines. *JSAE Rev* 1998;19(1):9–14.
- [52] Dahnz C, Spicher U. Irregular combustion in supercharged spark ignition engines—pre-ignition and other phenomena. *Int J Engine Res* 2010;11(6):485–98.
- [53] Cavina N, Rojo N, Businaro A, Ceschini L, Balducci E, Cerofolini A. Analysis of pre-ignition combustions triggered by heavy knocking events in a turbocharged GDI engine. *Energy Procedia* 2016;101:893–900.
- [54] Sasaki N, Nakata K. Effect of fuel components on engine abnormal combustion. *Tech. Rep.*, (2012-01-1276). SAE Technical Paper; 2012.
- [55] Cavina N, Rojo N, Poggio L, Calogero L, Cevolani R. Investigation on pre-ignition combustion events and development of diagnostic solutions based on ion current signals. *SAE Int J Engines* 2017;10(4):1518–23.
- [56] Ottenwälder T, Burke U, Hoppe F, Budak O, Brammertz S, Klintworth K, et al. Experimental and numerical study of abnormal combustion in direct injection spark ignition engines using conventional and alternative fuels. *Energy Fuels* 2019;33(6):5230–42.
- [57] Hülser T, Grünfeld G, Brands T, Günther M, Pischinger S. Optical investigation on the origin of pre-ignition in a highly boosted SI engine using bio-fuels. *Tech. Rep.*, (2013-01-1636). SAE Technical Paper; 2013.
- [58] Winklhofer E, Hirsch A, Kapus P, Kortschak M, Philipp H. TC GDI engines at very high power density—irregular combustion and thermal risk. *Tech. Rep.*, (2009-24-0056). SAE Technical Paper; 2009.
- [59] Palaveev S, Magar M, Kubach H, Schieß I R, Spicher U, Maas U. Premature flame initiation in a turbocharged DISI engine-numerical and experimental investigations. *SAE Int J Engines* 2013;6(1):54–66.
- [60] Dahnz C, Han K-M, Spicher U, Magar M, Schieß I R, Maas U. Investigations on pre-ignition in highly supercharged SI engines. *SAE Int J Engines* 2010;3(1):214–24.
- [61] Kubach H, Weidenleiner A, Pfeil J, Koch T, Kittel H, Roisman IV, et al. Investigations on the influence of fuel oil film interaction on pre-ignition events in highly boosted DI gasoline engines. *Tech. Rep.*, (2018-01-1454). SAE Technical Paper; 2018.
- [62] Gao J, Yao A, Zhang Y, Qu G, Yao C, Zhang S, et al. Investigation into the relationship between super-knock and misfires in an SI GDI engine. *Energies* 2021;14(8):2099.
- [63] Kalaskar V, Moore T, Swarts A. On optical semi-quantitative spectral study of low-speed pre-ignition sources in spark ignition engines. *SAE Int J Adv Curr Pract Mobil* 2021;3(5):2581–93.
- [64] He Y, Liu Z, Stahl I, Zhang G, Zheng Y. Comparison of stochastic pre-ignition behaviors on a turbocharged gasoline engine with various fuels and lubricants. *Tech. Rep.*, (2016-01-2291). SAE Technical Paper; 2016.
- [65] Colliou T, Giarracca L, Lahaussais D, Sasaki T, Fukazawa Y, Iida Y, et al. Impact of diesel and detergent contamination on gasoline low-speed pre-ignition and their characterization using unwashed gums. *Fuel* 2022;318:122754.
- [66] Costanzo VS, Yu X, Chapman E, Davis R, Haenel P. Fuel & lubricant effects on stochastic preignition. *SAE Int J Adv Curr Pract Mobil* 2019;1(1):259–77.
- [67] Boronat Colomer V, Splitter D, Neupane S, Partridge Jr. W. Particle matter index and fuel wall-wetting relations on stochastic pre-ignition. *SAE Int J Adv Curr Pract Mobil* 2021;1(1):636–48.
- [68] Splitter D, Colomer VB, Neupane S, Chuahy FDF, Partridge W. In situ laser induced fluorescence measurements of fuel dilution from low load to stochastic pre ignition prone conditions. *Tech. Rep.*, (2021-01-0489). SAE Technical Paper; 2021.
- [69] Swarts A, Chapman E, Costanzo V. Detailed analyses and correlation of fuel effects on stochastic preignition. *Tech. Rep.*, (2020-01-0612). SAE Technical Paper; 2020.
- [70] Swarts A, Kalaskar V. Market fuel effects on low speed pre-ignition. In: SAE WCX digital summit. *Tech. Rep.*, (2021-01-0487). SAE Technical Paper; 2021.
- [71] Niegemann P, Fikri M, Kaiser S, Schulz C. Ignition of individual droplets in a reactive fuel/air mixture behind reflected shock waves. *SAE Int J Adv Curr Pract Mobil* 2019;2(2019-01-2162):301–9.
- [72] Kar A, Huisjen A, Aradi A, Reitz J, Iqbal A, Haumann K, et al. Assessing the impact of lubricant and fuel composition on LSPI and emissions in a turbocharged gasoline direct injection engine. *SAE Int J Adv Curr Pract Mobil* 2020;2(2020-01-0610):2568–80.
- [73] Kalghatgi GT, Bradley D. Pre-ignition and 'super-knock' in turbo-charged spark-ignition engines. *Int J Engine Res* 2012;13(4):399–414.
- [74] Takeno T. Ignition criterion by thermal explosion theory. *Combust Flame* 1977;29:209–11.
- [75] Zhou L, Zhang X, Zhong L, Yu J. Effects of flame propagation velocity and turbulence intensity on end-gas auto-ignition in a spark ignition gasoline engine. *Energies* 2020;13(19):5039.
- [76] Kalghatgi G. Fuel anti-knock quality-part I. Engine studies. *Tech. Rep.*, (2001-01-3584). SAE Technical Paper; 2001.
- [77] Szymbist JP, Splitter DA. Pressure and temperature effects on fuels with varying octane sensitivity at high load in SI engines. *Combust Flame* 2017;177:49–66.
- [78] Yates AD, Swarts A, Viljoen CL. Correlating auto-ignition delays and knock-limited spark-advance data for different types of fuel. *Tech. Rep.*, (2005-01-2083). SAE Technical Paper; 2005.
- [79] Prakash A, Wang C, Janssen A, Aradi A, Cracknell R. Impact of fuel sensitivity (RON-mon) on engine efficiency. *SAE Int J Fuels Lubr* 2017;10(1):115–25.
- [80] Cai L, Pitsch H, Mohamed SY, Raman V, Bugler J, Curran H, et al. Optimized reaction mechanism rate rules for ignition of normal alkanes. *Combust Flame* 2016;173:468–82.
- [81] Feng D, Buresheid K, Zhao H, Wei H, Chen C. Investigation of lubricant induced pre-ignition and knocking combustion in an optical spark ignition engine. *Proc Combust Inst* 2019;37(4):4901–10.
- [82] Chun KM, Kim KW. Measurement and analysis of knock in a SI engine using the cylinder pressure and block vibration signals. *SAE Trans* 1994;56–62.
- [83] Wang Z, Liu H, Song T, Qi Y, He X, Shuai S, et al. Relationship between super-knock and pre-ignition. *Int J Engine Res* 2015;16(2):166–80.
- [84] Kalghatgi G, Algunaibet I, Morganti K. On knock intensity and superknock in SI engines. *SAE Int J Engines* 2017;10(3):1051–63.
- [85] Haenel P, Seyfried P, Kleeberg H, Tomazic D. Systematic approach to analyze and characterize pre-ignition events in turbocharged direct-injected gasoline engines. *Tech. Rep.*, (2011-01-0343). SAE Technical Paper; 2011.
- [86] Haenel P, Tomazic D, Kleeberg H, Ciaravino J. Fuel properties and their impact on stochastic pre-ignition occurrence and mega-knock in turbocharged direct-injection gasoline engines. *Tech. Rep.*, (2020-01-0614). SAE Technical Paper; 2020.
- [87] Chapman E, Studzinski W, Monroe R, Tolou A, Wagle M, Ciaravino J, et al. Impact of fuel detergent type and concentration on the rate and severity of stochastic preignition in a turbocharged spark ignition direct injection gasoline engine. *Tech. Rep.*, (2021-01-0490). SAE Technical Paper; 2021.
- [88] Truffin K, Angelberger C, Richard S, Pera C. Using large-eddy simulation and multivariate analysis to understand the sources of combustion cyclic variability in a spark-ignition engine. *Combust Flame* 2015;162(12):4371–90.
- [89] Robert A, Richard S, Colin O, Poinot T. LES study of deflagration to detonation mechanisms in a downsized spark ignition engine. *Combust Flame* 2015;162(7):2788–807.
- [90] Zeldovich YB. Regime classification of an exothermic reaction with nonuniform initial conditions. *Combust Flame* 1980;39(2):211–4.

- [91] Khokhlov AM, Oran ES, Wheeler JC. A theory of deflagration-to-detonation transition in unconfined flames. *Combust Flame* 1997;108(4):503–17.
- [92] Meyer J, Oppenheim A. Dynamic response of a plane-symmetrical exothermic reaction center. *AIAA J* 1972;10(11):1509–13.
- [93] Vinkeloe J, Zander L, Szeponik M, Djordjevic N. Tailoring the temperature sensitivity of ignition delay times in hot spots using fuel blends of dimethyl ether, methane, and hydrogen. *Energy Fuels* 2019;34(2):2246–59.
- [94] Rudloff J, Zaccardi J-M, Richard S, Anderlohr J. Analysis of pre-ignition in highly charged SI engines: Emphasis on the auto-ignition mode. *Proc Combust Inst* 2013;34(2):2959–67.
- [95] Peters N, Kerschgens B, Paczko G. Super-knock prediction using a refined theory of turbulence. *SAE Int J Engines* 2013;6(2):953–67.
- [96] Lutz AE, Kee RJ, Miller JA, Dwyer HA, Oppenheim AK. Dynamic effects of autoignition centers for hydrogen and C1, 2-hydrocarbon fuels. In: *Symposium (International) on combustion*. 22, (1);Elsevier; 1989, p. 1683–93.
- [97] Dai P, Qi C, Chen Z. Effects of initial temperature on autoignition and detonation development in dimethyl ether/air mixtures with temperature gradient. *Proc Combust Inst* 2017;36(3):3643–50.
- [98] Gorbatenko I, Singh E, Sarathy M, Nicolle A. Effects of fuel composition on auto-ignition and detonation development in boosted spark-ignited engines. *Tech. Rep.*, (2021-24-0022). SAE Technical Paper; 2021.
- [99] Cai L, Pitsch H. Tailoring fuels for a shockless explosion combustor. In: *Active flow and combustion control* 2014. Springer; 2015, p. 299–315.
- [100] Wang Y, Qi Y, Liu W, Wang Z. Investigation of methanol ignition phenomena using a rapid compression machine. *Combust Flame* 2020;211:147–57.
- [101] Bobusch BC, Berndt P, Paschereit CO, Klein R. Shockless explosion combustion: An innovative way of efficient constant volume combustion in gas turbines. *Combust Sci Technol* 2014;186(10–11):1680–9.
- [102] Dec JE. Advanced compression-ignition engines—understanding the in-cylinder processes. *Proc Combust Inst* 2009;32(2):2727–42.
- [103] Berndt P, Klein R. Modeling the kinetics of the shockless explosion combustion. *Combust Flame* 2017;175:16–26.
- [104] Su J, Dai P, Chen Z. Detonation development from a hot spot in methane/air mixtures: Effects of kinetic models. *Int J Engine Res* 2020;1468087420944617.
- [105] Guerouani A, Robert A, Zaccardi J-M. Detonation peninsula for TRF-air mixtures: assessment for the analysis of auto-ignition events in spark-ignition engines. *Tech. Rep.*, (2018-01-1721). SAE Technical Paper; 2018.
- [106] Gao Y, Dai P, Chen Z. Numerical studies on autoignition and detonation development from a hot spot in hydrogen/air mixtures. *Combust Theory Model* 2020;24(2):245–61.
- [107] Dai P, Chen Z. Effects of NO<sub>x</sub> addition on autoignition and detonation development in DME/air under engine-relevant conditions. *Proc Combust Inst* 2019;37(4):4813–20.
- [108] Dai P, Chen Z, Gan X. Autoignition and detonation development induced by a hot spot in fuel-lean and CO<sub>2</sub> diluted n-heptane/air mixtures. *Combust Flame* 2019;201:208–14.
- [109] Zhang X, Wei H, Zhou L, Cai X, Deiterding R. Relationship of flame propagation and combustion mode transition of end-gas based on pressure wave in confined space. *Combust Flame* 2020;214:371–86.
- [110] Blumenthal R, Fieweger K, Komp K, Adomeit G. Gas dynamic features of self ignition of non diluted fuel/air mixtures at high pressure. *Combust Sci Technol* 1996;113(1):137–66.
- [111] Pan J, Wei H, Shu G, Pan M, Feng D, Li N. LES analysis for auto-ignition induced abnormal combustion based on a downsized SI engine. *Appl Energy* 2017;191:183–92.
- [112] Wei H, Zhao J, Zhang X, Pan J, Hua J, Zhou L. Turbulent flame–shock interaction inducing end-gas autoignition in a confined space. *Combust Flame* 2019;204:137–41.
- [113] Wang Z, He X, Liu H, Qi Y, Zhang P, Wang J. Initiation of detonation in iso-octane/air mixture under high pressure and temperature condition in closed cylinder. In: *25th int. colloq. dyn. explos. react. syst.* 2015.
- [114] Wang Z, Qi Y, Liu H, Zhang P, He X, Wang J. Shock wave reflection induced detonation (SWRID) under high pressure and temperature condition in closed cylinder. *Shock Waves* 2016;26(5):687–91.
- [115] Liu H, Wang Z, He X, Qi Y, Wang Y, Wang J. Super-knock suppression for highly turbocharged gasoline engines using lean mixture control strategy with the same energy density. *Int J Engine Res* 2021;22(2):665–73.
- [116] Xu H, Weng C, Gao J, Yao C. The effect of energy intensification on the formation of severe knock in internal combustion engines. *Appl Energy* 2020;266:114854.
- [117] Xu H, Yao A, Yao C, Gao J. Energy convergence of shock waves and its destruction mechanism in cone-roof combustion chambers. *Energy Convers Manage* 2016;127:342–54.
- [118] Zhou L, Kang R, Wei H, Feng D, Hua J, Pan J, et al. Experimental analysis of super-knock occurrence based on a spark ignition engine with high compression ratio. *Energy* 2018;165:68–75.
- [119] Morikawa K, Moriyoshi Y, Kuboyama T, Imai Y, Yamada T, Hatamura K. Investigation and improvement of LSPI phenomena and study of combustion strategy in highly boosted SI combustion in low speed range. *Tech. Rep.*, (2015-01-0756). SAE Technical Paper; 2015.
- [120] Döhler A, Schaffner P. Optical diagnostic tools for detection and evaluation of glow ignitions. In: *International conference on knocking in gasoline engines*. Springer; 2017, p. 55–70.
- [121] Passow EJ, Sethi P, Maschewske M, Bieneman J, Karris K, Truckel P. An introduction to how low speed pre ignition affects engine components. *Tech. Rep.*, (2017-01-1042). SAE Technical Paper; 2017.
- [122] Kocsis MC, Briggs T, Anderson G. The impact of lubricant volatility, viscosity and detergent chemistry on low speed pre-ignition behavior. *SAE Int J Engines* 2017;10(3):1019–35.
- [123] Willand J, Daniel M, Montefrancesco E, Geringer B, Hofmann P, Kieberger M. Limits on downsizing in spark ignition engines due to pre-ignition. *MTZ Worldwide* 2009;70(5):56–61.
- [124] Heiß M. Approach for modelling the initiation process of low-speed pre-ignition in downsized SI-engines [Ph.D. thesis], Wien; 2015.
- [125] Inoue T, Inoue Y, Ishikawa M. Abnormal combustion in a highly boosted SI engine—the occurrence of super knock. *Tech. Rep.*, (2012-01-1141). SAE Technical Paper; 2012.
- [126] Singh E, Dibble R. Effectiveness of fuel enrichment on knock suppression in a gasoline spark-ignited engine. *Tech. Rep.*, (2018-01-1665). SAE Technical Paper; 2018.
- [127] Rönn K, et al. Low-speed pre-ignition and super-knock in spark-ignition engines. 2020.
- [128] Boese D, Ritchie A, Young AW. Controlling low-speed pre-ignition in modern automotive equipment: Defining approaches to and methods for analyzing data in new studies of lubricant and fuel-related effects (part 2). *Tech. Rep.*, (2016-01-0716). SAE Technical Paper; 2016.
- [129] Fleishman AI. A method for simulating non-normal distributions. *Psychometrika* 1978;43(4):521–32.
- [130] Kalaskar VB, Swarts A, Alger T. Impact of engine age and engine hardware on low-speed pre-ignition. *Tech. Rep.*, (2018-01-1663). SAE Technical Paper; 2018.
- [131] Fletcher KA, Dingwell L, Yang K, Lam WY, Styer JP. Engine oil additive impacts on low speed pre-ignition. *SAE Int J Fuels Lubr* 2016;9(3):612–20.
- [132] Andrews A, Burns R, Dougherty R, Deckman D, Patel M. Investigation of engine oil base stock effects on low speed pre-ignition in a turbocharged direct injection SI engine. *SAE Int J Fuels Lubr* 2016;9(2):400–7.
- [133] Teng H, Luo X, Hu T, Miao R, Wu M, Chen B, et al. Influence of crankcase oil properties on low-speed pre-ignition encountered in a highly-boosted gasoline direct injection engine. *SAE Int J Fuels Lubr* 2016;9(3):603–11.
- [134] Luo X, Teng H, Hu T, Miao R, Cao L. An experimental investigation on low speed pre-ignition in a highly boosted gasoline direct injection engine. *SAE Int J Engines* 2015;8(2):520–8.
- [135] Mansfield AB, Chapman E, Briscoe K. Effect of market variations in gasoline composition on aspects of stochastic pre-ignition. *Fuel* 2016;184:390–400.
- [136] Jatana GS, Splitter DA, Kaul B, Szybist JP. Fuel property effects on low-speed pre-ignition. *Fuel* 2018;230:474–82.
- [137] Kaul B, Finney C, Stiffler R, Drallmeier J. Advanced intra-cycle detection of pre-ignition events through phase-space transforms of cylinder pressure data. *Tech. Rep.*, (2020-01-2046). SAE Technical Paper; 2020.
- [138] Haenel P, Kleeberg H, de Bruijn R, Tomazic D. Influence of ethanol blends on low speed pre-ignition in turbocharged, direct-injection gasoline engines. *SAE Int J Fuels Lubr* 2017;10(1):95–105.
- [139] Singh E, Dibble R. Pre-ignition detection followed by immediate damage mitigation in a spark-ignited engine. *Tech. Rep.*, (2021-01-0437). SAE Technical Paper; 2021.
- [140] Moriyoshi Y, Kuboyama T, Takaki T, Hitosugi H. Investigation on relationship between LSPI and lube oil consumption and its countermeasure. *Tech. Rep.*, (2021-01-0567). SAE Technical Paper; 2021.
- [141] Kumano K, Akagi Y, Matohara S, Uchise Y, Yamasaki Y. Using an ion-current sensor integrated in the ignition system to detect precursory phenomenon of pre-ignition in gasoline engines. *Appl Energy* 2020;275:115341.
- [142] Tong S, Yang Z, He X, Deng J, Wu Z, Li L. Knock and pre-ignition detection using ion current signal on a boosted gasoline engine. *Tech. Rep.*, (2017-01-0792). SAE Technical Paper; 2017.
- [143] Ayad S, Sharma S, Verma R, Henein N. Combustion ionization for detection of misfire, knock, and sporadic preignition in a gasoline direct injection engine. *J Energy Res Technol* 2019;141(11).
- [144] Wang J, Hu Z, Zhu D, Ding W, Li L, Yan W, et al. In cycle pre-ignition diagnosis and super-knock suppression by employing ion current in a GDI boosted engine. *Tech. Rep.*, (2020-01-1148). SAE Technical Paper; 2020.
- [145] Kuzhagaliev N, Thabet A, Singh E, Ghanem B, Sarathy SM. Using deep neural networks to diagnose engine pre-ignition. *Proc Combust Inst* 2020.
- [146] Michlberger A, Sutton M. LSPI durability, a study of LSPI over the life of a vehicle. *SAE Int J Engines* 2018;11(1):23–38.
- [147] Zhang R, Howard K, Browne D. A real-world fleet test of the effects of engine oil on low speed pre-ignition occurrence in TGD<sub>i</sub> engine. (2019-01-2294). SAE Technical Paper; 2019.
- [148] Chapman E, Davis R, Studzinski W, Geng P. Fuel octane and volatility effects on the stochastic pre-ignition behavior of a 2.0 l gasoline turbocharged DI engine. *SAE Int J Fuels Lubr* 2014;7(2):379–89.

- [149] Kocsis MC, Anderson G, Briggs T. Real fuel effects on low speed pre-ignition. Tech. Rep., (2018-01-1456). SAE Technical Papers; 2018.
- [150] Maharjan S, Elbaz AM, Roberts WL. Study of the effect of research octane number on the auto-ignition of lubricant oil surrogates (n-hexadecane). ACS Omega 2022.
- [151] Mitsudharmadi H, Maharjan S, Elbaz AM, Qahtani YA, Roberts WL. Auto-ignition of a hexadecane droplet mixed with different octane number fuels at elevated pressures to investigate the pre-ignition behavior. Energy Fuels 2019;34(1):806–16.
- [152] Andrae JC. Development of a detailed kinetic model for gasoline surrogate fuels. Fuel 2008;87(10–11):2013–22.
- [153] Ghosh P, Hickey KJ, Jaffe SB. Development of a detailed gasoline composition-based octane model. Ind Eng Chem Res 2006;45(1):337–45.
- [154] Budak O, Hoppe F, Heuser B, Pischinger S, Burke U, Heufer A. Hot surface pre-ignition in direct-injection spark-ignition engines: Investigations with Tailor-Made Fuels from Biomass. Int J Engine Res 2018;19(1):45–54.
- [155] Farrell JT, Johnston R, Androulakis I. Molecular structure effects on laminar burning velocities at elevated temperature and pressure. SAE Trans 2004;1404–25.
- [156] Downs D, Theobald F. The effect of fuel characteristics and engine operating conditions on pre-ignition. Proc Inst Mech Eng Automob Div 1963;178(1):89–108.
- [157] Singh E, Dibble R. Knock, auto-ignition and pre-ignition tendency of fuels for advanced combustion engines (FACE) with ethanol blends and similar RON. Tech. Rep., (2020-01-0613). SAE Technical Paper; 2020.
- [158] Mansfield AB, Chapman E, Briscoe K. Impact of fuel octane rating and aromatic content on stochastic pre-ignition. Tech. Rep., (2016-01-0721). SAE Technical Paper; 2016.
- [159] Xu Z, Zhou Z, Wu T, Li T, Cheng C, Yin H. Investigations of smoke emission, fuel dilution and pre-ignition in a 2.0 l turbo-charged GDI engine. Tech. Rep., (2016-01-0698). SAE Technical Paper; 2016.
- [160] Haynes WM. CRC handbook of chemistry and physics. CRC Press; 2014.
- [161] Tanaka D, Uchida R, Noda T, Kolbeck A, Henkel S, Hardalupas Y, et al. Effects of fuel properties associated with in-cylinder behavior on particulate number from a direct injection gasoline engine. Tech. Rep., (2017-01-1002). SAE Technical Paper; 2017.
- [162] Sethi P, Passow E, Karpri K, Maschewske M, Bieneman J, Truckel P. A study to determine factors that have influence on the propensity of natural LSPI occurring in GTDI engines. In: ASME 2018 internal combustion engine division fall technical conference. American Society of Mechanical Engineers Digital Collection; 2018.
- [163] Kassai M, Torii K, Shiraishi T, Noda T, Goh TK, Wilbrand K, et al. Research on the effect of lubricant oil and fuel properties on LSPI occurrence in boosted SI engines. Tech. Rep., (2016-01-2292). SAE Technical Paper; 2016.
- [164] Mayer M, Hofmann P, Geringer B, Williams J, Moss J. Influence of different fuel properties and gasoline-ethanol blends on low-speed pre-ignition in turbocharged direct injection spark ignition engines. SAE Int J Engines 2016;9(2):841–8.
- [165] Long Y, Wang Z, Qi Y, Xiang S, Zeng G, Zhang P, et al. Effect of oil and gasoline properties on pre-ignition and super-knock in a thermal research engine (TRE) and an optical rapid compression machine (RCM). Tech. Rep., (2016-01-0720). SAE Technical Paper; 2016.
- [166] Costanzo V, Yu X, Chapman E, Davis R. Fuel effects on the propensity to establish propagating flames at SPI-relevant engine conditions. SAE Int J Adv Curr Pract Mobil 2021;3(2021-01-0488):3194–203.
- [167] Downs D, Pigneguy J. An experimental investigation into pre-ignition in the spark-ignition engine. Proc Inst Mech Eng Automob Div 1950;4(1):125–49.
- [168] Günther M, Uygun Y, Kremer F, Pischinger S. Pre-ignition and glow-ignition of gasoline biofuels. MTZ Worldwide 2013;74(12):46–53.
- [169] Pischinger S, Günther M, Budak O. Abnormal combustion phenomena with different fuels in a spark ignition engine with direct fuel injection. Combust Flame 2017;175:123–37.
- [170] Nomura T, Ueura H, Tanaka Y, Iida Y, Yuan Z, Ando A. The effect of gasoline metallic additives on low speed pre-ignition. Tech. Rep., (2018-01-0936). SAE Technical Paper; 2018.
- [171] Joedicke A, Krueger-Venus J, Bohr P, Cracknell R, Doyle D. Understanding the effect of DISI injector deposits on vehicle performance. Tech. Rep., (2012-01-0391). SAE Technical Paper; 2012.
- [172] Van Basshuysen R, Schäfer F. Internal combustion engine handbook-basics, components, systems and perspectives. vol. 345, 2004.
- [173] Ritchie A, Boese D, Young AW. Controlling low-speed pre-ignition in modern automotive equipment part 3: Identification of key additive component types and other lubricant composition effects on low-speed pre-ignition. SAE Int J Engines 2016;9(2):832–40.
- [174] Takeuchi K, Fujimoto K, Hirano S, Yamashita M. Investigation of engine oil effect on abnormal combustion in turbocharged direct injection-spark ignition engines. SAE Int J Fuels Lubr 2012;5(3):1017–24.
- [175] Haas FM, Won SH, Dryer FL, Pera C. Lube oil chemistry influences on autoignition as measured in an ignition quality tester. Proc Combust Inst 2019;37(4):4645–54.
- [176] Tormos B, García-Oliver JM, Carreres M, Moreno-Montagud C, Domínguez B, Cárdenas MD, et al. Experimental assessment of ignition characteristics of lubricating oil sprays related to low-speed pre-ignition (LSPI). Int J Engine Res 2021;1–12.
- [177] Hourani N, Muller H, Adam FM, Panda SK, Witt M, Al-Hajji AA, et al. Structural level characterization of base oils using advanced analytical techniques. Energy Fuels 2015;29(5):2962–70.
- [178] Pan K, Deng J, Chen Y, Zhang E, Xie W, Qin Q, et al. Auto-ignition characteristics of lubricant droplets under hot co-flow atmosphere. Tech. Rep., (2018-01-1807). SAE Technical Paper; 2018.
- [179] Inada Y, Tanaka J. Lubricating oil droplets from piston crown on abnormal combustion in supercharged SI engine. Tech. Rep., (2020-32-2302). SAE Technical Paper; 2020.
- [180] Liu Y, Pei Y, Wang C, Guo R, Xu B. Characteristics of the deposited fuel liquid film when GDI spray impacts viscous oil film. Energy 2019;188:116011.
- [181] Wang QJ, Chung Y-W. Encyclopedia of tribology. Springer; 2013.
- [182] Guibet J-C, Duval A. New aspects of preignition in European automotive engines. SAE Trans 1972;399–417.
- [183] Fujimoto K, Yamashita M, Hirano S, Kato K, Watanabe I, Ito K. Engine oil development for preventing pre-ignition in turbocharged gasoline engine. SAE Int J Fuels Lubr 2014;7(3):869–74.
- [184] Mayer M, Hofmann P, Geringer B, Williams J, Moss J. Influence of different fuel properties and gasoline-ethanol blends on low-speed pre-ignition in turbocharged direct injection spark ignition engines. SAE Int J Engines 2016;9(2):841–8.
- [185] Haenel P, de Bruijn R, Tomazic D, Kleeberg H. Analysis of the impact of production lubricant composition and fuel dilution on stochastic pre-ignition in turbocharged, direct-injection gasoline engines. Tech. Rep., (2019-01-0256). SAE Technical Paper; 2019.
- [186] Elliott I, Sztenderowicz M, Sinha K, Takeuchi Y, Ushioda N. Understanding low speed pre-ignition phenomena across turbo-charged gdi engines and impact on future engine oil design. Tech. Rep., (2015-01-2028). SAE Technical Paper; 2015.
- [187] Splitter D, Kaul B, Szybist J, Speed L, Zigler B, Luecke J. Fuel-lubricant interactions on the propensity for stochastic pre-ignition. Tech. Rep., (2019-24-0103). SAE Technical Paper; 2019.
- [188] Lattuada M, Manni M. Evolution of the additive technology for top tier lubricating oils: Use of calixarene detergents for fuel economy improvement. Tech. Rep., (2021-01-1212). SAE Technical Paper; 2021.
- [189] Onodera K, Kato T, Ogano S, Fujimoto K, Kato K, Kaneko T. Engine oil formulation technology to prevent pre-ignition in turbocharged direct injection spark ignition engines. Tech. Rep., (2015-01-2027). SAE Technical Paper; 2015.
- [190] Gupta A, Devlin M. Impact of engine oil detergent on low speed pre-ignition (LSPI) and fuel economy performance. Tech. Rep., (2020-01-1424). SAE Technical Paper; 2020.
- [191] Liu H, Jin J, Li H, Yamamori K, Kaneko T, Yamashita M, et al. 0W-16 fuel economy gasoline engine oil compatible with low speed pre-ignition performance. SAE Int J Fuels Lubr 2017;10(3):842–7.
- [192] Kaneko T, Yamamori K, Suzuki H, Onodera K, Ogano S. Friction reduction technology for low viscosity engine oil compatible with LSPI prevention performance. Tech. Rep., (2016-01-2276). SAE Technical Paper; 2016.
- [193] Elliott I, Cherpeck R, Maria A, Gunawan T. Alternative engine oil formulating solutions to reduce low speed pre-ignition. Tech. Rep., (2019-01-2153). SAE Technical Paper; 2019.
- [194] Kassai M, Shiraishi T, Noda T. Fundamental mechanism analysis on the underlying processes of LSPI using experimental and modeling approaches. In: International conference on knocking in gasoline engines. Springer; 2017, p. 89–111.
- [195] McQueen J, Gao H, Black E, Gangopadhyay A, Jensen R. Friction and wear of tribofilms formed by zinc dialkyl dithiophosphate antiwear additive in low viscosity engine oils. Tribol Int 2005;38(3):289–97.
- [196] Du D-C, Kim S-S, Chun J-S, Suh C-M, Kwon W-S. Antioxidation synergism between ZnDTC and ZnDDP in mineral oil. Tribol Lett 2002;13(1):21–7.
- [197] Guevremont JM, Guinther GH, Szemenyei D, Devlin MT, Jao T-C, Jaye C, et al. Enhancement of engine oil wear and friction control performance through titanium additive chemistry. Tribol Trans 2008;51(3):324–31.
- [198] Michlberger A, Sutton M, Dohner B. Low speed pre-ignition (LSPI) durability - a study of LSPI in fresh and aged engine oils. Tech. Rep., (2018-01-0934). SAE Technical Paper; 2018.
- [199] Swarts A, Kostan T, Kalaskar V. Combined effects of engine and oil age on low speed pre-ignition. SAE Int J Adv Curr Pract Mobil 2019;1(2019-01-0033):227–35.
- [200] Singh E. Mechanism triggering pre-ignition events and ideas to avoid and suppress pre-ignition in turbocharged spark-ignited engines [Ph.D. thesis], 2019.
- [201] Han L, Zhu T, Qiao H, Zhang D, Fu D, Zhang J. Investigation of low-speed pre-ignition in boosted spark ignition engine. Tech. Rep., (2015-01-0751). SAE Technical Paper; 2015.
- [202] Mayer M, Hofmann P, Geringer B, Williams J, Moss J. Influence of different fuel properties and gasoline-ethanol blends on low-speed pre-ignition in turbocharged direct injection spark ignition engines. SAE Int J Engines 2016;9(2):841–8.

- [203] Arnold Kaden A, Gildein H, Kraus E, Schaupp U. Knocking simulation at mercedes-benz—application in series production development. *Knocking in Gasol Engines* 2013.
- [204] Singh E, Hlaing P, Shi H, Dibble RW. Effect of different fluids on injection strategies to suppress pre-ignition. Tech. Rep., (2019-01-0257). SAE International; 2019.
- [205] Singh E, Morganti K, Dibble R. Optimizing split fuel injection strategies to avoid pre-ignition and super-knock in turbocharged engines. *Int J Engine Res* 2021;22(1):199–221.
- [206] Schulz F, Samenfink W, Schmidt J, Beyrau F. Systematic LIF fuel wall film investigation. *Fuel* 2016;172:284–92.
- [207] Splitter D, Kaul B, Szybist J, Jatana G. Engine operating conditions and fuel properties on pre-spark heat release and SPI promotion in SI engines. *SAE Int J Engines* 2017;10(3):1036–50.
- [208] Zaccardi J-M, Serrano D. A comparative low speed pre-ignition (LSPI) study in downsized si gasoline and CI diesel-methane dual fuel engines. *SAE Int J Engines* 2014;7(4):1931–44.
- [209] Martin S, Beidl C, Mueller R. Responsiveness of a 30 bar BMEP 3-cylinder engine: Opportunities and limits of turbocharged downsizing. Tech. Rep., (2014-01-1646). SAE Technical Paper; 2014.
- [210] Alger T, Chauvet T, Dimitrova Z. Synergies between high EGR operation and GDI systems. *SAE Int J Engines* 2009;1(1):101–14.
- [211] Radwan M, Helali A, Elfeky S, Attai Y. An investigation on knock and pre-ignition with tumble induced turbulence. Tech. Rep., (2007-01-3557). SAE Technical Paper; 2007.
- [212] Franqueville L, Michel J-B. On the effects of EGR on spark-ignited gasoline combustion at high load. *SAE Int J Engines* 2014;7(4):1808–23.
- [213] Hoepke B, Jannsen S, Kasseris E, Cheng WK. EGR effects on boosted SI engine operation and knock integral correlation. *SAE Int J Engines* 2012;5(2):547–59.
- [214] Sekarapandian N, Kannaiyan A, Arivukkaranu H, Mani R, Muthu S. Advanced methods to handle LSPI in TGDI engines. *SAE Int J Adv Curr Pract Mobil* 2020;3(1):614–20.
- [215] Park S, Woo S, Oh H, Lee K. Effects of various lubricants and fuels on pre-ignition in a turbocharged direct-injection spark-ignition engine. *Energy Fuels* 2017;31(11):12701–11.
- [216] Mounce F. Development of a standardized test to evaluate the effect of gasoline engine oil on the occurrence of low speed pre-ignition-the sequence IX test. Tech. Rep., (2018-01-1808). SAE Technical Paper; 2018.
- [217] Kouchi S, Okamoto S, Ozawa K, Kawashima H, Ishima T, Uchida R, et al. Observation and analysis of behavior of spray impingement on a liquid film. Tech. Rep., (2015-01-2006). SAE Technical Paper; 2015.
- [218] Lee C, Ahmed A, Nasir EF, Badra J, Kalghatgi G, Sarathy SM, et al. Autoignition characteristics of oxygenated gasolines. *Combust Flame* 2017;186:114–28.
- [219] Javed T, Lee C, AlAbbad M, Djebbi K, Beshir M, Badra J, et al. Ignition studies of n-heptane/iso-octane/toluene blends. *Combust Flame* 2016;171:223–33.
- [220] Cheng S, Kang D, Fridlyand A, Goldsborough SS, Saggese C, Wagon S, et al. Autoignition behavior of gasoline/ethanol blends at engine-relevant conditions. *Combust Flame* 2020;216:369–84.
- [221] Wei H, Xu Z, Zhou L, Zhao J, Yu J. Effect of hydrogen-air mixture diluted with argon/nitrogen/carbon dioxide on combustion processes in confined space. *Int J Hydrogen Energy* 2018;43(31):14798–805.
- [222] Sarathy SM, Westbrook CK, Mehl M, Pitz WJ, Togbe C, Dagaut P, et al. Comprehensive chemical kinetic modeling of the oxidation of 2-methylalkanes from C7 to C20. *Combust Flame* 2011;158(12):2338–57.
- [223] Westbrook CK, Pitz WJ, Herbinet O, Curran HJ, Silke EJ. A comprehensive detailed chemical kinetic reaction mechanism for combustion of n-alkane hydrocarbons from n-octane to n-hexadecane. *Combust Flame* 2009;156(1):181–99.
- [224] Soejima M, Harigaya Y, Hamatake T, Wakuri Y. Study on lubricating oil consumption from evaporation of oil-film on cylinder wall for diesel engine. *SAE Int J Fuels Lubr* 2017;10(2):487–501.
- [225] Wang FC-Y, Zhang L. Chemical composition of group II lubricant oil studied by high-resolution gas chromatography and comprehensive two-dimensional gas chromatography. *Energy Fuels* 2007;21(6):3477–83.
- [226] Birkigt A, Michels K, Theobald J, Seeger T, Gao Y, Weikl M, et al. Investigation of compression temperature in highly charged spark-ignition engines. *Int J Engine Res* 2011;12(3):282–92.
- [227] Ohtomo M, Miyagawa H, Koike M, Yokoo N, Nakata K. Pre-ignition of gasoline-air mixture triggered by a lubricant oil droplet. *SAE Int J Fuels Lubr* 2014;7(3):673–82.
- [228] Ohtomo M, Suzuoki T, Miyagawa H, Koike M, Yokoo N, Nakata K. Fundamental analysis on auto-ignition condition of a lubricant oil droplet for understanding a mechanism of low-speed pre-ignition in highly charged spark-ignition engines. *Int J Engine Res* 2019;20(3):292–303.
- [229] Gong Z, Hu M, Fang Y, Zhang D, Feng L. Mechanism study of natural gas pre-ignition induced by the auto-ignition of lubricating oil. *Fuel* 2022;315:123286.
- [230] Yi P, Long W, Feng L, Wang W, Liu C. An experimental and numerical study of the evaporation and pyrolysis characteristics of lubricating oil droplets in the natural gas engine conditions. *Int J Heat Mass Transfer* 2016;103:646–60.
- [231] Welling O, Moss J, Williams J, Collings N. Measuring the impact of engine oils and fuels on low-speed pre-ignition in downsized engines. *SAE Int J Fuels Lubr* 2014;7(1):1–8.
- [232] Coultas DR. The role of NOx in engine lubricant oxidation. *SAE Tech Pap* 2020;2(2020-01-1427).
- [233] Chen Y, Li L, Zhang Q, Deng J, Xie W, Zhang E, et al. Effects of lubricant additives on auto-ignition under a hot co-flow atmosphere. Tech. Rep., (2017-01-2231). SAE Technical Paper; 2017.
- [234] Kassai M, Shiraishi T, Noda T, Hirabe M, Wakabayashi Y, Kusaka J, et al. An investigation on the ignition characteristics of lubricant component containing fuel droplets using rapid compression and expansion machine. *SAE Int J Fuels Lubr* 2016;9(3):469–80.
- [235] Miyasaka T, Miura K, Hayakawa N, Ishino T, Iijima A, Shoji H, et al. A study on the effect of a calcium-based engine oil additive on abnormal SI engine combustion. *SAE Int J Engines* 2015;8(1):206–13.
- [236] Miura K, Shimizu K, Hayakawa N, Miyasaka T, Iijima A, Shoji H, et al. Influence of Ca-, Mg-and Na-based engine oil additives on abnormal combustion in a spark-ignition engine. *SAE Int J Engines* 2016;9(1):452–7.
- [237] Tamura K, Utaka T, Kamano H, Hayakawa N, Miyasaka T, Ishino T, et al. Abnormal combustion induced by combustion chamber deposits derived from engine oil additives in a spark-ignited engine. *SAE Int J Engines* 2015;8(1):200–5.
- [238] Moriyoshi Y, Yamada T, Tsunoda D, Xie M, Kuboyama T, Morikawa K. Numerical simulation to understand the cause and sequence of LSPI phenomena and suggestion of CaO mechanism in highly boosted SI combustion in low speed range. Tech. Rep., (2015-01-0755). SAE Technical Paper; 2015.
- [239] Kyaw K, Matsuda H, Hasatani M. Applicability of carbonation/decarbonation reactions to high-temperature thermal energy storage and temperature upgrading. *J Chem Eng Japan* 1996;29(1):119–25.
- [240] Maharjan S, Qahtani Y, Roberts W, Elbaz A. The effect of pressure, temperature and additives on droplet ignition of lubricant oil and its surrogate. Tech. Rep., (2018-01-1673). SAE Technical Paper; 2018.
- [241] Hayakawa N, Miura K, Miyasaka T, Ishino T, Iijima A, Shoji H, et al. A study on the effect of Zn-and Mo-based engine oil additives on abnormal SI engine combustion using in-cylinder combustion visualization. *SAE Int J Engines* 2015;8(1):214–20.
- [242] Yasueda S, Takasaki K, Tajima H. Abnormal combustion caused by lubricating oil in high BMEP gas engines. *MTZ Ind* 2013;3(1):34–9.
- [243] Yasueda S, Takasaki K, Tajima H. The abnormal combustion affected by lubricating oil ignition in premixed gas engine. In: Proceedings of the ASME 2012 internal combustion engine division spring technical conference. ASME 2012 internal combustion engine division spring technical conference. 2012, p. 29–36.
- [244] Yasueda S, Tozzi JL. Conseil international des machines a combustion international council on combustion engines paper no.: 37 predicting autoignition caused by lubricating oil in gas engines. Tech. Rep., 2013.
- [245] Yasueda S, Zhu S, Sotiropoulou E, Tozzi L. The working process of the internal combustion engine. Tech. Rep., 2015.
- [246] Serrano D, Obiols J, Lecoite B. Optimization of dual fuel diesel-methane operation on a production passenger car engine-thermodynamic analysis. Tech. Rep., (2013-01-2505). SAE Technical Paper; 2013.
- [247] Chen R, Kuboyama T, Moriyoshi Y, Yasueda S, Doyen V, Martin J-B. Effects of engine operating condition and fuel property on pre-ignition phenomenon in a highly boosted premixed natural gas engine. Tech. Rep., (2019-01-2154). SAE Technical Paper; 2019.
- [248] Königsson F. On combustion in the CNG-diesel dual fuel engine [Ph.D. thesis], KTH Royal Institute of Technology; 2014.
- [249] Gong Z, Feng L, Li L, Qu W, Wei L. Shock tube and kinetic study on ignition characteristics of methane/n-hexadecane mixtures. *Energy* 2020;201:117609.
- [250] Tsujimura T, Suzuki Y. The utilization of hydrogen in hydrogen/diesel dual fuel engine. *Int J Hydrogen Energy* 2017;42(19):14019–29.
- [251] Kriek M, Günther M, Pischinger S, Kramer U, Thewes M. Effects of LPG fuel formulations on knock and pre-ignition behavior of a DI SI engine. *SAE Int J Engines* 2016;9(1):237–51.
- [252] Eto K, Kihara M. Calcium in oil effects on pre-ignition of two-stroke engine. Tech. Rep., (2019-32-0579). SAE Technical Paper; 2020.
- [253] Devlin MT. Common properties of lubricants that affect vehicle fuel efficiency: a north American historical perspective. *Lubricants* 2018;6(3):68.
- [254] Onodera K, Watanabe H, Sato T, Lee GH, Kaneko T, Yamamori K, et al. Fuel economy improvement by engine oil with ultra-high viscosity index. Tech. Rep., (2019-01-2203). SAE Technical Paper; 2019.
- [255] Matsui T, Featherstone T, Wright P. Art of fuel economy lubricant formulation: How appropriate fuel economy assessment tools and new technologies are opening-up new formulation spaces for the next generation fuel economy lubricants. Tech. Rep., (2019-01-2242). SAE Technical Paper; 2019.
- [256] Yamamori K, Uematsu Y, Manabe K, Miyata I, Kusuhara S, Misaki Y. Development of ultra low viscosity 0W-8 engine oil. Tech. Rep., (2020-01-1425). SAE Technical Paper; 2020.
- [257] D8291 A. Standard test method for evaluation of performance of automotive engine oils in the mitigation of low-speed, preignition in the sequence IX gasoline turbocharged direct-injection, spark-ignition engine. Tech. Rep., ASTM International, West Conshohocken, PA.

**Kristian Rönn** is a doctoral student at Aalto School of Engineering, conducting research on low-speed pre-ignition through experiments and chemical simulations. He received his master's degree in 2020 from Aalto University, majoring in Sustainable Energy Conversion Processes.

**Dr Andre Swarts** is a staff engineer at Southwest Research Institute, where he works in fuels and lubricant research and fluids for electrified vehicles, including battery cooling. He has published more than 30 papers including several articles on low-speed pre-ignition. He obtained his Ph.D. from the University of Cape Town in 2006.

**Dr Vickey Kalaskar** is a Senior Research Engineer at Southwest Research Institute, where he has participated in several articles on low-speed pre-ignition.



**Dr. Alger** graduated from the US Military Academy as a Distinguished Cadet in 1992 and was commissioned as a 2nd Lieutenant in the US Army Corps of Engineers. He received his Ph.D. in Mechanical Engineering from The University of Texas at Austin in 2001. Dr. Alger joined Southwest Research Institute in 2003 in the Advanced Combustion and Emissions Section. During his career, he has worked on topics including improved efficiency and advanced combustion modes in SI engines, heat transfer and thermal management in motors and energy storage systems, abnormal combustion, connected vehicle energy optimization, grid storage and defense-related mobility challenges. He is currently the Executive Director of Sustainable Energy and Mobility and his team focuses on developing sustainable mobility technologies for the transportation industry and low carbon intensity solutions for other industries, including utilities and manufacturing. He is a Fellow of the Society of Automotive Engineers.

**Dr Rupali Tripathi** has been working as a researcher at Neste Corporation since 2019. She obtained her doctorate from Rheinisch-Westfälische Technische Hochschule Aachen in Combustion Technology. She has published many articles in various prestigious combustion journals. Her research interests include renewable fuel development, ignition behavior of biofuels, and combustion kinetics.

**Dr Juha Keskiväli** obtained his Ph.D. from the Department of Chemistry in University of Helsinki in 2018. After that, he worked for Neste Oyj as a product researcher.

**Associate Professor Ossi Kaario** at Aalto University School of Engineering has a background in engine modeling and experiments and has published more than 30 journal papers related to engine modeling and more than 20 journal papers on engine experiments.



**Assistant professor Annukka Santasalo-Aarnio** was appointed as the head of Energy Storage research team at Aalto School of Engineering in September 2018. The research focus areas in her team are power-to-fuels, thermal energy storage systems and materials, non-battery energy storage systems for grid stabilization and harvesting energy from end-of-use batteries. She is the project manager of an industrial research project on future fuels and has 3 Academy of Finland projects on Energy Storage. Annukka currently has a research team of 15 researchers and she is also the responsible professor at Aalto for the InnoEnergy Energy Storage master program.

Annukka obtained her Ph.D. on Fuel Cell material development and testing at Helsinki University of Technology in 2012. She did her postdoctoral work with Li-ion battery development and as a leader a work package in a Horizon 2020 project on Solar to Hydrogen, for task in the development of an electrolyzer technology and complete process integration. She obtained a University Teacher position in 2015 at the Department of Materials Science and Metallurgy, and became the responsible teacher on a variety of materials science, particularly on circular economy.



**Professor Rolf D. Reitz** is an emeritus professor at the University of Wisconsin-Madison. His career has included pioneering work on reactivity controlled compression ignition (RCCI) combustion for high efficiencies and low emissions and development of computer models of fuel injected engines. Professor Reitz has authored and co-authored more than 500 journal publications and he has 5 patents. He is the co-founding editor (Americas) of the International Journal of Engine Research. He has served on the executive board of the Institute of Liquid Atomization and Spraying Systems and was the director of the UWMadison Mechanical Engineering Department's Engine Research Center.



**Professor Martti Larmi** is the Head of the Research Group of Energy Conversion at Aalto University School of Engineering. He obtained his degree in Doctor of Science in Technology in 1993 from Helsinki University of Technology in Mechanical Engineering and has been a Professor of Internal Combustion Engine Technology since 2002 at Helsinki University of Technology and later at Aalto University. In 2005, he received the Reward of Finnish Technology Industry 100-year Foundation for the development of low emission combustion. He has examined or supervised 30 doctoral theses.